Società Geologica Italiana

ISPRA
Istituto Superiore per la Protezione e la Ricerca Ambientale
SERVIZIO GEOLOGICO D'ITALIA
Organo Cartografico dello Stato (legge N°68 del 2-2-1960)
Dipartimento Difesa del Suolo

Geological Field Trips

2015
Vol. 7 (1.2)

ISSN: 2038-4947

Geothermal resources, ore deposits and carbon mineral sequestration in hydrothermal areas of Southern Tuscany

Goldschmidt Conference - Florence, 2013

DOI: 10.3301/GFT.2015.02

GFT - *Geological Field Trips*

Periodico semestrale del Servizio Geologico d'Italia - ISPRA e della Società Geologica Italiana
Geol.F.Trips, Vol.**7** No.1.2 (2015), 91 pp., 67 figs. (DOI 10.3301/GFT.2015.02)

Geothermal resources, ore deposits and carbon mineral sequestration in hydrothermal areas of Southern Tuscany

Goldschmidt Conference, 2013

Marco Benvenuti[1], Chiara Boschi[2], Andrea Dini[2], Giovanni Ruggieri[3], Alessia Arias[4]

[1] Dipartimento di Scienze della Terra, University of Florence, Via G. La Pira, 4, 50121 Florence, Italy
[2] Istituto di Geoscienze e Georisorse, CNR, Via Moruzzi 1, 56124 Pise, Italy
[3] Istituto di Geoscienze e Georisorse, CNR, Via G. La Pira 4, 50121 Florence, Italy
[4] Enel Green Power SpA, Via Andrea Pisano 120, 56122 Pise, Italy

Corresponding Author e-mail address: m.benvenuti@unifi.it c.boschi@igg.cnr.it a.dini@igg.cnr.it ruggieri@igg.cnr.it

ISSN: 2038-4947 [online]

http://www.isprambiente.gov.it/it/pubblicazioni/periodici-tecnici/geological-field-trips

DOI: 10.3301/GFT.2015.02

INDEX

Information

Excursion notes

Itinerary

DOI: 10.3301/GFT.2015.02

2nd Day - The geothermal field of Larderello and the Malentrata mine

DOI: 10.3301/GFT.2015.02

Riassunto

Questa escursione geologica di tre giorni permette di conoscere i differenti aspetti dell'attività idrotermale della Toscana meridionale, prodotta da una diffusa anomalia termica e da magmatismo che ha interessato la regione in uno stadio post-collisionale dell'orogenesi appenninica (dal tardo Miocene al Pleistocene). L'attività idrotermale, passata ed attuale, della Toscana meridionale è di grande importanza sotto il punto di vista storico, economico e scientifico poiché ha prodotto numerosi giacimenti, alcuni dei quali sono stati coltivati dal tardo Calcolitico per i loro alti contenuti di metalli, ed è responsabile della carbonatazione delle rocce serpentinitiche che rappresentano un analogo naturale del sequestro mineralogico di anidride carbonica. L'attività idrotermale attuale fornisce il vapore caldo che è estratto nelle aree di Larderello-Travale e Monte Amiata, che rappresentano due delle più importanti aree geotermiche del mondo.
L'escursione prevede una visita al campo geotermico di Larderello, ad alcune interessanti emergenze giacimentologiche metallifere (lo skarn a Cu-Pb-Zn-Ag del Temperino, Campiglia Marittima; miniera di Cu del Pavone, Montecastelli) ed a spettacolari esempi naturali di sequestro di biossido di carbonio (miniera di magnesite di Malentrata; depositi superficiali di carbonati idrati di magnesio nell'area di Montecastelli). A questi aspetti squisitamente scientifici si accompagnerà la visita ad emergenze storiche ed archeologiche di grande rilevanza (la Rocca altomedievale di San Silvestro; la città medievale di Massa Marittima; le tombe etrusche nelle necropoli di Baratti a Populonia).

Parole chiave: Toscana meridionale, attività idrotermale, Etruschi, giacimenti minerari, campo geotermico di Larderello, sequestro mineralogico di CO_2

Abstract

This three-day geological field trip is focused on different aspects of the Southern Tuscany hydrothermal district, produced by the wide thermal anomaly and magmatism which affected the region in the post-collisional stage of the Apennine orogeny (from Late Miocene to Pleistocene). Past and present hydrothermal activity of southern Tuscany is of great importance from many historical, economic and scientific points of view as it produced numerous ore deposits, some of which were exploited for their metal contents since the late Chalcolithic, and it was also responsible for carbonation of serpentinites, that is a good example of natural

DOI: 10.3301/GFT.2015.02

carbon dioxide sequestration. Present-day hydrothermal activity supplies the hot steam exploited in the Larderello-Travale and Mt. Amiata areas, one of the most important geothermal districts of the world.
The excursion includes a visit to the Larderello geothermal field, as well as to some relevant ore deposits (the Cu-Pb-Zn-Ag skarn deposit of Temperino, Campiglia Marittima; the Cu mine of Pavone, Montecastelli), and to spectacular natural examples of carbon dioxide sequestration (magnesite mine of Malentrata; surface deposits of hydrated Mg-carbonates at Montecastelli). These exquisitely scientific aspects will be accompanied by a visit to historical and archaeological emergencies of great importance (the medieval towns of Rocca S. Silvestro and Massa Marittima; the Etruscan necropolis of Baratti-Populonia).

Keywords: Southern Tuscany, hydrothermal activity, Etruscan, ore deposits, Larderello geothermal field, CO_2 sequestration.

Program

The three-day field trip starts with the visit to one of the most important skarn localities of Tuscany, i.e., the classical Cu-Pb-Zn-Ag skarn deposit of Temperino mine (Campiglia Marittima: **Stops 1.1-1.3**), which has been exploited since pre-Etruscan times up to a few decades ago. In the nearby Archaeological Park of Baratti-Populonia (**Stops 1.4-1.6**) we shall visit the Etruscan Acropolis, Necropolis and beach slag deposit, where abundant metallurgical wastes dating at the Etruscan to Roman periods have been discharged. The 1st day will conclude in Massa Marittima, one of the medieval jewels of Tuscany. The ancient city name ("Massa Metallorum") clearly refers to the mining activity for silver and copper, which has been such a distinctive feature of the city's economic and social history.
The 2nd day starts with the visit (**Stops 2.1-2.4**) to the world-famous Larderello geothermal area. More than 100 years have passed since July 4th, 1904, when at Larderello, five light bulbs were lighted thanks to the conversion into electricity of the steam power stored in the Earth. Italy is currently one of the main producers of geothermal electricity in the world with over 700 MW. Indeed, geothermal power covers one fourth of the Tuscan region's energy needs. The field trip would comprise the visit to the Geothermal Museum at Larderello, the opening of the demonstrative geothermal well, a visit along the perimeter of "Nuova San Martino" power plant, where geothermal equipment are exposed, and finally a visit to the natural manifestations of Monterotondo Marittimo.
The field trip continues with the visit (**Stops 2.5-2.9**) to the magnesite deposit of Malentrata (Southern

DOI: 10.3301/GFT.2015.02

Tuscany), providing a spectacular example of natural analogues of carbon dioxide mineral sequestration. Carbon dioxide sequestration by mineral carbonation is a potentially attractive way to mitigate increasing global warming on the basis of industrial imitation of natural weathering processes. In the Malentrata deposit several carbonate-silica veins are hosted by silicified, carbonated and argillified serpentinites, embedded in pelite-carbonate formations.

On the 3rd day of the field trip, the program provides the visit (**Stops 3.1-3.3**) to the deposits of hydrated Mg-carbonates in the Montecastelli area. At Montecastelli site, a plurichilometric body of serpentinite, embedded in shales, has been deeply eroded by the Pavone River providing good geological exposures. The central portion of the serpentinite body (near the river) hosts a small copper ore deposit that was intermittently exploited during the 19th century up to 1869. The mining dump, as well as the main adit of the mine, is characterized by an intense carbonation with crusts of hydrated Mg-carbonates coating the serpentinite clasts. On the other side of the Pavone River, wide and incoherent escarpments of serpentinites show scattered white spots where the rock was superficially coated and veined by hydrated Mg-carbonates, near an alkaline spring water. The visits to the main tunnel of the mine, the mine dump and the escarpment of serpentinite permit to fully evaluate different extents of atmospheric CO_2 uptake (sequestration) through ongoing carbonation.

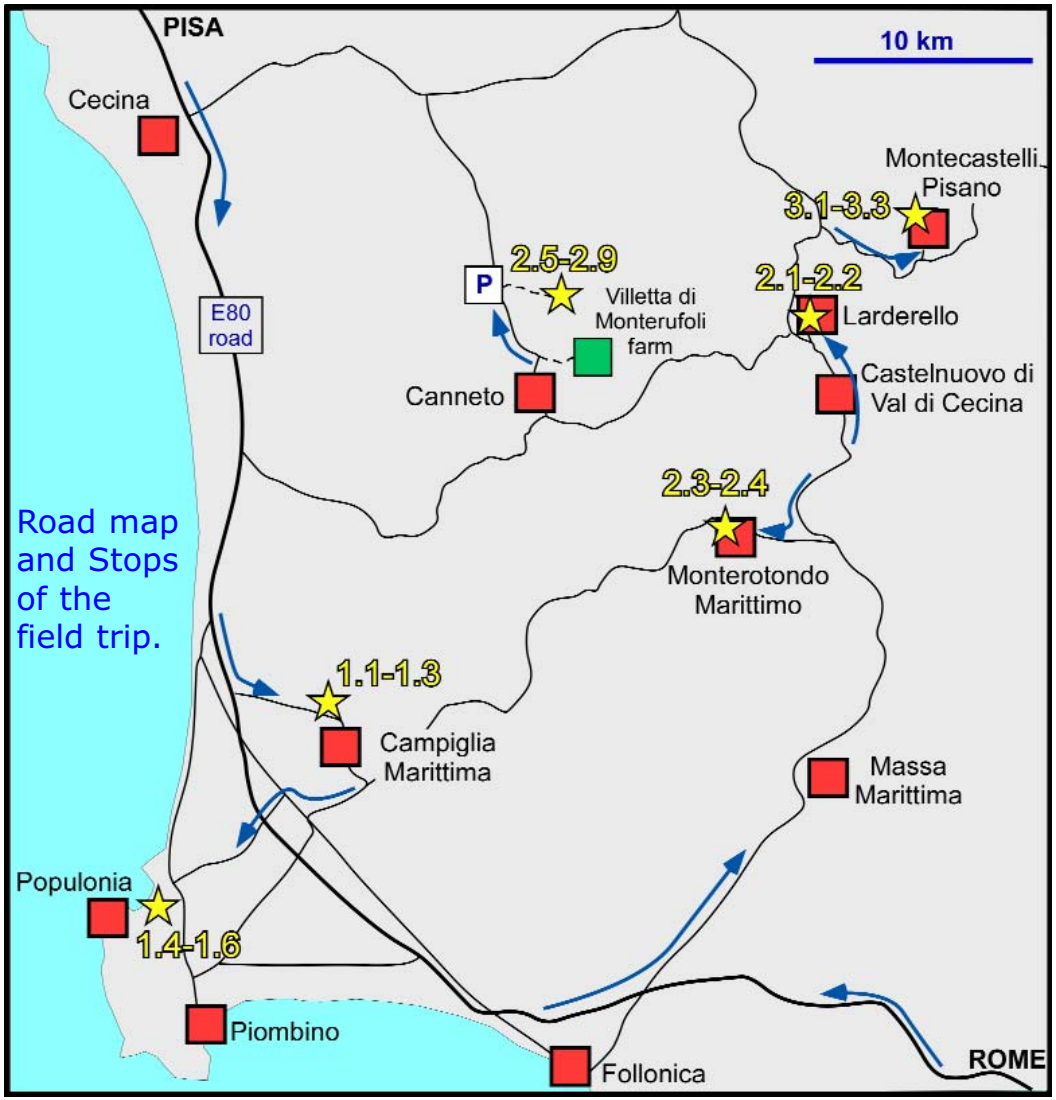

DOI: 10.3301/GFT.2015.02

Safety

Hat, hiking boots, sunglasses and sunscreen are strongly recommended. Depending on weather conditions, the path in the Montecastelli area could be slippery.

Hospital

Ospedale Sant'Andrea, Via Risorgimento 43 - 58024 Massa Marittima (Gr); Tel:+39 0566909111.

Emergency Contact Numbers

Medical Emergencies 118; Fire Department 115; State Police 113

Accomodation

A list of hotels located in the Northern area of Massa Marittima is available at the following website:
http://www.altamaremmaturismo.it/en/
In the Malentrata area, the farm resort very close to the outcrops is:
http://www.villettadimonterufoli.it/english.asp

Visit

For the visit to the Archaeological Mines Park of San Silvestro:
http://www.parchivaldicornia.it/...

For the visit to the Archaeological Park of Baratti and Populonia:
http://www.parchivaldicornia.it/...

For the visit to the Larderello Geothermal museum and the close areas:
http://www.museivaldicecina.it/...

For the visit (only guided tours) to the Montecastelli area, please contact the owner of the mine:
https://sites.google.com/...

DOI: 10.3301/GFT.2015.02

1. Introduction

A general introduction to the main topics of the field trip is described in the following pages. For more details please refer to the papers cited in the text and in the reference list. All the scheduled stops are described in detail at the end of the guide.

2. Geological setting of Southern Tuscany

2.1 Geological background

Southern Tuscany is structurally located in the inner part of the Northern Apennines (Fig. 1). Its structural setting is a consequence of two contrasting processes: the first is related to the convergence and collision (from Late Cretaceous to Early Miocene) of the Adria

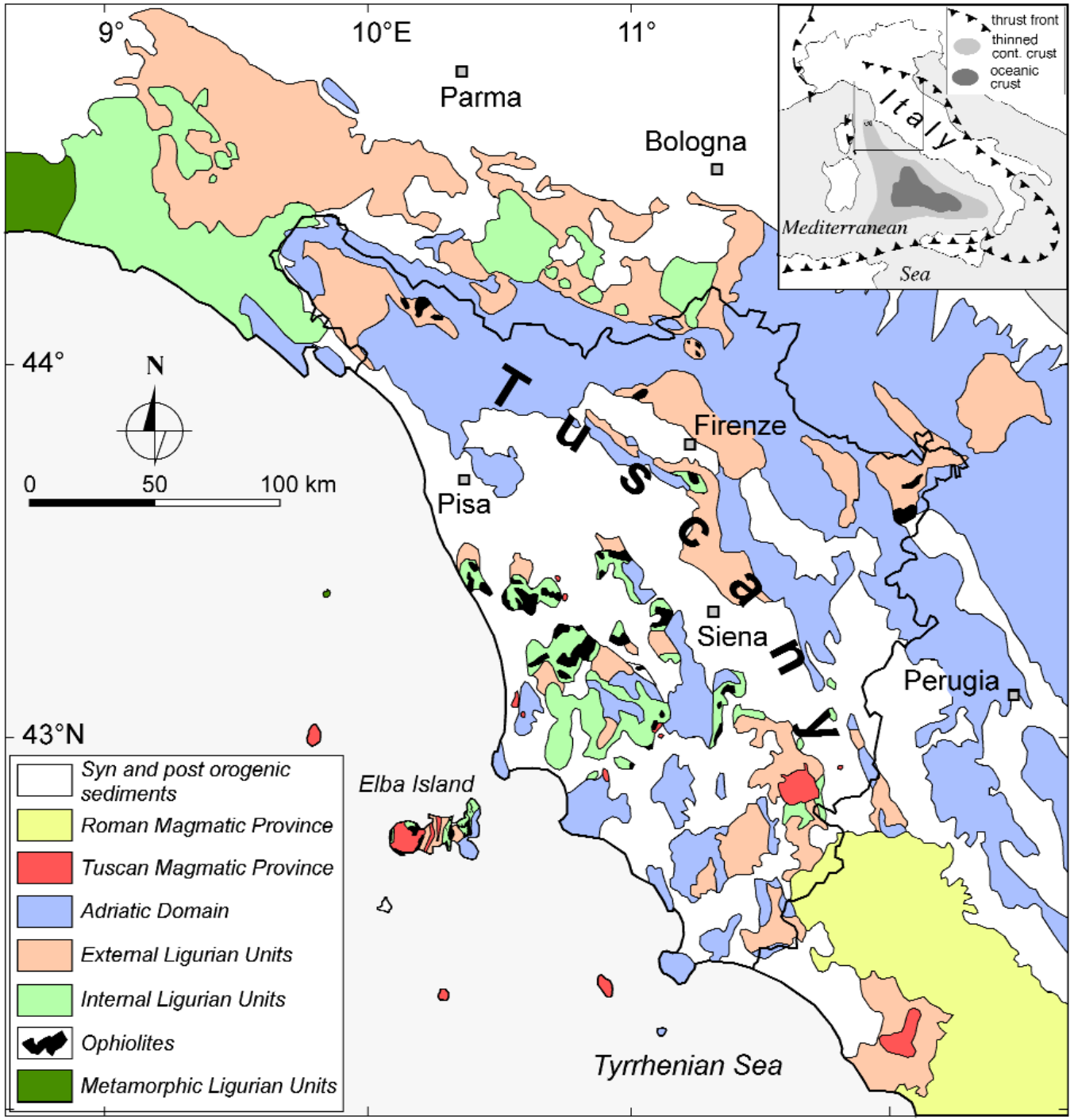

Fig. 1 - Schematic geological map of Tuscany, showing the tectonic units of the Northern Apennines (modified after Boschi et al., 2013).

DOI: 10.3301/GFT.2015.02

microplate and the European plate, represented by the Sardinia-Corsica Massif (Boccaletti et al., 1971; Elter, 1975; Molli, 2008); the second is related to extensional tectonics, which developed since the Early-Middle Miocene (Jolivet et al., 1990; Carmignani et al., 1994; Brunet et al., 2000). The Adria/European collision determined the stacking of tectonic units that were derived from the palaeogeographic domains of the inner Northern Apennines (Fig. 2).
These are, from the top:

(a) The Ligurian units, composed of remnants of Jurassic-Cretaceous oceanic crust and its Jurassic-Cretaceous sedimentary cover.

(b) The Subligurian units made up of arenaceous and calcareous turbidites of Late Cretaceous-Oligocene age. Ligurian and Subligurian units were thrust eastwards over the Tuscan domain during the Late Oligocene-Early Miocene.

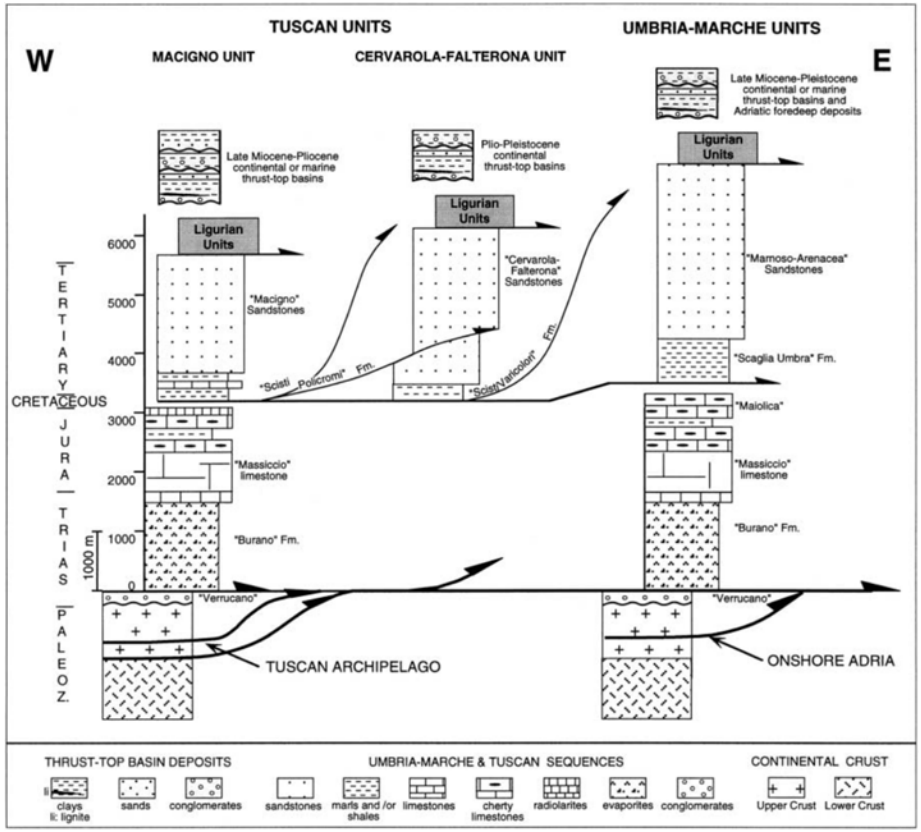

Fig. 2 - Schematic stratigraphic columns of the Tuscan and Umbria-Marche units (from Finetti et al., 2001).

(c) The Tuscan nappe that includes sedimentary rocks, ranging from Upper Triassic evaporites (Anidriti di Burano Fm.) to Jurassic-Cretaceous carbonates and Cretaceous-Lower Miocene marine clastic deposits (Scaglia Toscana group and Macigno Fm.). During the Early Miocene, the Tuscan nappe, already involved in duplex structures, detached along the Upper Triassic evaporite level to thrust over the external Tuscan domain and the inner part of the Umbria-Marche domain.

(d) The metamorphic Tuscan unit, belonging to the external Tuscan domain, consisting of greenschist-facies metamorphic rocks deriving from a Triassic-Oligocene sedimentary succession, similar to that one

DOI: 10.3301/GFT.2015.02

characterizing the inner Tuscan domain. The substratum of the Tuscan domain was involved in the collisional stage determining isoclinal folds and duplex structures. It is composed of a Palaeozoic metamorphic basement and its Triassic cover (Verrucano group; quartzites and phyllites).

(e) The Umbria-Marche domain consists of continental-margin deposits (Triassic to Late Miocene); this domain represents the external zone of the Northern Apennines, where a fold-and-thrust belt developed from the Middle Miocene (Brozzetti et al., 2002).

Kinematic indicators invariably show a NE direction of tectonic transport. During this contractional event, rocks belonging to the Verrucano group overthrust the external Tuscan succession, thus determining the metamorphic conditions in which deformation occurred (Liotta, 2002).

Tuscan succession is exposed in Larderello and Monte Amiata areas as isolated outcrops ("*Nuclei toscani*" Auct.) surrounded by the Ligurian units (Brogi et al., 2005). Tuscan succession is characterized by Oligocene-Early Miocene thrusts, developed under very low-metamorphic conditions. The Upper Triassic evaporites and the Cretaceous-Oligocene clayey marls (Scaglia Toscana group) acted as the main detachment horizons. After the emplacement of the tectonic units, extension produced lateral segmentation of the Tuscan succession and of the basal Verrucano group through low-angle normal faults. The tectonism that occurred in the Burdigalian-Messinian time span created tectonic depressions, where continental to marine Middle-Late Miocene sediments were deposited (Brogi & Liotta, 2008). The deeper structural levels within this framework, such as the Late Triassic evaporites, the Verrucano group and the palaeozoic phyllites, were directly overlain by the Ligurian units. A second extensional event was characterized by NW-SE high-angle normal faults that dissected the previous compressional and extensional structures. Marine sediments were deposited during Early-Middle Pliocene in these tectonic depressions. The main tectonic depressions are dissected by SW-NE transfer zones. The present crustal and lithospheric thicknesses, ranging between 22-24 km and 30-40 km, respectively (Locardi & Nicolich, 1988), are a clear evidence of this extensional process. An alternative view of the structural evolution of the Northern Apennines suggests a basically continuous (Bonini et al., 1999; Bonini et al., 2001; Finetti et al., 2001) or pulsing (Bonini & Sani, 2002) collisional process, active from the Cretaceous to Pliocene-Pleistocene times (Finetti, 2006).

DOI: 10.3301/GFT.2015.02

2.2 Neogene-Quaternary magmatism

The Tuscan magmatic province consists of a series of intrusive and extrusive centres scattered through southern Tuscany and the Tuscan Archipelago. The acid centres of the Tolfa-Cerveteri-Manziana area, northwest of Rome, are also traditionally included within the Tuscan province. Fig. 3 gives an overview of locations, ages and main compositional characteristics of the Tuscan magmatism. Magmatic rocks consist of plutons, stocks, laccoliths, sills, dykes, necks, lava flows and domes, and of the large volcanic edifices of Monte Amiata, Monti Cimini and Capraia Island. Ages range from 14 Ma to 0.2 Ma, and show a tendency to decrease from west to east (Serri et al., 1993). The Tuscan magmatic province is very complex and includes crustal anatectic acid peraluminous rhyolites and granites, and a wide range of mafic to intermediate magmas. These vary among high-potassium calcalkaline, shoshonitic, potassic alkaline and ultrapotassic lamproitic rocks. Mixing appears to have affected both mafic and acid rocks; the latter bear textural (mafic enclaves, xenocrysts, etc.) and geochemical evidence of mingling and mixing with various types of mantle-derived calcalkaline to potassic melts.

Fig. 3 - Location map for intrusive and volcanic rocks of the Tuscan Magmatic Province (modified after Dini et al., 2005).

DOI: 10.3301/GFT.2015.02

The thermal anomaly related to this prolonged magmatic activity drove intense deep convective fluid circulation that formed mineralization and ore deposits, some of which were extensively mined in the past. The anomaly is now responsible for the active geothermal systems of southern Tuscany (i.e., Larderello–Travale and Mt Amiata geothermal fields) (Tanelli, 1983; Lattanzi et al., 1994; Lattanzi, 1999; Dini et al., 2005, and references therein). Presently, southern Tuscany is characterized by high heat flow that averages 120 mW/m^2, with local peaks up to 1000 mW/m^2 in the Larderello geothermal area.

2.3 Ore geology: state of the art

For about 30 centuries, Tuscany has been one of the most important mining regions of Italy and has produced a large variety of resources, including pyrite, iron, base metals, geothermal steam and several industrial minerals and rocks (Lattanzi et al. 1994, and references therein). Today, the mining industry in Tuscany is limited to industrial minerals (feldspars, halite), ornamental stones, and building materials. The Tuscan metallogenic province includes (Fig. 4): the Fe oxide deposits of Elba Island, the pyrite (± barite ± Fe oxides) deposits of Southern Tuscany and Apuane Alps, the base- and precious-metals deposits of the "Colline Metallifere" district (Southern Tuscany), the Hg deposits of the Monte Amiata area, and the Sb deposits of the Capalbio-Monti Romani belt (Cipriani & Tanelli, 1983; Tanelli, 1983). The newest addition to the metallogenic framework of Tuscany is the discovery in the mid '80s of "Carlin-type" epithermal gold mineralization. Most of the Au prospects, of limited economic importance, are closely related to Sb deposits (Lattanzi, 1999).

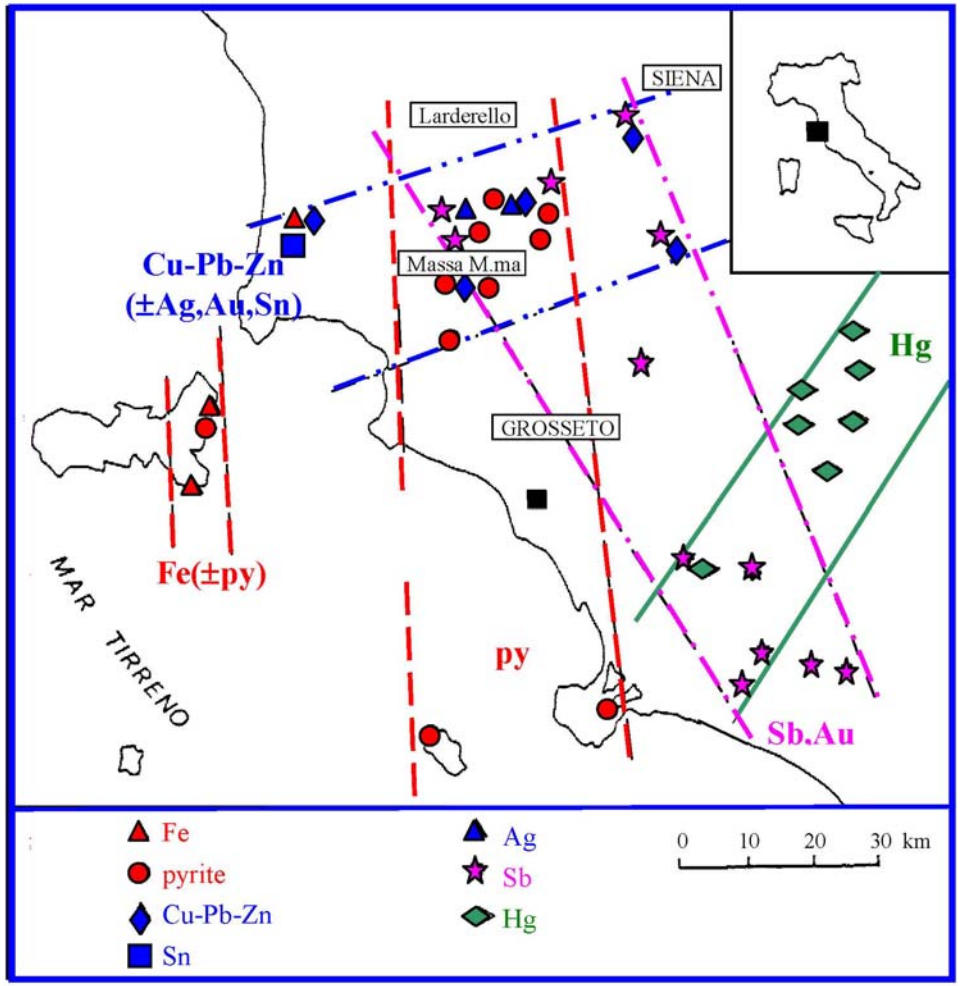

Fig. 4 - Distribution of main ore types of Southern Tuscany.

DOI: 10.3301/GFT.2015.02

A number of different skarn deposits occur in the southwestern portion of the Tuscan metallogenic province (Fig. 5): they include calcic iron skarns (Capo Calamita, Ginevro, Sassi Neri and Ortano at Elba Island; Niccioleta in the Colline Metallifere district) and lead-zinc (-copper) skarns (Temperino mine in the Campiglia M.ma district; Serrabottini near Massa Marittima). These deposits have been studied by several authors (for details see Benvenuti et al., 2004, and reference therein). According to Tanelli (1977), the Tuscan skarn deposits formed by replacement of Triassic carbonate rocks of the Tuscan unit by metasomatic processes triggered by the emplacement at shallow crustal levels of the Neogene magmatic rocks of the Tuscan Province. Skarn bodies may be in contact with magmatic rocks (e.g., at Temperino mine), or at various distances from them (Niccioleta, Ortano). The presence of magmatic rocks in close proximity to skarn bodies does not necessarily imply a genetic link: at Ginevro, for instance, aplitic dikes appear to predate skarn formation. Source(s) of elements for Tuscan skarn deposits are still poorly constrained. Corsini et al. (1980) maintain that isotopic composition of sulfur from the Temperino skarn deposit is compatible with a local, non-magmatic source (i.e., sulfides/sulfates from Permo-Triassic country rocks). On the other hand, the uniform lead isotope composition of pyrite and galena from the Campiglia Marittima and Niccioleta deposits may reflect contribution of lead (and other metals?) from Neogene-Quaternary magmatic rocks (Lattanzi et al., 1994).

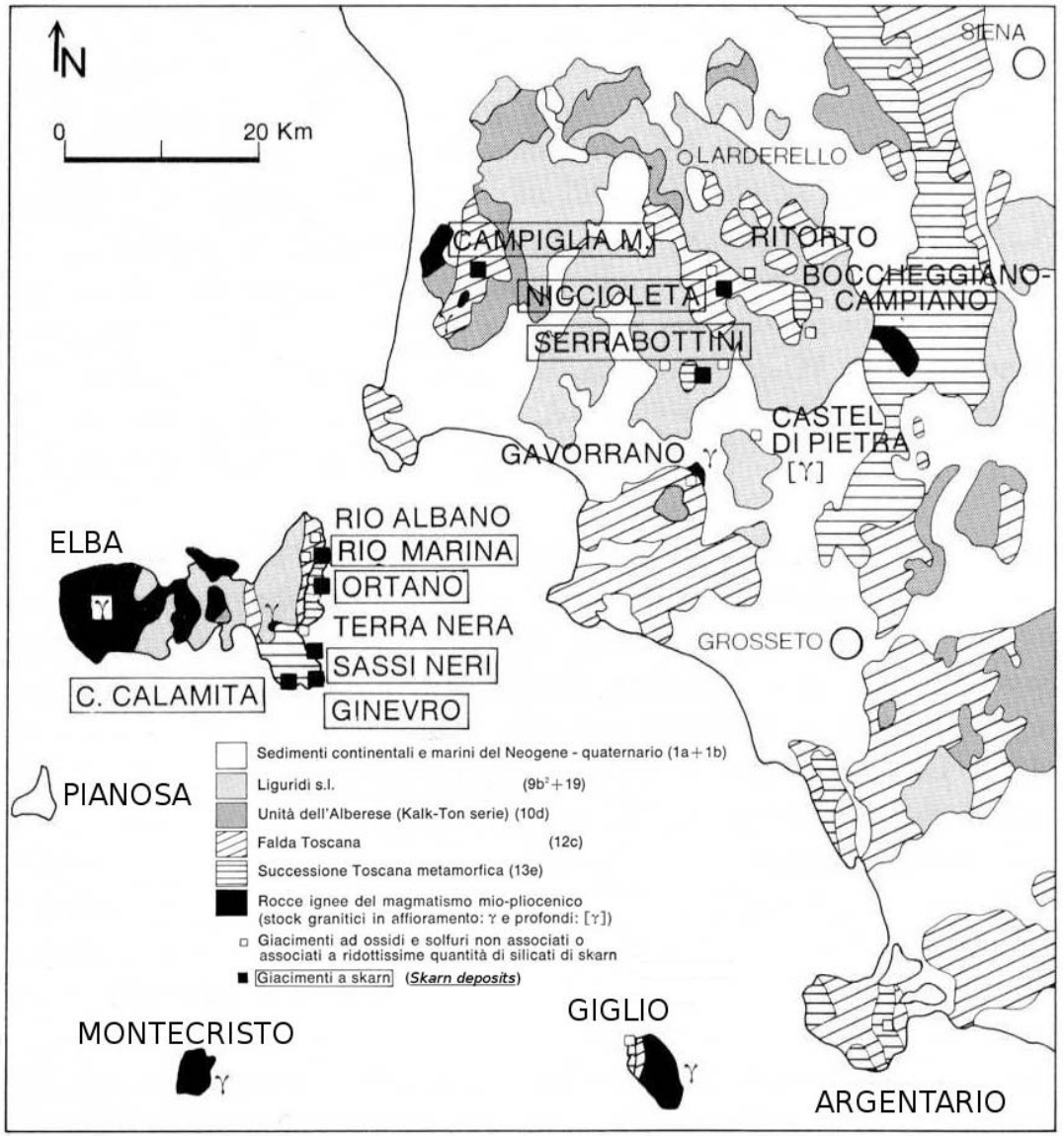

Fig. 5 - Location of Tuscan skarn deposits (after Tanelli, 1977).

DOI: 10.3301/GFT.2015.02

3. Campiglia Marittima

3.1 Geological framework

The ore-deposits of Valle del Temperino (for details see Benvenuti et al., 2004 and references therein) are located 2 km north of Campiglia Marittima village (Livorno) (Fig. 6). Several formations of the Tuscan unit sequence crop out in this area, which can be described as a N-S trending wedge-shaped horst ("Campiglia ridge") bordered by high angle N-S and NW-SE trending faults on the western and eastern margins, respectively (Acocella et al., 2000, and references therein). The Campiglia ridge is made up of several formations, which belong to the Tuscan unit, ranging from Liassic massive limestone (Calcare Massiccio) to Oligocene turbiditic sandstone (Macigno). The Tuscan unit formations are tectonically overthrust by the allochthonous "Ligurian" and "Subligurians" units, consisting of calcareous, marly and shaly turbidites of Upper Jurassic to Eocene age. The latter sequences are then unconformably overlain by Quaternary sediments, consisting of

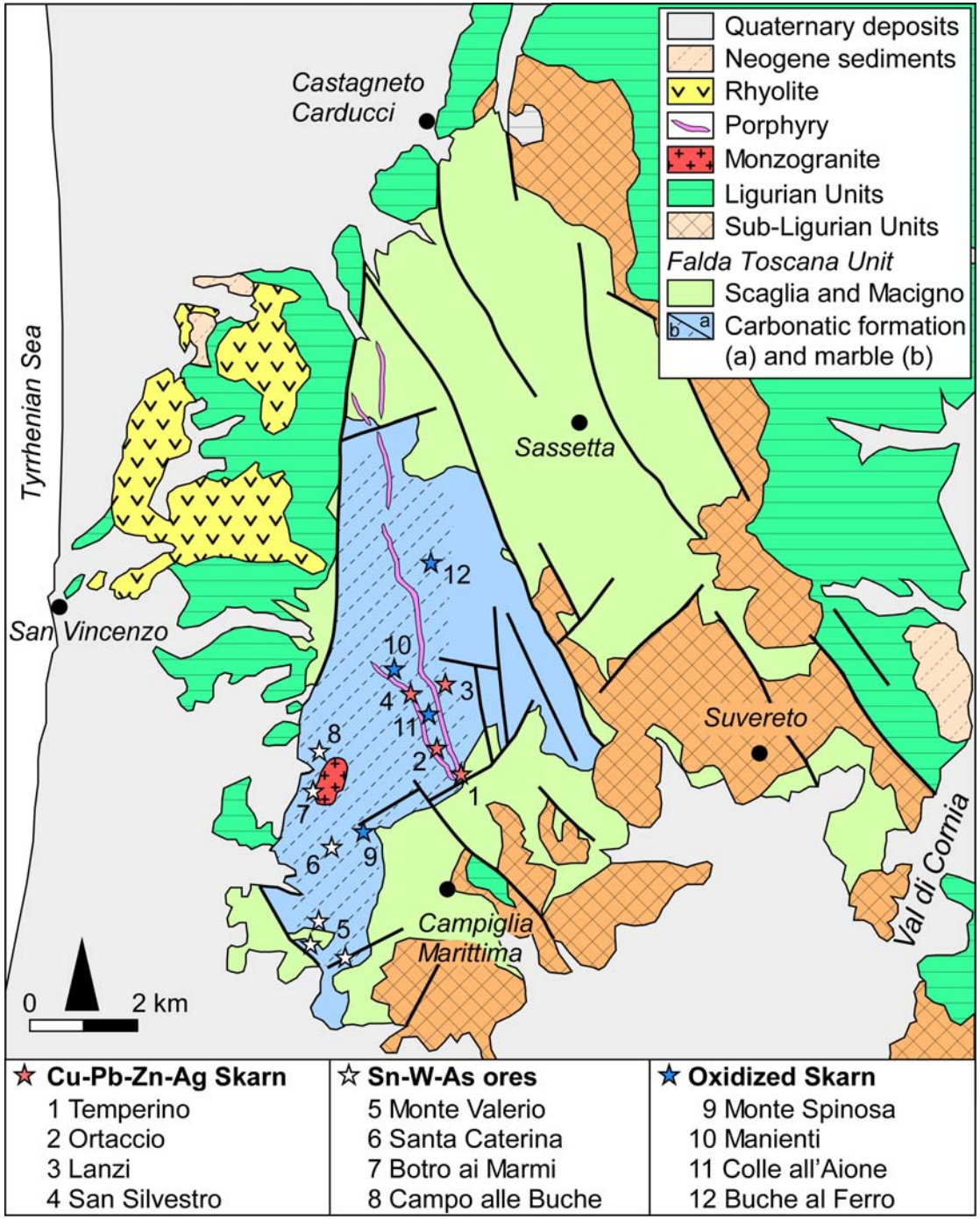

Fig. 6 - Geological sketch map of the Campigliese area showing the distribution of magmatic rocks and ore deposits (modified after Da Mommio et al., 2010).

DOI: 10.3301/GFT.2015.02

alluvium, fluvial and beach deposits. Magmatic activity strongly affected the Campiglia Marittima area in Late Miocene-Lower Pliocene time. Several kinds of both plutonic and volcanic bodies were emplaced, mostly with an overall acid to intermediate composition. The earliest emplaced magmatic body, exposed in the Campiglia Marittima area, is the "granito di Botro ai Marmi", dated at 5.7 Ma. Most chemical data for the Botro ai Marmi stock plot in the syenogranite field; some rocks encountered in drill holes have granodioritic compositions.

The contact with the host rocks (mainly represented by the Calcare Massiccio Formation) is marked by a N-S trending thermo-metamorphic aureole, approximately 5 km long, 1.5 km wide and 300 m thick. The dominant calcite-tremolite-diopside skarn assemblage suggests emplacement conditions characterized by temperatures ≤500°C and pressures ≤1 kb.

Between 5 and 4 Ma, several swarms of porphyry dikes intruded the eastern part of the Campiglia area. Three types of dikes can be distinguished: quartz-monzonite, monzonitic (also called "green porphyry"), and potassic alkaline porphyries ("yellow porphyry"). The "green porphyry" ("porfido verde"), also known as "augitic porphyry", represents a diopside-bearing mafic differentiate, with intermediate silica contents, high Mg#, high Ni and Cr, and relatively low Al_2O_3 and Na_2O contents. All the fertile skarn bodies exploited in the Campiglia Marittima district are closely related to the "green porphyry". The "yellow porphyry" (Fig. 7) and the quartz-monzonitic porphyry are acidic in composition (i.e., very similar to the "Botro ai Marmi" intrusion), and display

Fig. 7 - Road cut showing an acidic porphyry dyke hosted by marble.

DOI: 10.3301/GFT.2015.02

a strong potassic alteration. The extensive degree of alteration of the Campiglia porphyry dikes makes it difficult to establish whether the quartz-monzonite and "yellow" porphyries are both evolved products from the "green porphyry" or represent independent magmas. To the north of the Botro ai Marmi intrusion, the San Vincenzo rhyolites were erupted at about 4.4 Ma. They probably resulted from mixing between a crustal "anatectic" melt and minor but significant amounts of subcrustal, mafic-intermediate melt of possible calcalkaline affinity. According to Acocella et al. (2000) a releasing bend formed during right-lateral strike-slip faulting on the western margin of the Campiglia ridge favoured the emplacement of the Botro ai Marmi intrusion. Pliocene extensional tectonics reactivated the strike-slip lineaments and probably controlled the emplacement of the Campiglia dikes as well as extrusion of the San Vincenzo rhyolites.

3.2 Ore geology and mineralogy

The Campiglia Marittima area has long been known for Cu-Pb-Zn (±Fe,Ag,Sn) skarn deposits (Corsini et al., 1980), which have been exploited since pre-Etruscan times up to a few decades ago. In the "Relazione Generale Mineraria" published by the Direzione Generale delle Miniere (1975), the reserves in the district were estimated to be in the order of 250,000 tons at 4% Zn, 2% Pb, 0.8-1% Cu, and 20-70 g/t Ag (with inferred reserves of about 700,000 tons: data from Cipriani & Tanelli, 1983). These deposits lie 1-2 km E and NE of the Botro ai Marmi stock, in strict spatial association with (4-5 Ma?) porphyry dikes; only minor skarn occurs in the immediate proximity of the intrusion (Fig. 6). A number of industrial minerals and rocks are also mined in the district. The skarn-sulfide deposits of Campiglia Marittima can be subdivided between those outcropping in the area of Valle dei Lanzi (predominant Pb-Zn, mostly with galena>sphalerite: e.g., Cava del Piombo) and the Cu (Pb-Zn) orebodies from Valle del Temperino (Fig. 6). Both skarn complexes are completely enclosed in white marbles, derived from contact metamorphism of the liassic Calcare Massiccio by the Botro ai Marmi and/or related intrusions. However, the skarn ores of the Campiglia area are not related to the Botro ai Marmi granite stock, but instead to the more extensive, though not outcropping, parent intrusion of the network of yellow and green porphyry dikes.

The Valle del Temperino deposits occur in an area of about 0.4 km^2 where they have been mined, even if on a small scale, from the surface at 250 m down to 50 m elevation. According to Corsini et al. (1980), the skarn complex of Valle del Temperino consists of two west-northwest-east-southeast elongated masses, which appear to be strictly associated with the green porphyry (Figs. 8 and 9).

DOI: 10.3301/GFT.2015.02

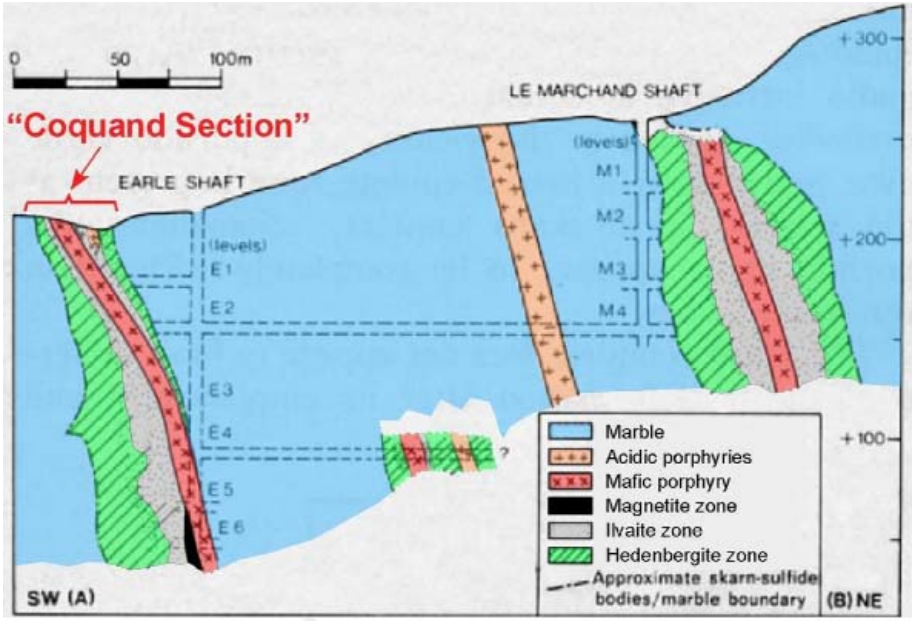

Fig. 8 - Interpretive section of Temperino skarn deposit (modified after Corsini et al, 1980).

Fig. 9 - A small dyke of mafic porphyry crosscutting the skarn at Temperino mine.

The latter seems to be completely embedded in the orebodies, and is crossed by small mineralized veinlets bearing the calcite-epidote-quartz, k-mica and k-feldspar association. The skarn complex consists of manganoan ilvaite (up to 9.5 wt % MnO), hedenbergite-johannsenite pyroxene, quartz, calcite, epidote, and traces of andradite, rhodonite, fluorite and ferroactinolite. End member johannsenite of the solid solution hedenbergite-johannsenite series occurs near Rocca San Silvestro (Fig. 10).

Epidote is particularly abundant in association with the yellow porphyry. Most common ore minerals include chalcopyrite, pyrrhotite, sphalerite, galena, pyrite, magnetite, hematite (traces), arsenopyrite, bismuthinite, mackinawite and galenobismuthinite (Tanelli, 1977). Supergene minerals are only present in the upper levels of the mines and in small gossans.

DOI: 10.3301/GFT.2015.02

Fig. 10 - Textural and mineralogical variations of the Temperino skarn.

The ilvaite zone occurs directly at the contact with the green porphyry: the typical ore assemblage consists of chalcopyrite and pyrrhotite, with minor magnetite, pyrite and Fe-rich sphalerite (Fig. 11). Beautiful crystals of ilvaite have been found in pockets, associated with quartz (Fig. 12). Magnetite occurs here generally only as pseudomorphs after lamellar hematite.

According to Corsini et al. (1980), three zones of mineralization, with prevailing magnetite, ilvaite and hedenbergite, occur between the green porphyry and the metamorphosed liassic limestone (Fig. 8). The magnetite zone occurs only in the deepest levels of the skarn-sulfide deposit; it consists of a 1m thick, massive aggregate of coarse subhedral crystals of magnetite with quartz and traces of pyrite, pyrrhotite and chalcopyrite.

Fig. 11 - Pyrite, chalcopyrite and pyrrhotite ore in hedenbergite-ilvaite skarn; Temperino mine.

DOI: 10.3301/GFT.2015.02

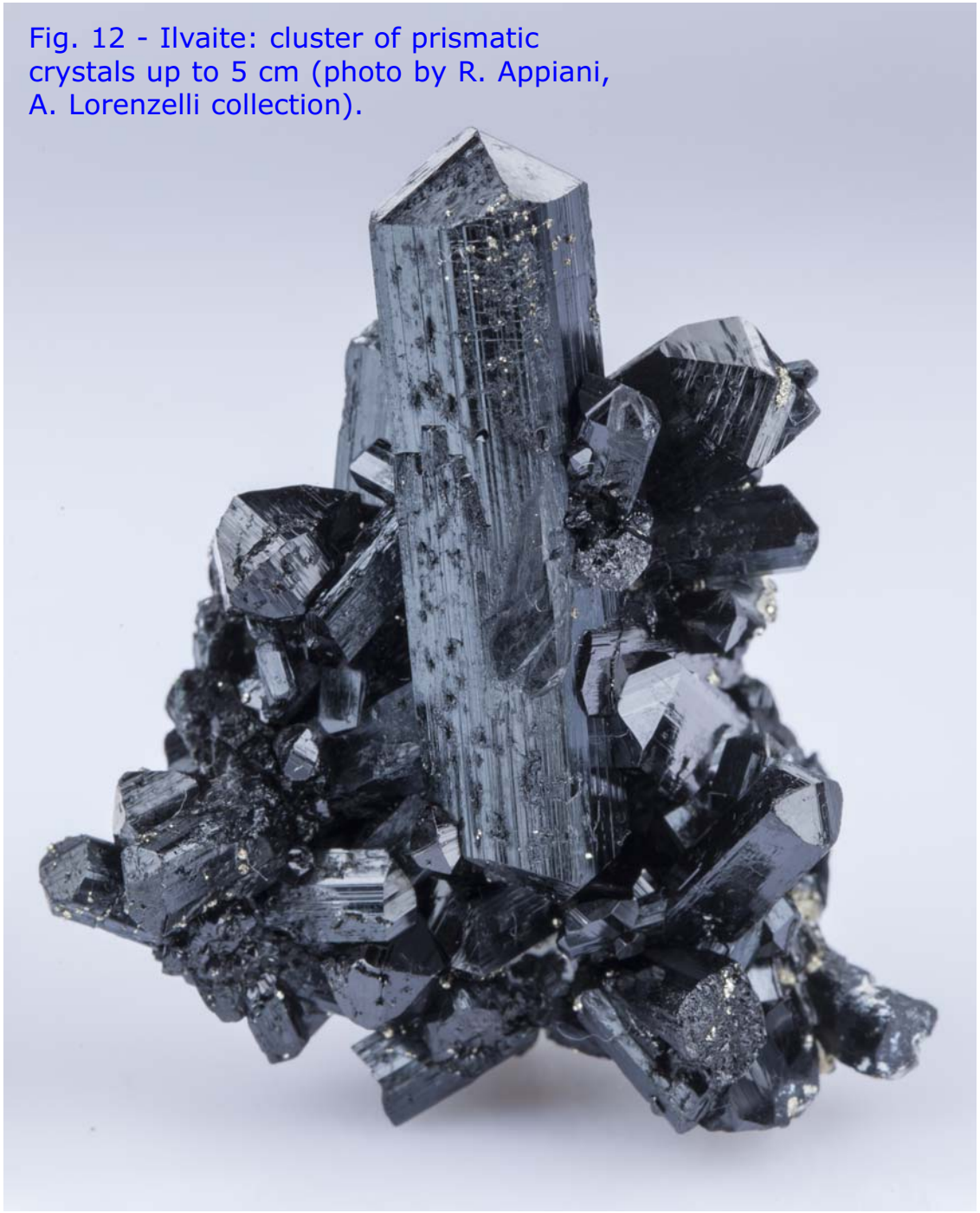

Fig. 12 - Ilvaite: cluster of prismatic crystals up to 5 cm (photo by R. Appiani, A. Lorenzelli collection).

Pyrrhotite seems to be one of the earliest mineral phases, and is replaced by the other sulfides, as well as by magnetite. Sphalerite is quite late in the sulfide paragenesis and has an iron content ranging from 17.2 to 21.3 mole % FeS.

The hedenbergite zone is characterized both by well-developed, radiating and concentric aggregates of clinopyroxene with long fibers (Fig. 10), and by marbles corroded and enclosed within the skarn bodies, showing that the skarn minerals were growing toward the limestone side of the complex. An increase in the Mn content of the clinopyroxene has been recorded, from manganoan hedenbergite (2.6 wt % MnO) in the core of the skarn body, to quite pure johannsenite (27.6 wt % MnO) at the contact with the marbles. The ore assemblage consists of chalcopyrite, pyrite, iron-poor sphalerite and finally of galena, with only minor lamellar magnetite and hematite remnants. Gangue minerals are quartz, calcite, epidote, minor ilvaite and andradite.

The ore mineral deposition at Valle del Temperino (Corsini et al., 1980) appears to have been a multi-stage process, which can be divided into three main stages. The first corresponds to the deposition of iron oxides,

DOI: 10.3301/GFT.2015.02

mainly magnetite. Temporary changes of physicochemical parameters allowed hematite to form at first in the outer zones, and to be quickly reduced again to magnetite before the second stage took place. In the second stage, a first pyrite generation (I) was formed, then pyrrhotite, and then a second generation of pyrite (II). During this second stage, crystallization of ilvaite and hedenbergite took place. The third stage brought the deposition of Cu-Pb-Zn sulfides. Chalcopyrite was the first to precipitate, followed by sphalerite and finally by galena. The banded rocks contain ilvaite, hedenbergite, chalcopyrite and pyrrhotite. The replacement of ilvaite by hedenbergite and vice versa indicates that these two minerals overlap. As mentioned above, absolute age measurements and the geological reconstruction of the Campiglia area indicate a Pliocene age for the formation of the Valle del Temperino skarn-sulfide complex. Regional stratigraphy indicates that the maximum thickness of the sediments over the Calcare Massiccio during the Pliocene was about 1500 to 2000 meters.

Based on mineralogy and S-isotope data, Corsini et al. (1980) estimated that sulfide deposition at Valle del Temperino occurred during decreasing temperatures from about 400 °C to 250 °C. They also suggest that sources of sulfur for these deposits may have been sulfate ($\delta^{34}S$ = 12 to 14.6 ‰) and/or sulfide ($\delta^{34}S$ = 5 to 12 ‰) associated with the Paleozoic/Mesozoic basement formations (namely, the "Filladi di Boccheggiano" and/or "Calcare Cavernoso"), both of them containing evaporites. A different type of mineralization, consisting of layered iron minerals (mainly goethite, hematite, siderite ± marcasite, chlorite) and sparry calcite crystals, with apparently karstic features, occurs in the old mining locality of Campo alle Buche. This deposit has been exploited by both underground and open pit mine workings in the 19th-20th centuries, although there is evidence of older (Etruscan?) mining activity. According to Bertolani (1958), skarn sulfide mineralization occurs at some depth below the calcite-iron oxyhydroxide mineralization. The Campo alle Buche deposit has been regarded as a gossan-type ore by early authors; alternatively, it can be considered the product of late-stage, low-temperature hydrothermal fluids still related to the Pliocene magmatism which was responsible of the emplacement of the Cu-Pb-Zn (Ag,Sn) skarn bodies of the Campiglia Marittima district (Tanelli, 1977).

DOI: 10.3301/GFT.2015.02

4. Populonia in the framework of "Etruria Mineraria"

Mineral resources of Tuscany have long been exploited, at least since Chalcolithic times, and were very important in the development of Etruscan and Roman civilizations; in medieval times, numerous city-states derived important revenues from mining exploitation and metal production. The same applies, on a larger scale, after the unification of Tuscany under the Medici government in the 16th century. Even in more recent times some mineral resources, such as the Elba iron ores, were successfully exploited (Cipriani & Tanelli, 1983; Mascaro et al., 1991; Benvenuti et al., 2012).

The western portion of ancient Etruria lying between Volterra to the north and Monti della Tolfa to the south is known in the archaeological literature as "Etruria Mineraria" because of the abundance of ore resources (incl. iron, copper, tin, etc., Fig. 13). The Etruscan town of Populonia played a key role in the production and trade of metals (especially,

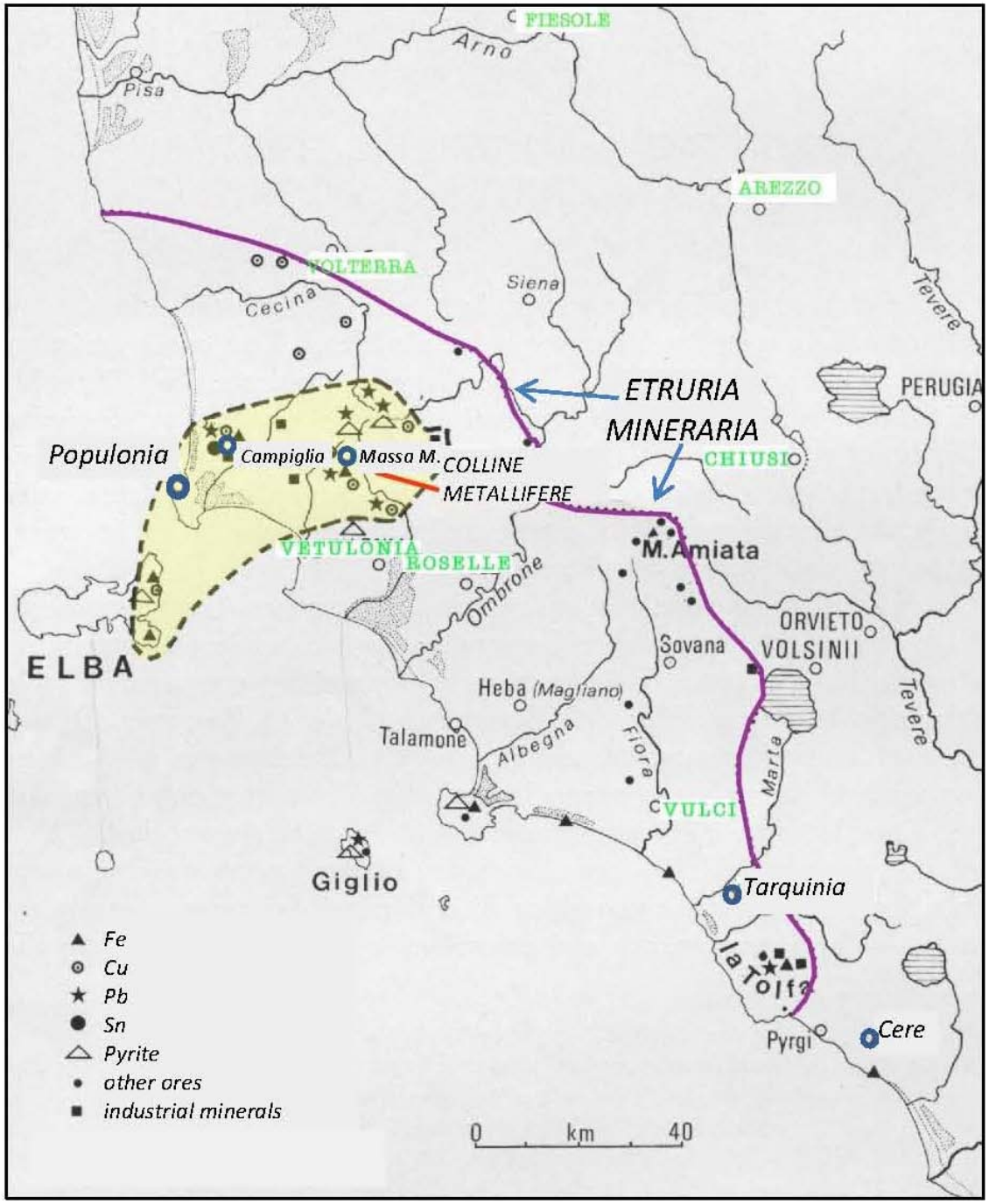

Fig. 13 – Sketch map of "Etruria Mineraria" with location of the main ore deposits, part of which exploited by the Etruscans and, later, by the Romans (modified after Sestini, 1981).

DOI: 10.3301/GFT.2015.02

but not exclusively, iron) in the Mediterranean area during the 1st Millennium BC. Populonia was an important iron production centre from the 6th century BC up to the 1st century AD (Corretti & Benvenuti, 2001). Such a prominent role was mainly due to its strategic location, midway between the large iron deposits of eastern Elba Island and the polymetallic Cu-Pb-Zn-Fe-Ag-Sn ores of the Campiglia Marittima area. The huge heaps of slags (probably in excess of 40,000 m^3), discharged along the foreshore of the Gulf of Baratti, could document a total iron production of some thousands tonnes of iron bloom (up to half a million tonnes according to Voss, 1988). In the last twenty years, a detailed research program in the Baratti area at Populonia (Fig. 14) has been undertaken, with the aim of establishing the types and extent of metallurgical activities, as well as the provenance of smelted ores in the 1st Millennium BC. The main results so far obtained have been published elsewhere (Benvenuti et al., 2000, 2002, 2003a, b; Cartocci et al., 2007; Chiarantini et al., 2009a, 2009b, with references), and will be briefly summarized here. Recent fieldwork in the Baratti area and detailed stratigraphic, mineralogical, textural, and chemical analyses of the metallurgical wastes still partly preserved gave some interesting results which can be briefly summarized as it follows:

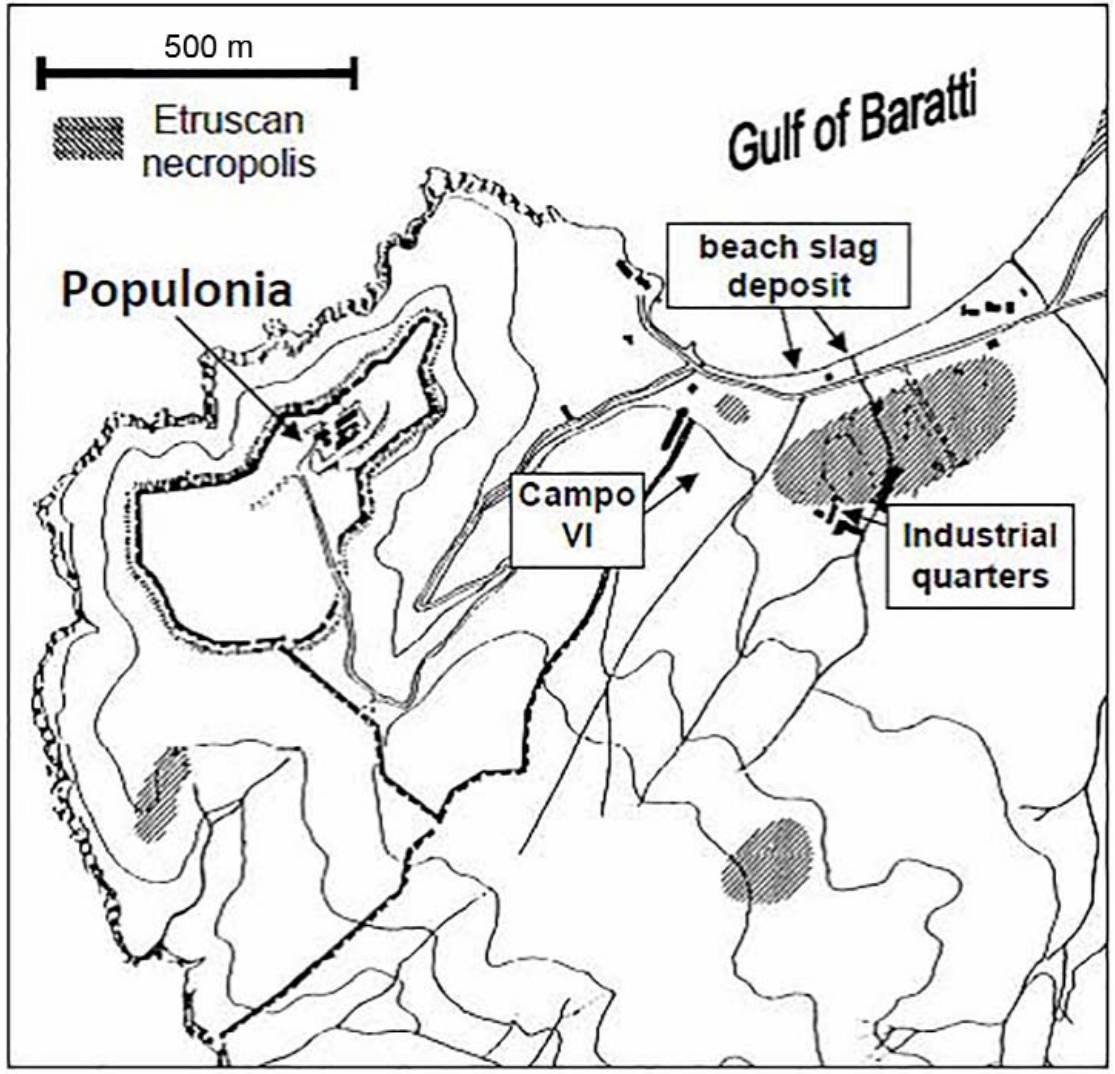

Fig. 14 - Sketch map of the Populonia-Baratti area with location of sites mentioned in the text (modified after Benvenuti et al., 2000).

• excavations carried out since 2002 in the so-called "beach slag deposit" (Fig. 14) - probably located some 100 m ahead from the shoreline

DOI: 10.3301/GFT.2015.02

in Etruscan times - indicate an earlier copper metallurgy, radiocarbon dated to the 9th–8th centuries BC (Cartocci et al., 2007), followed by predominant iron production between the 7th century and the 2nd century BC in agreement with archaeological and historical documents;

• characterization, output estimates and direct dating of primary iron production at Populonia are hindered by intense reworking of slag deposits during the past century for re-use in siderurgic plants at Piombino. Although abundant fragments of smelting furnaces can be found among metallurgical debris, any attempt to reconstruct their technological design is based upon assumptions (Benvenuti et al., 2003b) and preliminary archaeometallurgical experiments;

• smithing/reheating hearths employed for iron working, made with local sandstone blocks and bricks lined with clay, have been found in upper portion of the S. Cerbone deposit; they can be mostly dated to the V-II century BC;

• there is also evidence of local bronze production (dating to the 3rd century BC or earlier), particularly in the "Campo VI" site, adjacent to the ancient defensive walls of Etruscan Popluna (Populonia; Fig. 13);

• trace element geochemistry (e.g., tin+tungsten anomalous content of iron slags) and Pb-isotope analyses both indicate that iron was mainly from eastern hematite-rich ores from Elba Island (Benvenuti et al., 2013), whereas the most likely source area for smelted copper (and tin?) was the nearby Cu–Pb–Zn–Fe–Sn ore district of Campiglia Marittima (Fig. 14), and particularly the Cu-Zn,Pb,Ag skarn sulphide deposits of Valle del Temperino–Valle Lanzi (Chiarantini et al., 2009b).

DOI: 10.3301/GFT.2015.02

5. The Larderello-Travale geothermal field

Larderello-Travale is one of the few superheated steam geothermal systems in the world, i.e., with a reservoir pressure that is much lower than the hydrostatic gradient. This peculiarity is the consequence of a natural evolution of the system from the initial water-phase to the current steam phase. Larderello and Travale fields, initially considered separate, turned out to belong to the same geothermal system when drilling was extended to 3-4 km depth. Temperature and pressure distribution shows that the whole system is steam dominated with some 50°C of superheating (Barelli et al., 1995, 2000) (Fig. 15). At 3000 m depth, the 300°C isotherm contour includes both areas, with a total extension of about 400 km^2. The present installed capacity is 594.5 MW, with 22 units in Larderello, and 200 MW with 8 units in operation in Travale field.

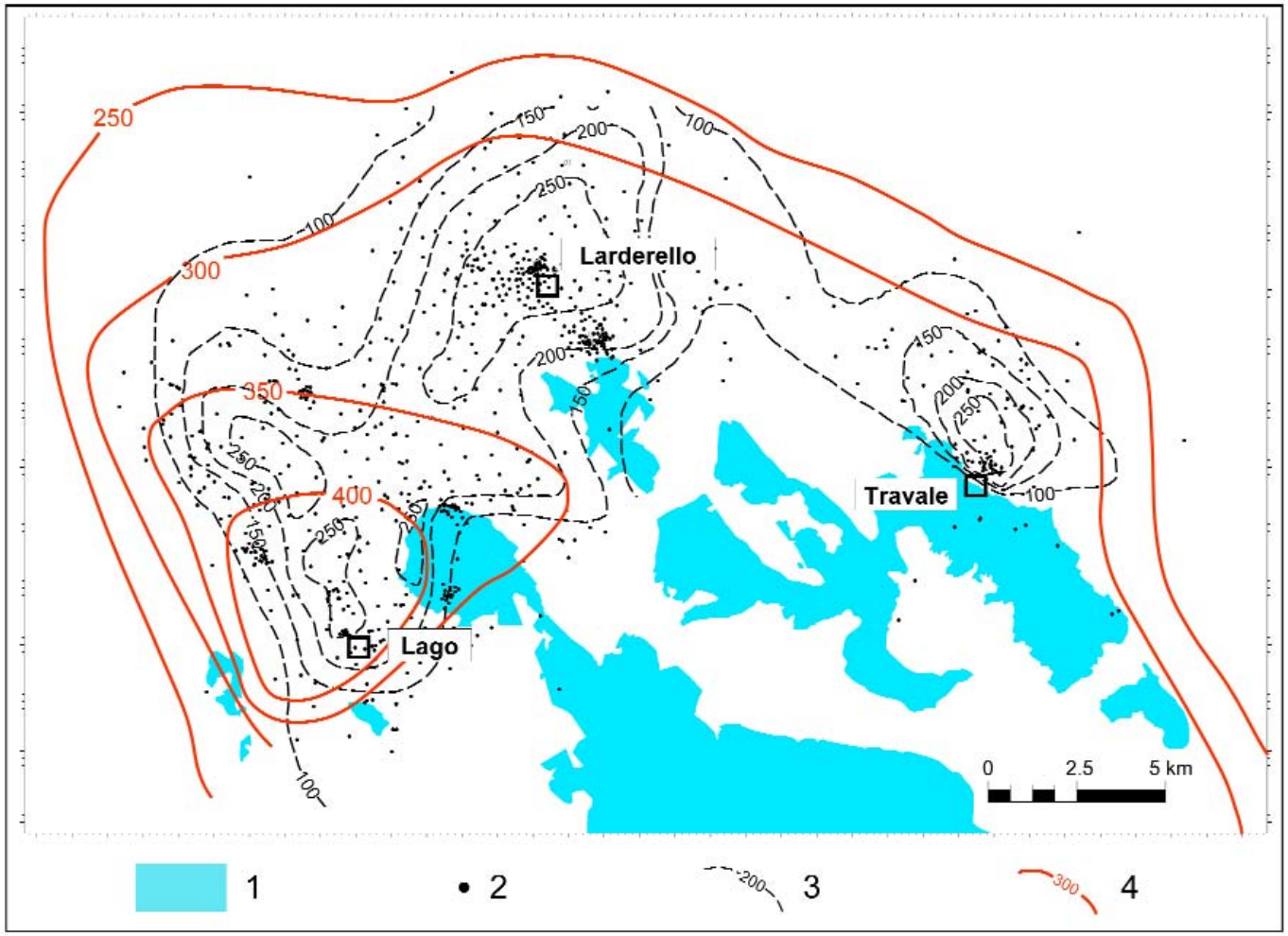

Fig. 15 - Temperature distribution in the Larderello–Travale geothermal field. (1) Outcrops of permeable formations; (2) geothermal wells; (3) temperature at the top of the shallow reservoir; (4) temperature at 3000m b.s.l. Modified from Cappetti et al. (2005).

DOI: 10.3301/GFT.2015.02

5.1 Geothermal development in Tuscany

Italy is the country where geothermal energy was first exploited for industrial purposes, and it is still one of the leading producers of geothermal energy. Natural geothermal manifestations as "lagoni" (small pools or craters where steam mixed with gas cause the water to bubble up) and "soffioni" (jets of steam, which can be violent) originally occurred in several localities (Larderello, Montecerboli, Castelnuovo Val di Cecina, Sasso Pisano, Serrazzano, Monterotondo Marittimo, Lagoni Rossi, Travale, etc.) lying between Pomarance and Massa Marittima. Temperatures reached 100-200°C, with pressures of several atmospheres. The first evidence of an intentional and organized use of geothermal phenomena came from the discovery of a large public bathing complex in the Sasso Pisano area (3rd century BC). However, the earliest scientific and economic appraisal of the "lagoni" area is due to Uberto Francesco Hoefer, director of the grand duchy's pharmacies, who, in 1777, demonstrated the occurrence of boric acid within the water of "Lagone Cerchiaio" of Monterotondo Marittimo (Fig. 16; Burgassi et al., 1995). Commercial power generation from geothermal resources began in Italy in

Fig. 16 - Plaque in memory of U. F. Hoefer that in 1777 discovered the presence of boric acid in the water of the pond called "Lagone Cerchiaio", at Monterotondo Marittimo.

DOI: 10.3301/GFT.2015.02

1913 with a 250 KW unit. A significant increase in the production of water-steam boric mixtures was obtained from wells drilled to increasing depths, up to 250-300 m, in early 1900 (Fig. 17). Power generation stayed at modest levels until 1938, but since then it has risen rapidly and continuously, interrupted only in 1944 by events occurring during World War II (UGI, 2007). The Italian experience of electricity generation from endogenous fluids remained the sole example in the world until 1958, when the first power generation unit was installed in Wairakei (New Zealand). In the same year more than 1900 GWh of electric energy was produced in the Larderello area, with an installed capacity of 300 MW (Cappetti et al., 2000).

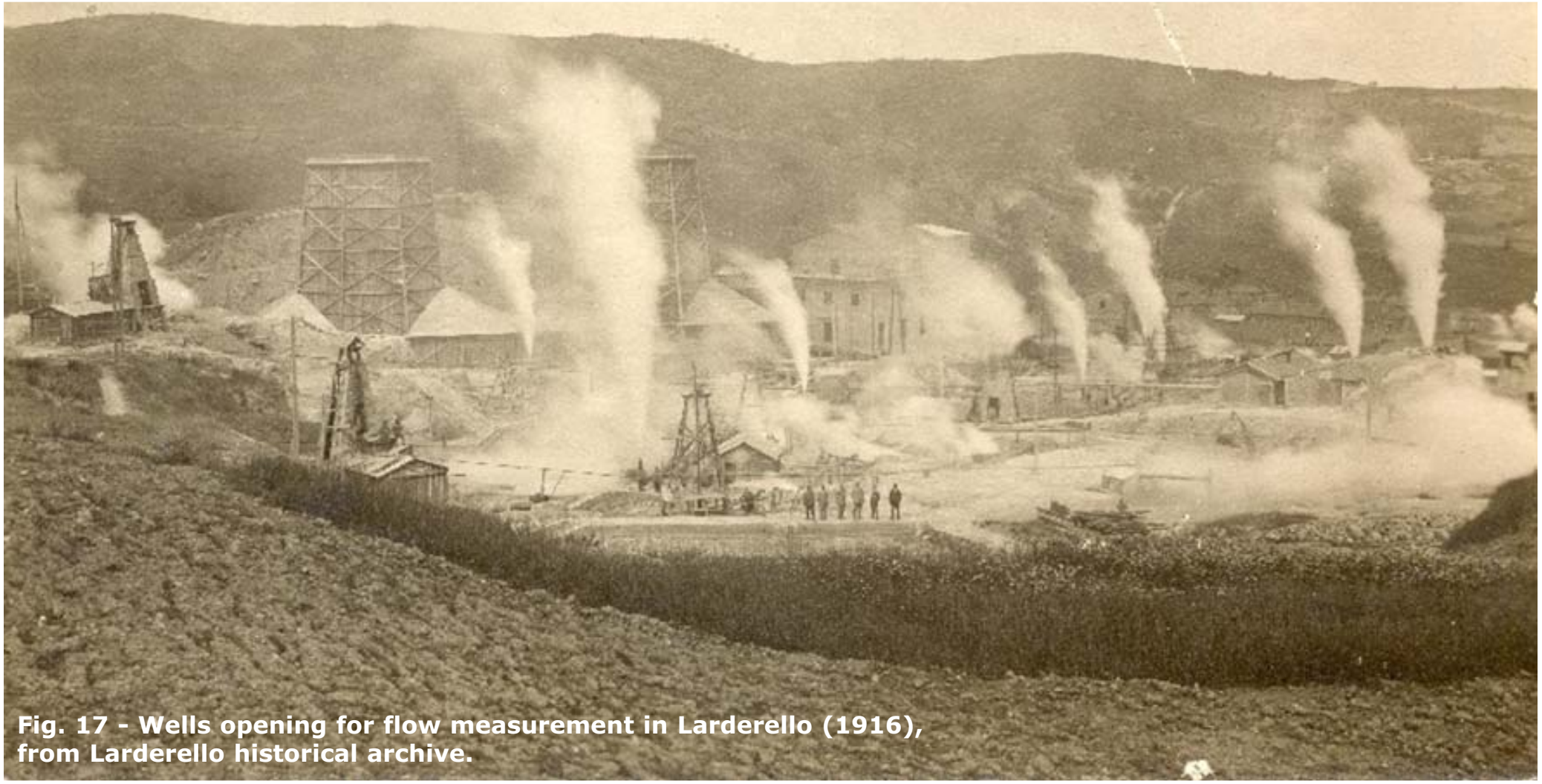

Fig. 17 - Wells opening for flow measurement in Larderello (1916), from Larderello historical archive.

DOI: 10.3301/GFT.2015.02

The positive results of deep exploration and reinjection programs, which began in the late 1970s, have made it possible to reassess the field potential of geothermal areas and to plan both development (involving additional wells and power plants) and renewal programs (replacement of old units with new ones, characterized by higher efficiency and lower environmental impact).

In 1995 the total installed capacity in Italy was 625.7 MW with an energy generation of 3436 GWh (Cappetti et al., 2000, and reference therein). In comparison, at present, Enel Green Power, with an installed capacity in Italy of 874.5 MW (running capacity of 722 MW), currently operates 33 geothermal power plants in Val di Cecina and Monte Amiata (Tuscany), with over 8700 users of district heating, 25 hectares of heated greenhouses, and an electrical production of about 5.2 TWh in 2012 (Fig. 18). In 2012, the geothermal production in Italy was 2% of total production, ≈7% of ENEL production, and ≈7% of the renewable production. The geothermal production covers ≈26% of the Tuscan region consumption.

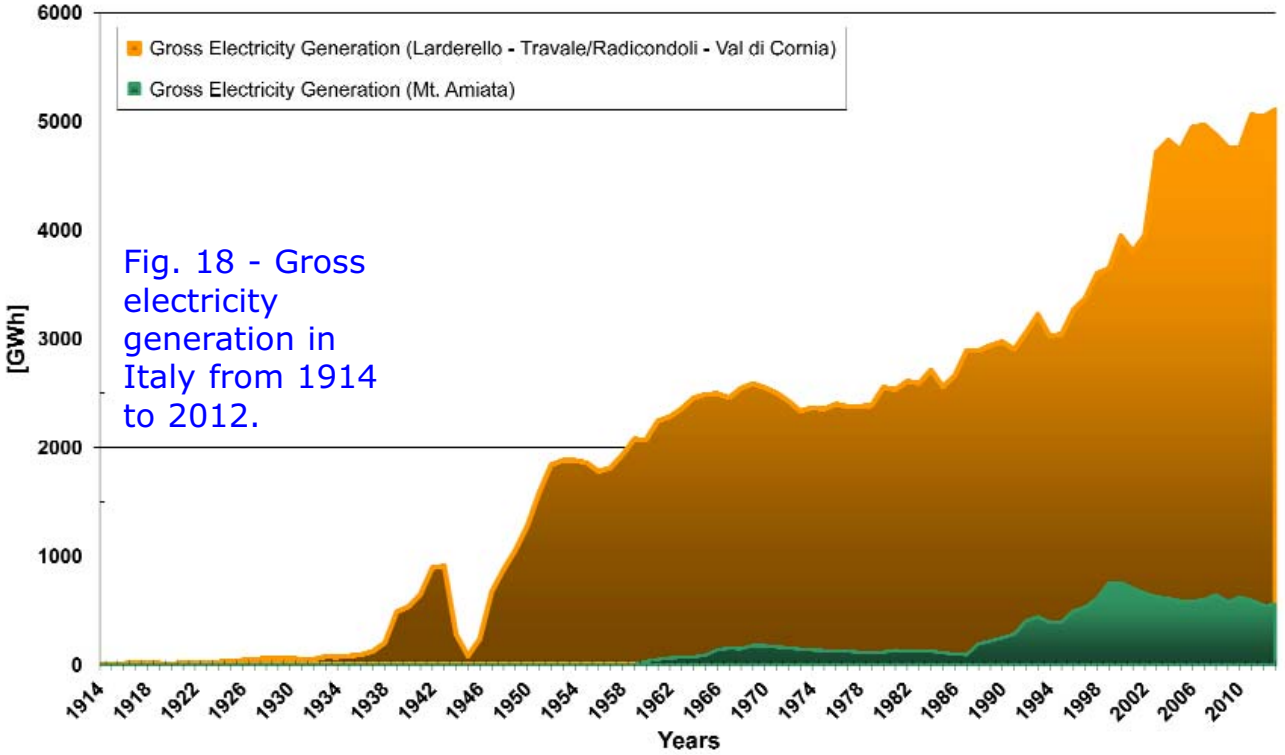

Fig. 18 - Gross electricity generation in Italy from 1914 to 2012.

5.2 Geological framework of the Larderello-Travale area

The Larderello-Travale geothermal area, shown in Fig. 19, is characterized by late-to post-orogenic basins (grabens or semi-grabens according to Bossio et al., 1993; Martini & Sagri, 1993; thrust-top basins according to Bonini et al., 2001) filled with Neogene, continental to marine sediments and separated by ridges where the Apenninic tectonic pile of nappes (i.e. Tuscan nappe and Ligurian and Sub-Ligurian units) crops out (Bertini et al., 1994; Vai, 2001, and

DOI: 10.3301/GFT.2015.02

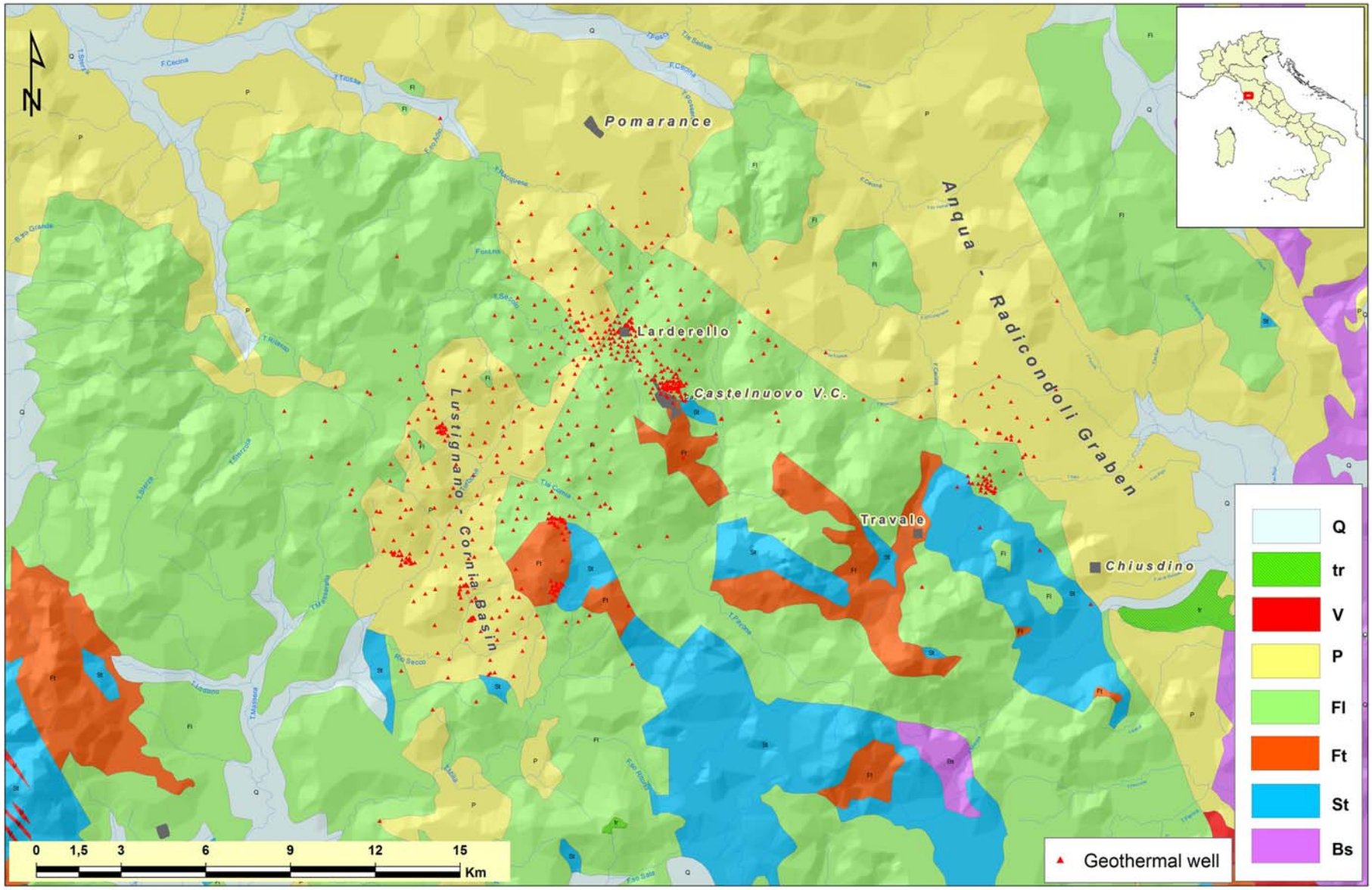

Fig. 19 - Schematic geology of the Larderello-Travale area. Geologic legend from top to bottom: **Q)** Quaternary deposits; **tr)** Plio-Quaternary travertines; **V)** vulcanites; **P)** neo-autochthonous terrigenous deposits (Lower Pliocene – Upper Miocene); **Fl)** Ligurian and sub-Ligurian complex (Jurassic-Eocene); **Ft)** terrigenous formations of Tuscan units (Upper Cretaceous – Lower Miocene); **St)** mainly carbonate formations of Tuscan units (Upper Triassic-Malm); **Bs)** crystalline basement (Upper Carboniferous). Modified from Arias et al. (2010).

DOI: 10.3301/GFT.2015.02

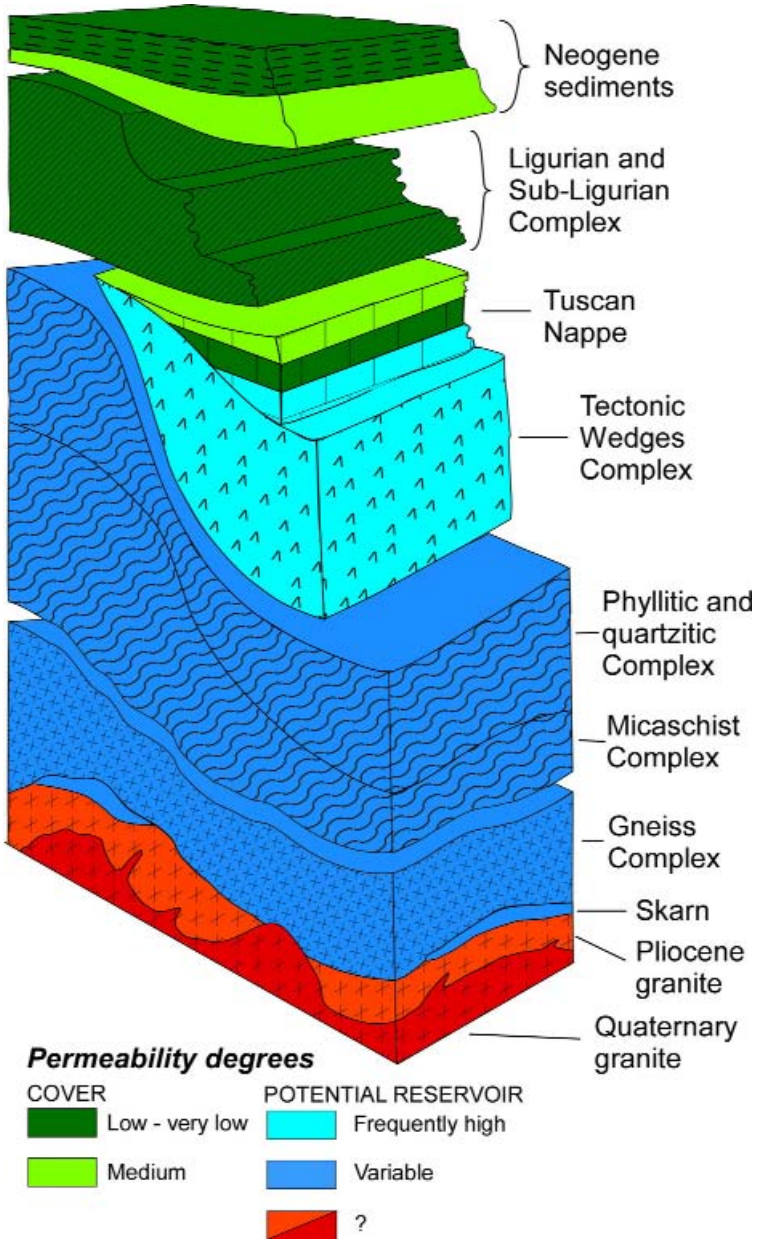

Fig. 20 - Structural-stratigraphic and hydrogeologic sketch of the geothermal area. Modified from Bertini et al. (2006).

references therein). The main tectono-stratigraphic units found in the Larderello-Travale deep geothermal drillings are shown in Fig. 20. They are from top to bottom:

(1) Neogene and Quaternary deposits: Late Miocene to Pliocene and Quaternary continental to marine sediments, filling up the extensional tectonic depressions, which, in the geothermal areas, unconformably overlie the pre-Neogene substratum;

(2) The Ligurian complex *sensu lato*: the Ligurian units *sensu stricto* (Jurassic-Eocene) composed by ophiolites and a pelagic sedimentary cover, and the Sub-Ligurian unit (Eocene–Oligocene) limestones and shales;

(3) The Tuscan unit (Tuscan nappe): evaporitic (Late Triassic), carbonate (Late Triassic–Early Cretaceous), and pelagic–turbiditic (Cretaceous-Early Miocene) successions;

(4) A tectonic wedge complex: Triassic quartzite and phyllite (Verrucano group), Palaeozoic phyllite and the Late Triassic evaporites of the Tuscan nappe;

(5) The phyllite-quartzite complex: Paleozoic phyllite and quartzite, layers of anhydritic dolomites and basic metavolcanites lenses, affected by the Alpine greenschist metamorphism, which overprints a previous Hercynian blastesis;

(6) The micaschist complex: Paleozoic rocks (garnet-bearing micaschists and quartzites with amphibolite zones) affected by Alpine and Hercynian deformations;

(7) The gneiss complex: pre-Alpine polymetamorphic gneiss and paragneiss with intercalations of amphibolites and orthogneiss. The Alpine orogeny did not affect the gneiss complex (Elter & Pandeli, 1990).

The two deepest units were found only in deep drillings. Deep boreholes encountered also numerous acidic intrusive and felsic

DOI: 10.3301/GFT.2015.02

dykes at different depths (from about 2000 to more than 4600 m below the ground level) whose emplacement gave rise to contact aureoles in the metamorphic host rocks (Gianelli & Ruggieri, 2002; Elter & Pandeli, 1990; Musumeci et al., 2002 and references therein) and related hydrothermal processes (Cavarretta et al., 1982). This magmatism is related to asthenosphere upwelling and underplating/intrusion of mantle-derived magmas which produced the wide thermal anomaly in the Tuscan crust since Miocene time. The thermal anomaly triggered the formation of the crustal magmas and the hybrid ones formed by mixing/mingling between crustal- and mantle-derived magmas (Dini et al. 2005). This thermal anomaly is still extremely high in the Larderello-Travale geothermal area and produces heat flow with values ranging from 120 to more than 1000 mW/m^2 and geothermal gradients greater than 100°C/km with maximum values of 300°C/km (Baldi et al., 1995; Fig. 21). This framework and the geophysical modeling suggest the existence of a long-lived and still active magmatic system in the Larderello-Travale geothermal area (Gianelli et al., 1997; Mongelli et al., 1998). The buried solidified granites have isotopic ages ranging from 3.8 to 1.3 Ma (Villa et al., 2006; Dini et al., 2005, and references therein), and, owing to the limited effects that erosion and tectonic exhumation played during such a relatively short time, their present depth (top of intrusions around 3–4 km below the ground level), and geologic setting, probably do not largely differ from those at the time of emplacement.

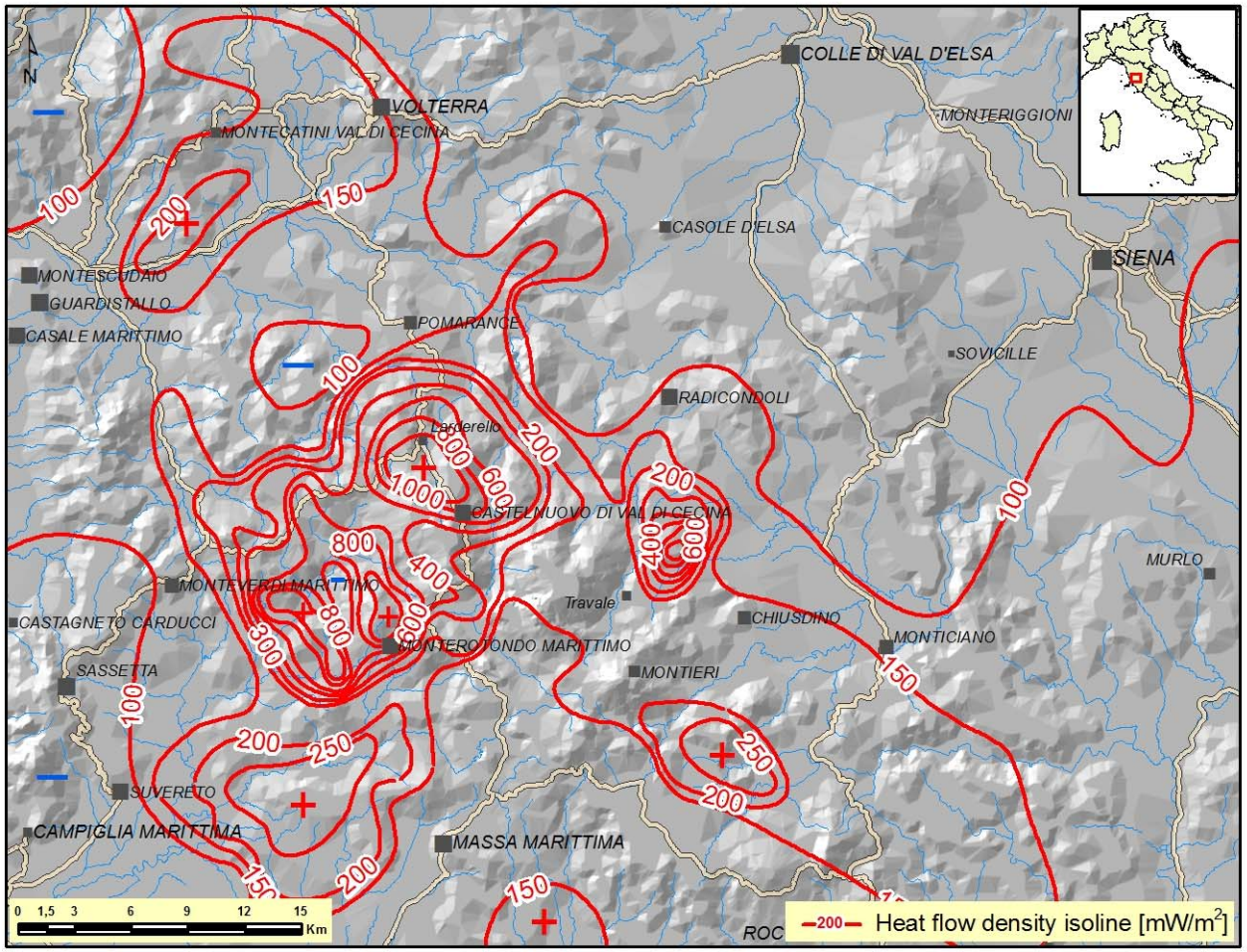

Fig. 21 - Heat flow density map of the Larderello-Travale geothermal field. Modified from Baldi et al. (1995).

DOI: 10.3301/GFT.2015.02

5.3 Reservoirs and present-day geothermal fluids

The cap rocks of the geothermal field are usually represented by flysch formations of the Ligurian complex and, where present, by Neogene formations (Batini et al. 2003; Romagnoli et al., 2010). Two geothermal reservoirs occur below the impermeable cover: 1) a shallow steam-dominated reservoir is hosted at 500-1500 m depth in the Mesozoic carbonate formations of the Tuscan nappe units and in the evaporitic levels of tectonic wedges complex, and is characterized by medium-high permeability, present-day temperatures of about 220-250°C and a pressure of about 20 bar at 1000 m depth; 2) a deep superheated steam reservoir, in vapor-static equilibrium with the shallow one, is hosted in the metamorphic basement and thermometamorphic rocks, and is characterized by a high anisotropic permeability distribution, temperatures ranging between 300-350°C and a reservoir pressure of 70 bar at 3000 m depth.

Both the reservoirs have a secondary permeability due to fractures. The high fracture variability, both in size and density, determines a wide range of permeability values that are in any case greater than 5 mD (Bertani & Cappetti, 1995). Otherwise, the primary porosity of all the reservoir rocks is homogeneous and very low (1-5%) (Cataldi et al., 1978). The fracture system is usually homogenously distributed in the shallow carbonate-anhydrite formations, with higher densities in structural highs. On the other hand, the fracturing in the rocks of the metamorphic basement is inhomogeneous and localized showing a wide range of permeability. The chemical composition of the geothermal fluids at Larderello is dominated by H_2O (up to 95%) with CO_2, CH_4, H_2S and N_2 as major components, with the noble gases present in ppm only (Scandiffio et al., 1995). Stable isotope data on H_2O (before re-injection) indicate meteoric water as the main source of the vapor (Craig, 1963; Ferrara et al., 1965). A simple mixing between two end-members could explain the isotopic composition of the steam produced in the field (Panichi et al., 1995; Scandiffio et al., 1995).

The former end-member is a primary deep steam having typical values of $\delta D = 40\pm2‰$ and $\delta^{18}O = 0\pm2‰$ (all isotope ratios are relative to VSMOW), resulting from extensive water-rock interactions, which shifted the original meteoric $\delta^{18}O$ value towards more positive values. The latter end-member is a secondary steam derived from the boiling of fresh waters, having $\delta D = 40\pm2‰$ and $\delta^{18}O = -7‰$, resulting from limited water-rock interactions due to a short residence time in the reservoir. An alternative explanation of the steam's origin has been proposed by D'Amore & Bolognesi (1994), who hypothesize the mixing of two end-members, meteoric waters, and magmatic fluids produced by the crystallization of a deep-seated magma body. A "large subduction-related magmatic

DOI: 10.3301/GFT.2015.02

contribution'' in the Larderello geothermal gases has been suggested by these authors on the basis of the stable isotope variations in the fluids, as well as the existing $^3He/^4He$ data and high N_2/He and N_2/Ar ratios, indicating a large N_2 excess. Moreover, a mantle component in the geothermal fluids at Larderello is suggested by the relatively high $^3He/^4He$ ratios (expressed as R/Ra, where R is the measured ratio and Ra is the typical value for air), reaching maximum values of 2.7–3.2 (Magro et al., 2003, and references therein). Thus, the observed R/Ra range (0.5-3.2) of the geothermal fluids was interpreted to be mainly the result of different mixing proportions between a ^3He-enriched fluid, derived from the mantle, and a ^4He-enriched fluid originating in the crust and most likely stored in the geothermal reservoir rocks. A good correlation exists between the depth to the seismic K-horizon (see description below) and the R/Ra areal distribution (Fig. 22). The culmination of the reflector at a depth of about 3000–3500 m matches the highest R/Ra contour lines very well; this may identify an area where rapid uplift of fluids of mantle origin allows the existence of relatively high R/Ra values in a typical crustal melting environment (Magro et al., 2003).

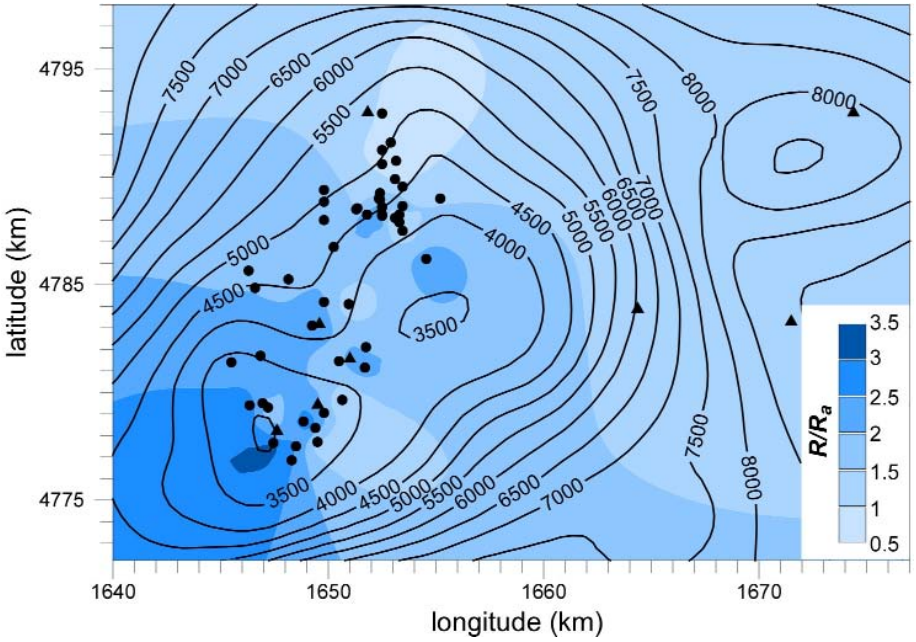

Fig. 22 - Correlation between depth of the top of K horizon (meters below the surface level) and R/Ra areal distribution in the Larderello geothermal area. Full dots: geothermal wells; full triangles: fumaroles; modified after Magro et al. (2003).

5.4 Past hydrothermal activity

The steam-dominated characteristic of the Larderello-Travale field arises from the natural evolution of the system. In fact, the thermal and structural context allowed the geothermal system to pass from an initial water phase (shown in fluid inclusions) to the current steam condition. The depressurization of the reservoir happened prior to the industrial exploitation of the geothermal resource, as verified by the first drilling data in the area (Celati et al., 1975). The liquid phase is presently confined to a few local structures that facilitate the seepage of meteoric waters into the reservoir (Barelli et al., 1995).

DOI: 10.3301/GFT.2015.02

The oldest hydrothermal circulation in the deeper levels of field is likely related to the emplacement of the granitoids (with isotopic ages of 1.3-3.8 Ma) and the related thermal metamorphism. Thermally metamorphosed phyllite, micaschist and gneiss are generally characterized by post-tectonic crystallization of quartz, biotite, andalusite, cordierite and tourmaline; moreover plagioclase, muscovite, pyrite, graphite and less frequently wollanstonite, spessartine and grossular-rich garnet, corundum and sanidine may also occur in variable amounts (Gianelli & Ruggieri, 2002; Pandeli et al., 2005).

Subsequent fluid circulation caused hydrothermal alteration of granite, contact-metamorphic rocks, metamorphic rocks not affected by contact-metamorphism and also of the sedimentary rocks of tectonic wedge complex and of the Tuscan nappe. Two main types of late hydrothermal alteration have been recognized (Cavarretta et al., 1982; Pandeli et al., 1994):

- propylitic-type alteration, characterized by veins of epidote, chlorite, quartz, calcite, K-feldspar, titanite, actinolite, anhydrite, albite and pyrite in variable proportions;
- sericitic-type, with K-mica, chlorite and quartz in different proportions. In addition hydrothermal calcite filling veins and voids also occurs in sedimentary rocks (Gianelli et al., 1997).

The long-lived geothermal activity in the Larderello-Travale fields is reflected by the occurrence of several types of fluids trapped as fluid inclusions within igneous quartz, contact-metamorphic and hydrothermal minerals. The different types of inclusion fluids within the magmatic and contact-metamorphic assemblages are the result of a complex sequence of fluid trapping during evolving pressure–temperature conditions (Cathelineau et al., 1994; Boiron et al., 2007, and references therein) (Fig. 23). Li-Na-rich saline fluids and compositionally complex brines (exsolved from granites), and aqueous-carbonic fluids (produced by heating of Paleozoic rocks during contact

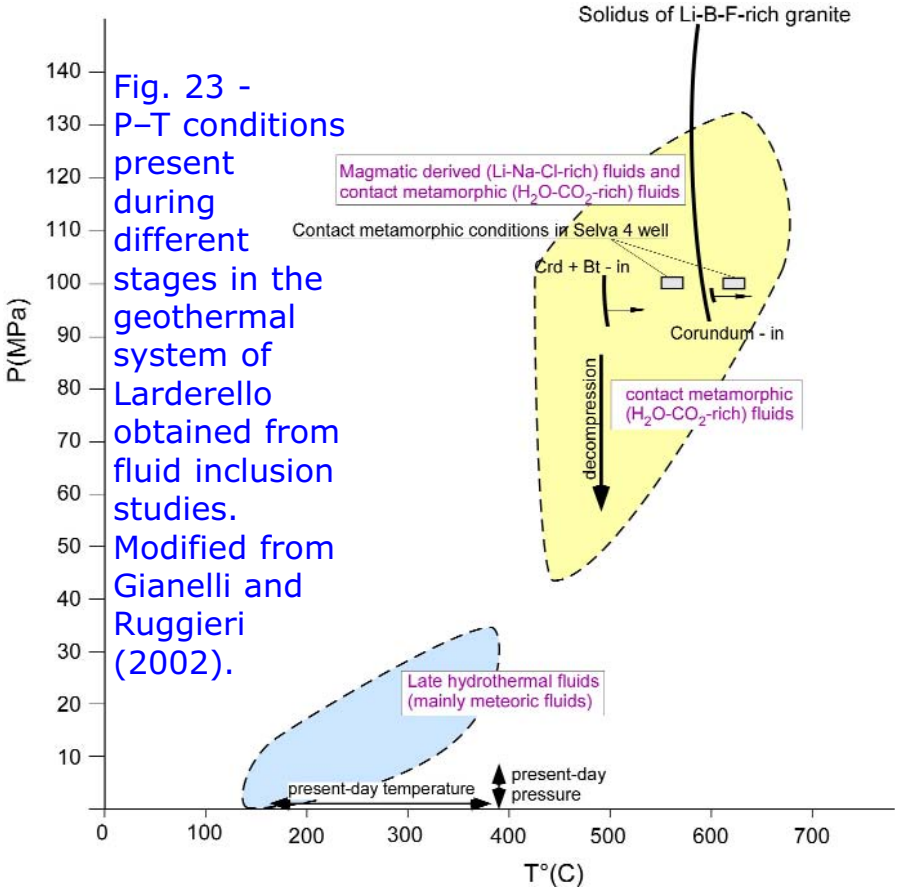

Fig. 23 - P–T conditions present during different stages in the geothermal system of Larderello obtained from fluid inclusion studies. Modified from Gianelli and Ruggieri (2002).

DOI: 10.3301/GFT.2015.02

metamorphism) circulated during early hydrothermal activity linked to the intrusion of granites (Cathelineau et al., 1994). These fluids probably circulated at depth >2500 m below the ground level, usually at temperatures of 425–690°C and under lithostatic pressures of approximately 90–130 MPa or at pressures below lithostatic values (only the aqueous-carbonic fluids) during system decompression (Fig. 23). A more recent hydrothermal stage is also recorded in fluid inclusions trapped in secondary minerals and also as late inclusions in magmatic and contact-metamorphic quartz. This stage is characterized by trapping temperature usually of 150-400°C, hydrostatic pressures (Fig. 23), and fluids with variable salinities (Ruggieri et al., 1999, and references therein). The relatively low-salinity aqueous liquids, sometimes containing small amounts of CO_2, are thought to be of prevalently meteoric origin, while liquids with variable salinities and containing dissolved Ca and Mg, in addition to Na, are believed to be derived from the interaction of (meteoric?) water with evaporite-carbonate sequences occurring in the Tuscan nappe and/or to represent connate waters mobilized during geothermal activity and/or to be the result of fluid boiling and mixing processes (Gianelli et al., 1997; Ruggieri et al., 1999).

5.5 The K-horizon

Reflection seismic data (Batini et al., 1983; Gianelli et al., 1997; Brogi et al., 2005) highlighted the presence of an intense and continuous reflector exhibiting local "bright spot" features inside the Palaeozoic crystalline basement, the so-called K-horizon. Its depth varies between 3–4 km in the western zone and 8–10 km in the Travale geothermal area (Bertini et al., 2006). The K-horizon is associated with the 400°C isotherm and is considered the base of the reservoir (Romagnoli et al., 2010). The K-horizon was never reached during deep drilling, except in the SANPOMPEO_2 well, which blew out on reaching this zone of pressurized fluids, and its nature is still a subject of debate. However, regardless of the interpretation of the K-horizon, the only phenomenon that is able to account for this seismic "bright spots" is the presence of micro-cracks and micro-fractures filled locally by fluids (Marini & Manzella, 2005). The K-horizon has been interpreted also as the upper boundary of an active shear zone at the top of the brittle-ductile transition (Liotta & Ranalli, 1999; Brogi et al., 2003). In this interpretation the lateral continuity of the K-horizon is interrupted by intersections with brittle shear zones where Pliocene-Present normal faults coalesce (Fig. 24). It has been hypothesized that the loss of seismic reflectivity in correspondence to the intersections between the shear zones and the top of the brittle-ductile transition is connected to fluid migration from the K-horizon to shallower levels along the shear zone (Brogi et al., 2003).

DOI: 10.3301/GFT.2015.02

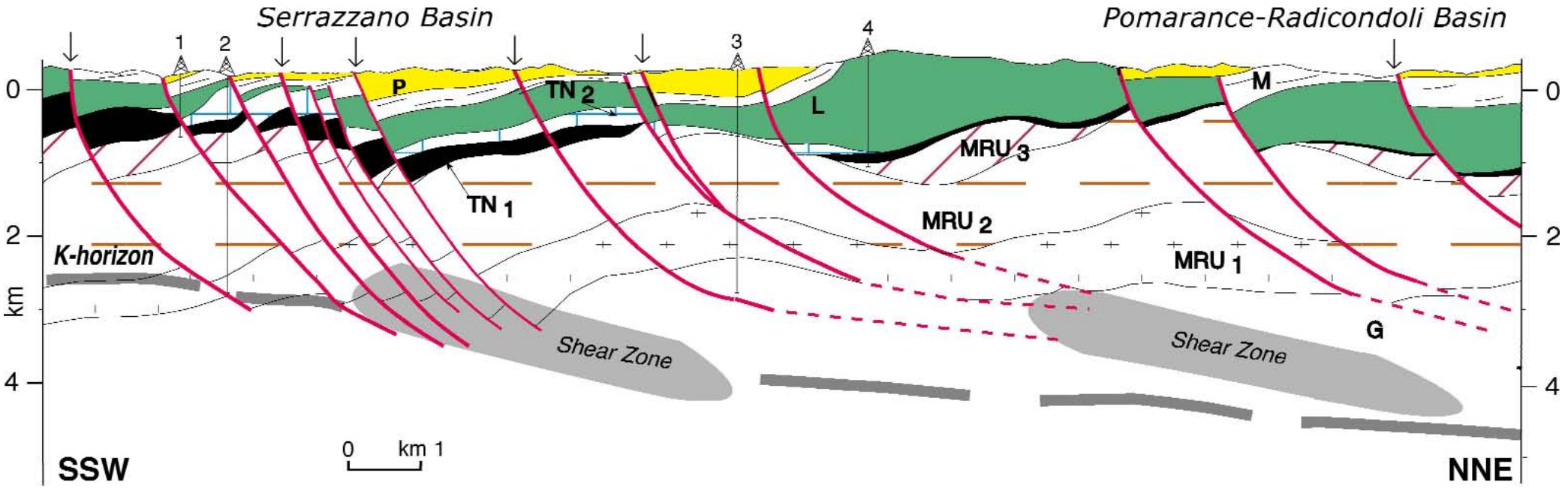

Fig. 24 - Geological section of the Larderello area obtained integrating borehole stratigraphies, field data, and reflection seismics interpretation. The K-horizon is interpreted as the upper boundary of an active shear zone (see text). Locations of outcropping normal faults are shown by black arrows. Key: P – Pliocene sediments; M – Miocene sediments; L: Ligurian and Sub-Ligurian complex; Tuscan nappe (TN): TN_2 – Early Miocene – Rhetic sequence; TN_1 – Late Triassic evaporites; Monticiano – Roccastrada unit (MRU): MRU_3 – Mesozoic – Paleozoic group; MRU_2 – phyllite – quartzitic group; MRU_1 – Paleozoic micaschist group; G: gneiss complex. Modified from Brogi et al. (2003).

On the other hand, Bertini et al. (2006) suggest that the K-horizon occurs at the top of a Quaternary granite and corresponds to the granite carapace and related contact metamorphic rocks which are permeated by supercritical fluid (Fig. 25). The fluids in the K-horizon are likely present in micro-cracks which can be re-activated by episodes of fluid overpressuring. This micro-crack reactivation process in rocks, in a plastic or semi-plastic condition, is vital for the life of the entire geothermal system because it enhances the cyclic advective heat transfer from a very high-temperature and very low-permeability zone to the 2–3.5 km depth where most of the geothermal wells are actually drilled.

Bertini et al. (2006) also characterized another seismic horizon (H-horizon) with seismic features similar to the K-horizon but occurring above the latter, at depths of 2–4 km, corresponding to the contact metamorphic rocks.

DOI: 10.3301/GFT.2015.02

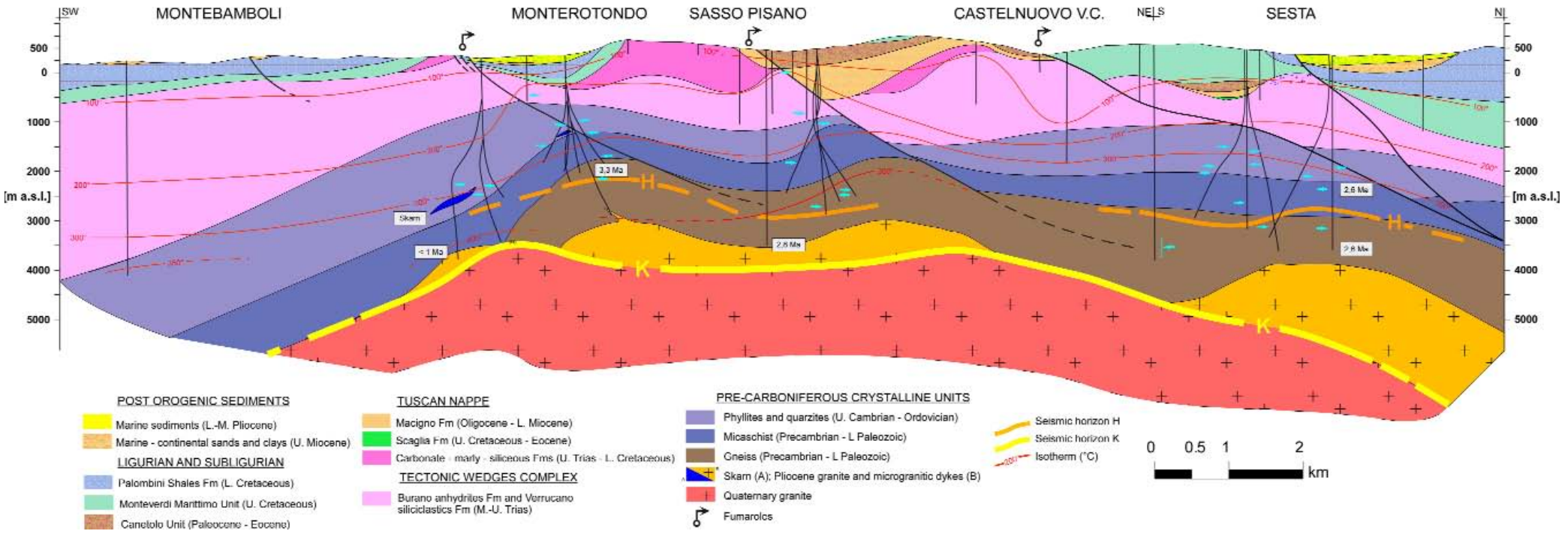

Fig. 25 - Geological cross-sections of the Larderello area; H and K seismic horizons, isotherms and the radiometric ages of "granites" and thermo-metamorphic rocks are also shown. From Bertini et al. (2006) modified.

The H-horizon is interpreted as a fossil K-horizon, corresponding to the top of older granite intrusions. The fluid hosted in this fractured horizon was supercritical and related to the magma, during an early magmatic stage of the system, as suggested by fluid inclusion data. The fractures were filled subsequently with fluids of meteoric origin, and are now filled by super-heated steam (Bertini et al., 2006). Another explanation for the presence of pore-fluids in the K-horizon was proposed by Marini & Manzella (2005), who suggest that the permeability in the K-horizon is related to the development of micro-cracks in quartz. Micro-cracking in quartz is favored by the α–β transition and by the very high volumetric thermal expansion at the pressure–temperature conditions around the depth of the K-horizon.

DOI: 10.3301/GFT.2015.02

5.6 Geothermal production process at Larderello-Travale

A geothermal development project begins with the identification of a geothermal resource that develops through the following steps:

• Surface exploration: investigation of geothermal manifestations (hot springs, fumaroles, geysers, steam jets, etc.), geological, geochemical and geophysical surveys. Drilling shallow boreholes (50 to 200 m) may give an indication of the local temperature gradient. The results of surface exploration indicate the most favorable area to focus the more expensive deep exploration phase.

• Deep exploration: drilling of slim-holes (up to 1000 m deep) and/or wells having commercial diameter (up to some km deep). The confirmation of the presence of the geothermal resource during the deep exploration will lead to the development phase.

• Development phase: drilling of wells for production and reinjection purposes, surface gathering system and geo-thermoelectric power plant construction.

A geothermal plant contains different elements that have an impact on our land. In the case of the Larderello-Travale geothermal system, the superheated steam extracted from the vapor-dominated reservoir arrives at the nearest power plant through a steam gathering system (Fig. 26). The total fluid composition, at wellhead, is usually 90-98% steam and 2-10% gas. The steam temperature in the reservoir is about 300°C while, when it arrives at the power plant, its temperature is in the range of 200-240°C depending on the inlet pressure.

ENEL drilled a total of 491 wells in Tuscany, 267 for production, 51 for reinjection, and the remaining 173 for other uses such as field monitoring and gas production. The steam pipe system (213 km long) is made up of steel pipes (150-800 mm diameter) insulated with rock wool and covered with a sheet of aluminum painted with colors according to the vegetation. At the power plant, the steam feeds the turbine for the conversion of thermal energy into mechanical energy. The exhaust steam leaving the turbine is returned to the liquid state

DOI: 10.3301/GFT.2015.02

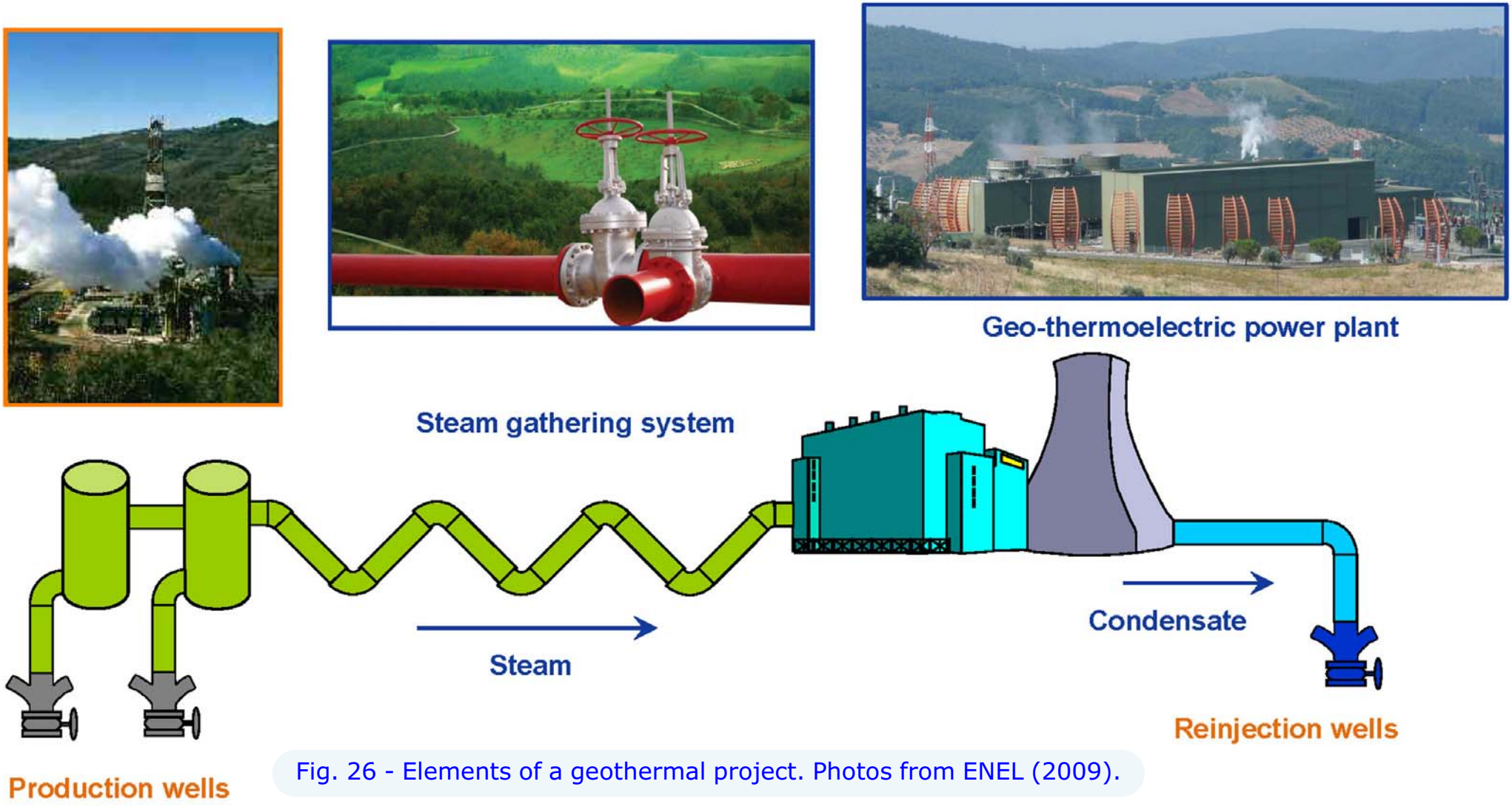

Fig. 26 - Elements of a geothermal project. Photos from ENEL (2009).

in a condenser, while the non-condensable gas contained in the steam is dispersed to the atmosphere after an appropriate treatment. The water produced by the power plant cooling towers must be injected at depth through appropriate drilled wells (reinjection wells) in order either to close the natural cycle or to give new fuel to the geothermal field. The ENEL water pipe system is 317 km long. The generator, connected to the

DOI: 10.3301/GFT.2015.02

turbine axis, transforms the mechanical energy into electrical energy that is subsequently transmitted to the step-up transformer (Fig. 27). The transformer raises the voltage to 132 kV and feeds it into the national grid. All of the ENEL power plants are remotely controlled by a "Remote Control Center" located in Larderello, where the operating parameters and any alarm messages are sent in order to alert the appropriate staff. In addition, ENEL personnel also may have remote supervision from any personal computer connected to the ENEL network which gives access to all the power plant data, their processing and diagnostics, etc. (ENEL, 2009).

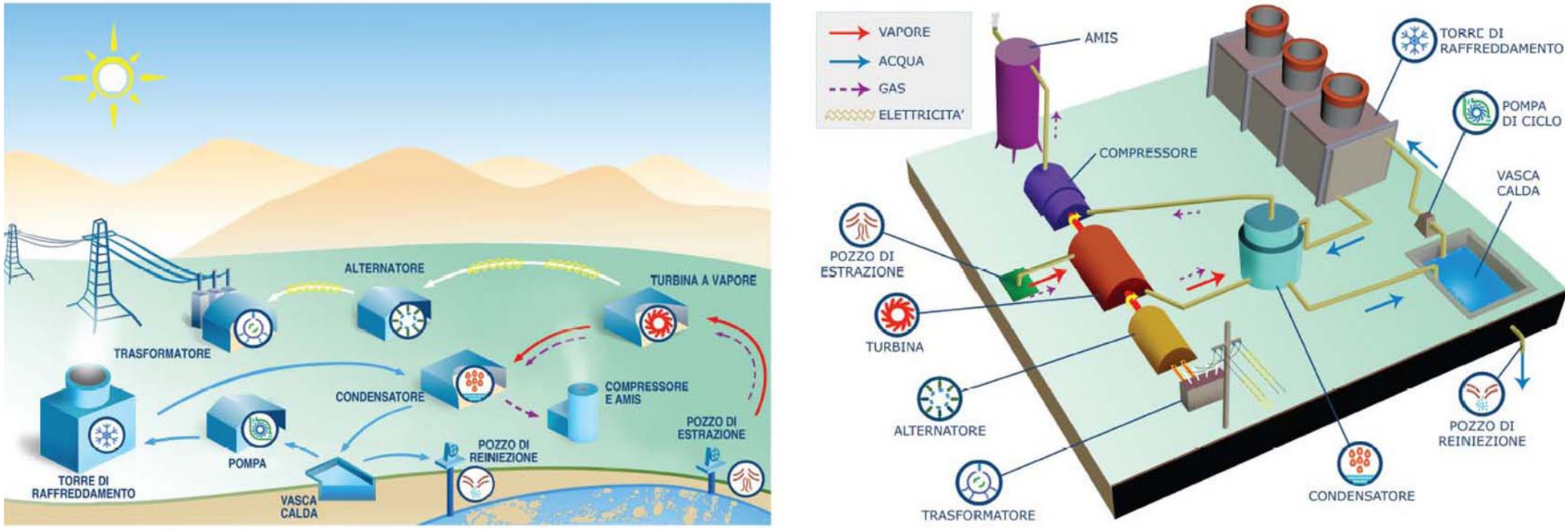

Fig. 27 - Simplified scheme of a standard geothermal power plant equipped with AMIS® abatement system (ENEL, 2009).

DOI: 10.3301/GFT.2015.02

6. Carbon dioxide sequestration by mineral carbonation in serpentinite rocks of Southern Tuscany

6.1 Geological framework

Carbon dioxide mineral sequestration through carbonation of natural silicate minerals is a potential alternative to CO_2 geological storage and consists of an induced exothermic alteration of metal-rich non-carbonate minerals (i.e., Mg_2SiO_4 forsterite, $Mg_3Si_2O_5(OH)_4$ serpentine, $CaSiO_3$ wollastonite) to geologically and thermodynamically stable mineral carbonates (i.e., $MgCO_3$ magnesite, $MgCa(CO_3)_2$ dolomite, $CaCO_3$ calcite, $FeCO_3$ siderite, $NaAl(CO_3)(OH)_2$ dawsonite). This technology attempts to mimic natural low-temperature alteration (carbonation) of widespread silicate rocks (i.e., peridotite, serpentinite, basalt) that trap CO_2 safely over geological times (Seifritz, 1990; Goff & Lackner, 1998; Lackner, 2003). Since Seifritz (1990) proposed the idea of an induced industrial *ex situ* mineral sequestration (where CO_2 and solid reactants require transport to a surface sequestration site), many carbonation approaches were proposed and several gas–solid and aqueous–solid carbonation processes have been investigated in order to design more effective and economic reactions. Most of the experimental studies on serpentine have shown that induced carbonation does not go to completion because precipitated carbonates or remaining silica-rich layers of the serpentine act as a diffusion barrier, inhibiting the evolution of the process (see Boschi et al., 2009, and references therein). In addition, the slow rate of serpentine dissolution and decrease of porosity during the reaction lower the efficiency of the reactions. The study of low-temperature carbonated ultramafic rocks and associated magnesite deposits, natural analogues of the induced carbon dioxide mineral sequestration, can complement laboratory and demonstration studies and provide opportunities to constrain the boundary conditions and the mechanisms for CO_2-bearing phases to form.

Magnesite deposits, hosted in extensively altered ultramafic rocks, are common throughout the world and occur as veins or stockwork bodies of cryptocrystalline magnesite, with minor amounts of talc, quartz and dolomite (Boschi et al., 2009, and references therein). Metric to kilometric magnesite veins are usually interpreted as ultramafic rocks that have interacted with CO_2-bearing meteoric/hydrothermal fluids where prolonged regional tectonics have been active, and have produced continuous networks of shallow crustal fractures.
Serpentinite-hosted magnesite deposits represent a relatively recent discovery in Tuscany, having been first noted in 1900 (Marinelli, 1955; Sartori, 1967; Grassellini-Troysi & Orlandi, 1972). They were actively exploited between 1914 and 1945, leading to a considerable production of magnesite (0.3 Mt) used for refractory bricks in the iron industry

DOI: 10.3301/GFT.2015.02

(Boschi et al., 2009, 2010). Several deposits are known from almost all the serpentinite outcrops in Tuscany (Monti Livornesi, Colline Metallifere, Elba Island). The inland Tuscan magnesite deposits are considerably large, being represented by tens of veins up to 15 m thick and 800 m on strike that were exploited over a vertical extent of at least 100 m. All the ore bodies show similar mineralogy (e.g., Fig. 28) and have a general sub-vertical attitude trending NNW–SSE, coherent with the main extensional, high-angle faults in the region.

The deposits lie at the northern periphery of the active Larderello–Travale geothermal field where granite intrusions were cored at depths of about 3300–4800 m in the Monteverdi 2A and 7, VC11 and Radicondoli 26B, 29 and 30 wells (Dini et al., 2005; Fig. 29). The presence of the Larderello geothermal field entails that the buried rocks are naturally heated at anomalous temperatures; in this area, at a deep less than 1000 m below ground level, the temperature is of about 150°C (see Boschi et al., 2008, for details). This peculiar geological situation enhances, in the presence of CO_2, a spontaneous carbonation of buried serpentinites and could be an ideal place to test in situ CO_2 mineralogical

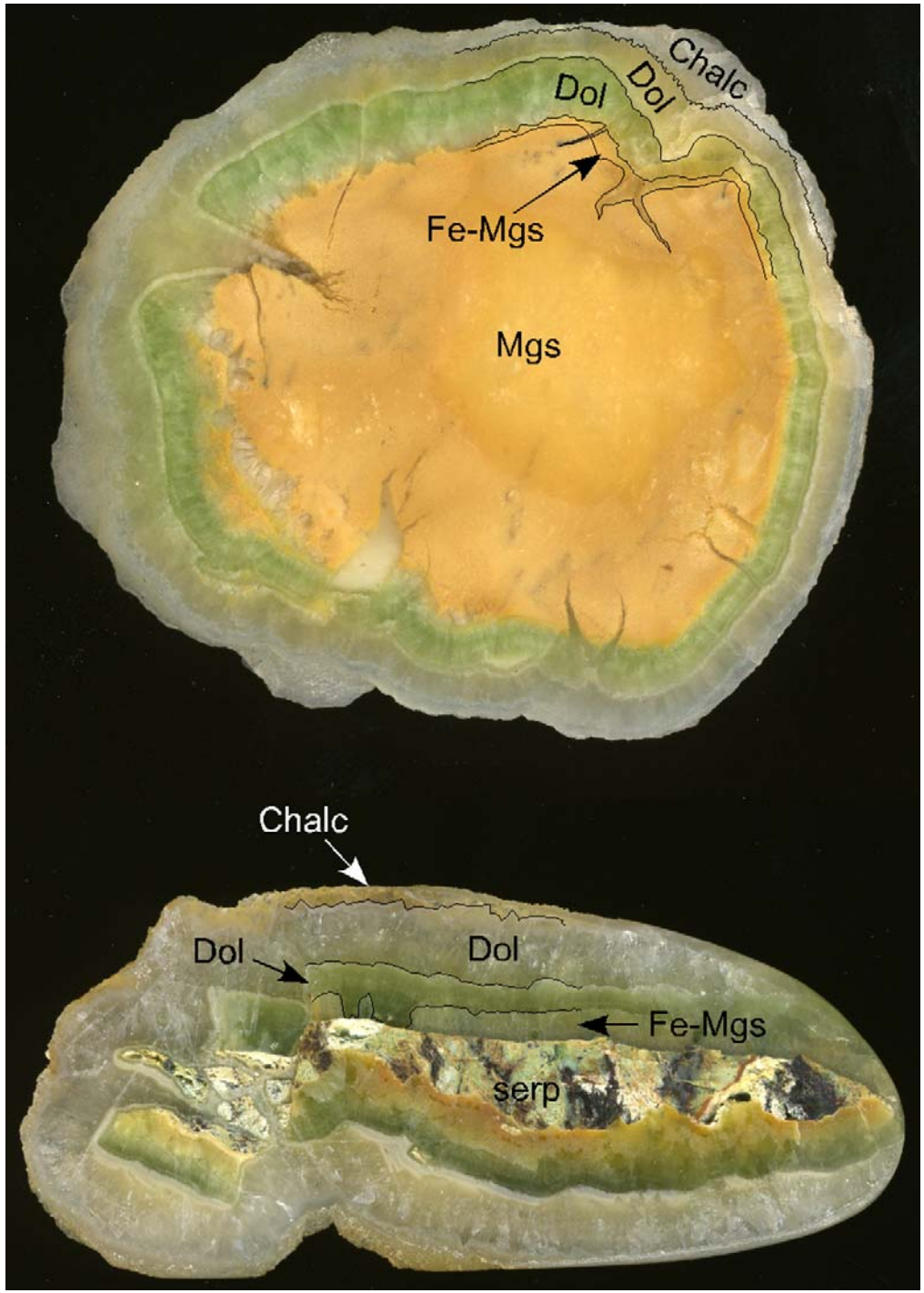

Fig. 28 - Two polished slabs of Malentrata ore displaying the brecciated-crustiform texture, and variations in color. (Mgs: magnesite, Fe–Mgs: Fe-rich magnesite, Dol: dolomite, Chalc: chalcedony, serp: silicified serpentinite; from Boschi et al., 2009).

DOI: 10.3301/GFT.2015.02

sequestration of unaltered buried serpentinites. Boschi et al. (2008) showed that outcropping Tuscan serpentinites can store up to 100 gigatons of CO_2, equivalent to 40-220 years of total Italian emissions (approximately 580 Mt/yr for the year 2010). Even assuming that only 10% of the ophiolite bodies can be transformed into magnesite, the amount of sequestered CO_2 is important. A new detailed study (Trumpy et al., 2010) reveal the most suitable areas in Tuscany and their CO2 storage potentials for applying in-situ and ex-situ mineral CCS technology.

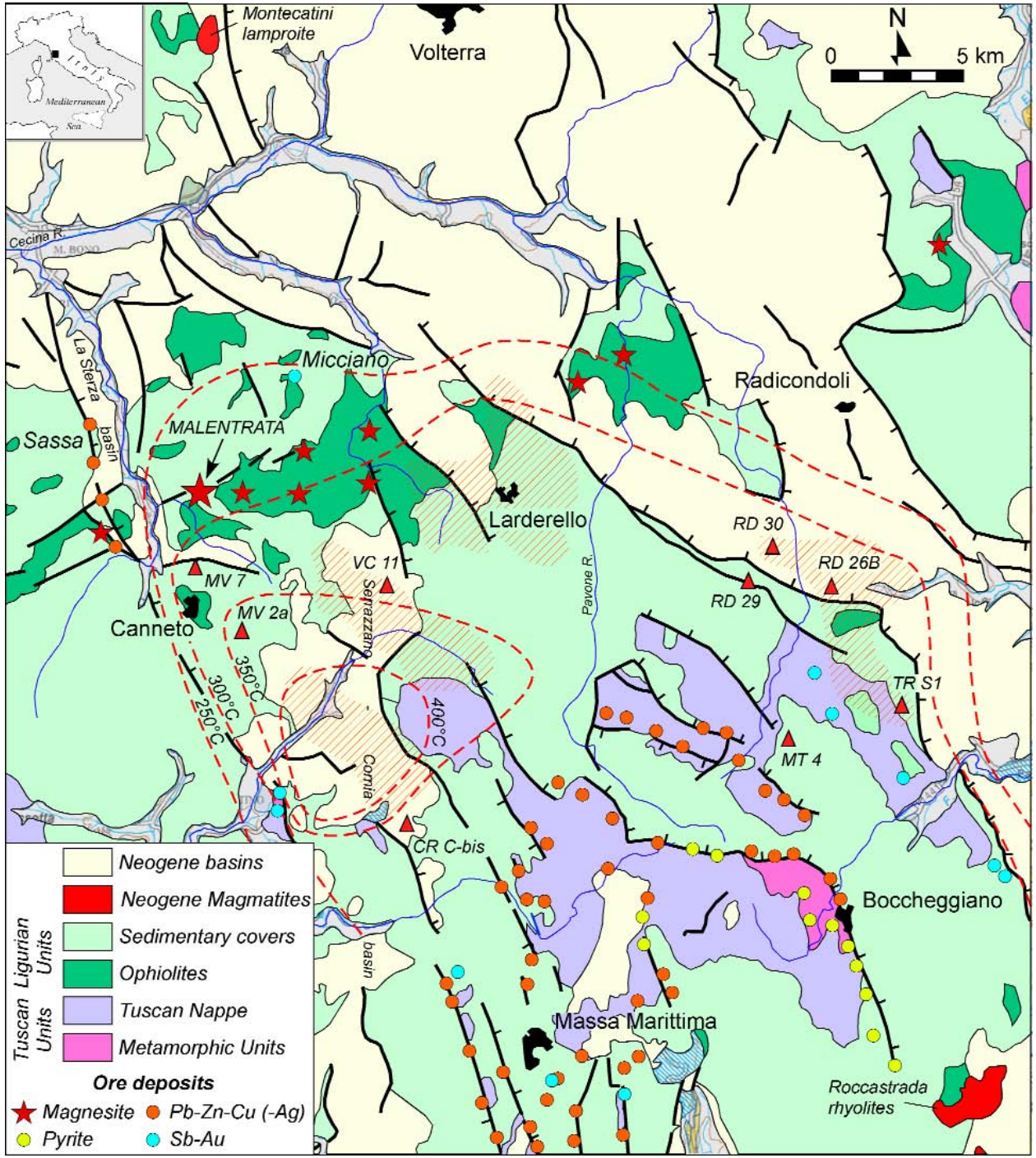

Fig. 29 - Geological map of Southern Tuscany (Italy) showing the distribution of magnesite, and other ore deposits with respect to the Larderello–Travale geothermal field. The occurrence of magmatic rocks at the surface and at depth (red triangles highlight geothermal wells that intersected Pliocene–Quaternary granites at depth of about 2500–5000 m) is also reported. Red dashed contour lines display the temperature distribution at depth of 3000 m below sea level. Super heated steam production reservoirs are indicated by dashed orange areas. Black areas indicate main towns (from Boschi et al., 2009).

DOI: 10.3301/GFT.2015.02

6.2 The Malentrata deposit

The ligurides in the Malentrata area are represented by a complex stacking sequence, made up by several tectonic units that include ophiolites, sedimentary cover (cherts, limestones and shales), and turbiditic sediments. The main ophiolitic bodies, dominated by serpentinites with minor gabbros and basalts, form an ENE trending discontinuous alignment (Fig. 29). The Ligurian units lie tectonically above a stack formed by units of continental affinity (Tuscan units). The Tuscan nappe and the Palaeozoic–Triassic metamorphic units crop out extensively to the south of the study area (Fig. 29), while below the Malentrata magnesite deposit they are buried at a depth of about 1300–1500 m below sea level, as indicated by some geothermal exploratory wells (Bertini et al., 2000; Barbier et al., 1998).

The Malentrata magnesite deposit consists of several carbonate–silica veins hosted by silicified, carbonated and argillified serpentinites of the Ligurian units (Fig. 30a, b). Serpentinite silicification and carbonate–silica veining is common in the Monterufoli district, but it reaches the highest intensity in the Malentrata–Poggio Castiglioni area. The ophiolite host constitutes disrupted decametric to pluri-kilometric masses embedded in a complex sequence of sedimentary formations (shales, calcilutites, siliciclastic–carbonatic arenites and calcarenites; Bertini et al., 2000). Carbonate–silica veins never occur in the sedimentary envelope. Serpentinite-hosted veins show sharp terminations against the sedimentary formations, as already reported for other Tuscan magnesite deposits (Marinelli, 1955). The Ligurian units in the Monterufoli area are limited to the west by the NNW–SSE Neogene La Sterza basin. This basin suddenly changes orientation 2 km south of the Malentrata deposit, developing an eastward segment connected to the N–S trending, Neogene Serrazzano–Cornia basin (Fig. 29).

The tectonic structures at the scale of the deposit reflect the previously described pattern with faults and fractures showing a bimodal distribution of their orientation: Apenninic (NNW–SSE) and anti-Apenninic (NE–SW and E–W). However, the carbonate–silica veins show a quite regular attitude with a dominance of NNW–SSE and minor NNE–SSW and NW–SE strikes (Fig. 30; see also Fig. 2 in Boschi et al., 2009). They are mostly sub-vertical (dip 50–90°) with a general immersion to the east and only few veins dipping to the west. The veins display sudden changes in thickness (from a few cm up to 4 m) and length (from a few meters up to 200 m), and they were explored/exploited by underground and open pit works over a vertical extent of about 100 m. $^{230}Th/^{234}U$ dating of dolomite from Malentrata indicates an age of less than 200,000 years for

DOI: 10.3301/GFT.2015.02

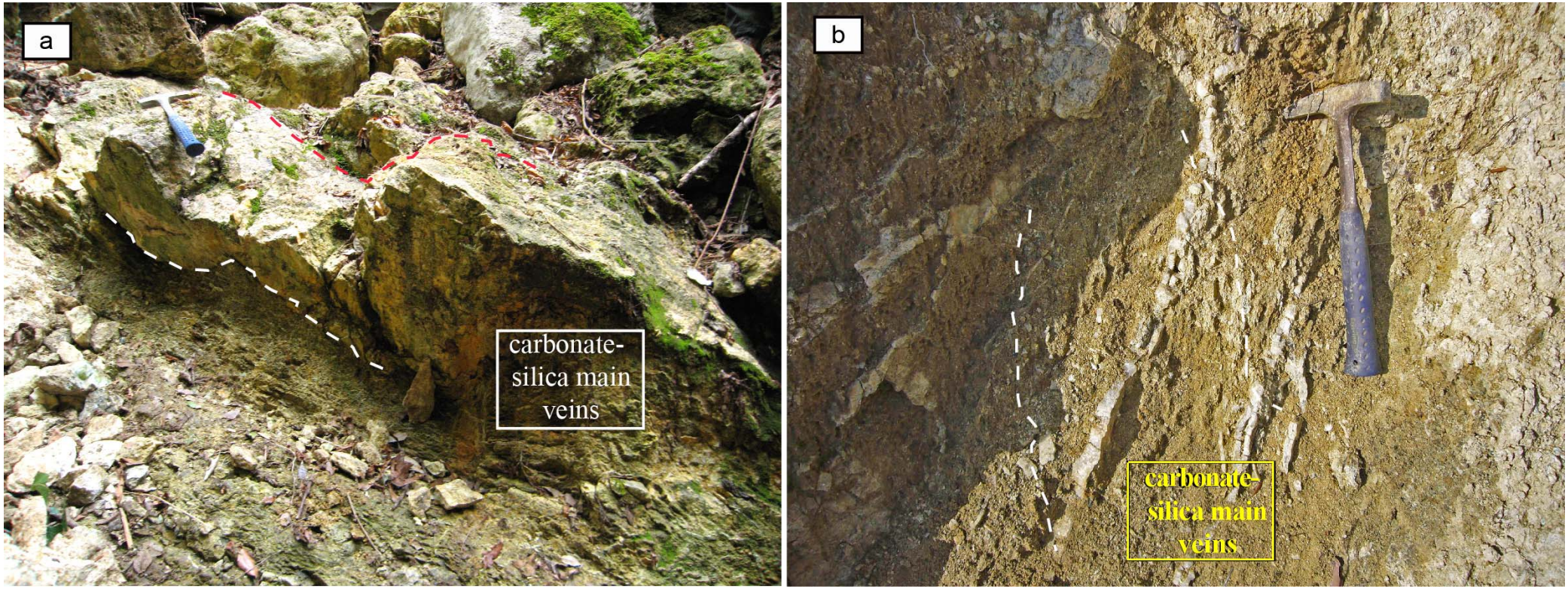

Fig. 30 - a, b) Representative examples of carbonate–silica veins hosted by silicified, carbonated and argillified serpentinites at Malentrata.

the veining event (Bertini et al., 1996). During such a short time span, erosion can have removed only a few tens of meters and suggests that the veins formed at very shallow crustal levels.

6.2.1 The silicified serpentinite host and the main carbonate–silica veins

Serpentinite host rocks were transformed into brownish friable rocks containing opal, montmorillonite, Fe-rich magnesite and minor iron sulfides and oxides. The silicified–carbonated serpentinites experienced several stages of brecciation and carbonate vein infilling. They are crosscut by a network of very small veins of magnesite and by a subsequent generation of dolomite veins, showing an attitude sub parallel to the main carbonate–silica veins, and a variable spacing (Fig. 31). In some brecciated portions, opal occurs as dispersed

DOI: 10.3301/GFT.2015.02

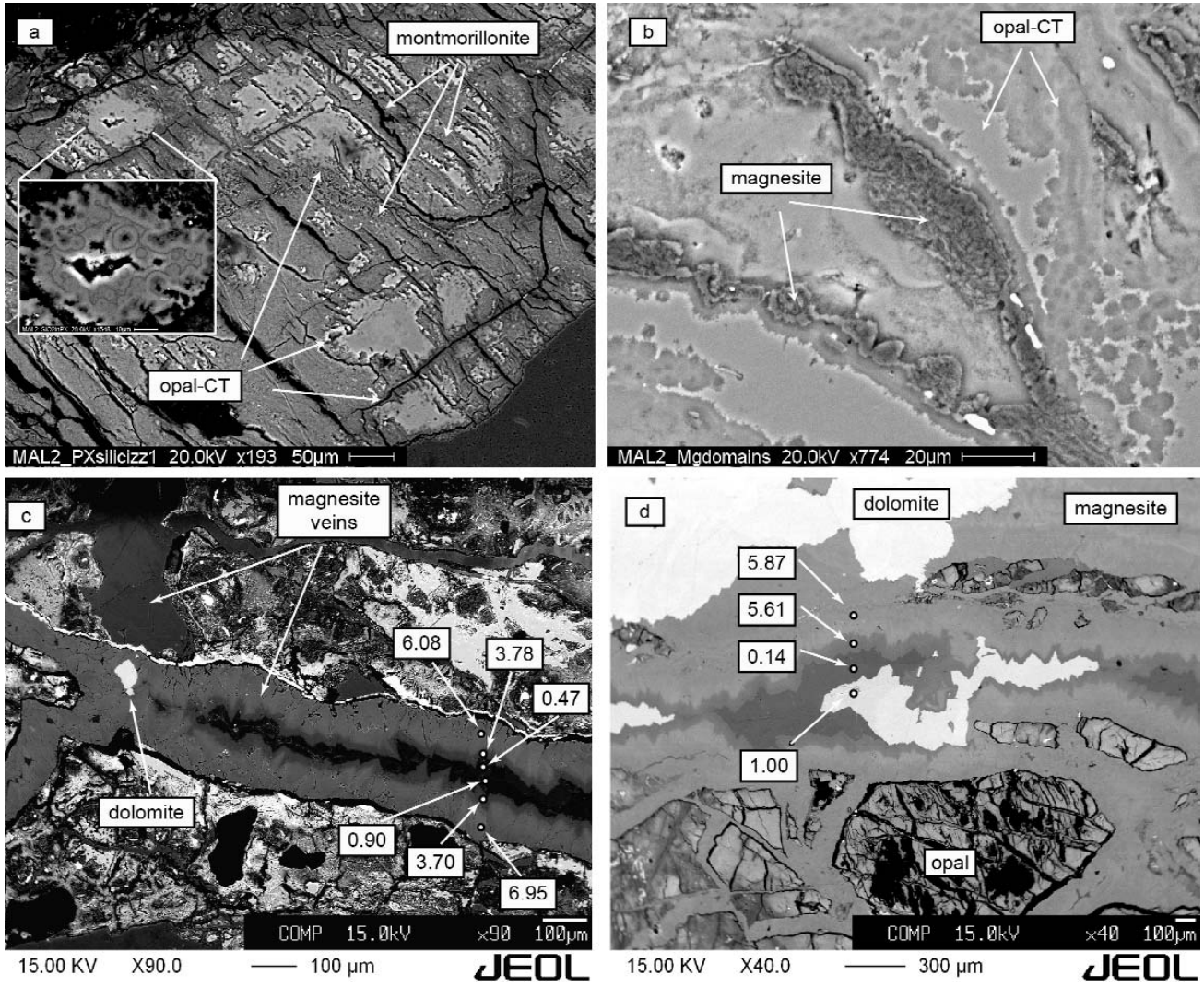

Fig. 31 - SEM images in backscattered electron mode showing the typical texture of the altered serpentinite host rock: a) example of bastite replaced by montmorillonite and opal-CT. Detail shows lepispheres of opal-CT; b) micrometric intergrowth of opal-CT (with variable amounts of water) and magnesite; c) Fe-zoned magnesite veinlets crosscutting altered serpentinite host; d) opal fragments cemented by magnesite and late dolomite (modified from Boschi et al., 2009).

fragments cemented by a magnesite matrix. In other portions, magnesite appears as fragments embedded in precipitated opal suggesting a non-systematic sequence of precipitation. Overall, the early stage of magnesite veining indicates that carbonate precipitation was associated with the silicification of the rock and repeated brecciation events, resulting in a complex brecciated-veined texture.

Main carbonate–silica veins are characterized by an early massive infill of cryptocrystalline creamy-white magnesite (Fig. 28) containing angular fragments (millimetric to decimetric in size) of the silicified serpentinite. Cryptocrystalline magnesite shows a polygonal texture with grains showing Fe-rich small nuclei surrounded by Fe-poor larger rims. Most of the massive veins are brecciated and show a "cement supported" brecciated structure with fragments of the early magnesite infill and host rocks cemented by banded Fe-rich magnesite, green and pale-brown dolomite, chalcedony, quartz and opal. Fragments vary from millimetric to

DOI: 10.3301/GFT.2015.02

centimetric (up to 15 cm). The fragments of the host rock display irregular shape, while cryptocrystalline magnesite fragments are mostly rounded although many angular fragments have been observed. Whole-rock chemical analyses of the altered serpentinites show that they are enriched in SiO_2 and depleted in MgO (see Boschi et al., 2009, particularly their Fig. 10). These data suggest that silicification of the Malentrata serpentinites was accompanied by external input of silica, and mobilization of magnesium to the vein system. Most likely, moderate/low pH Mg-bearing hydrothermal fluids escaped from their original reaction zones and were focused in the fractures, where they experienced pressure loss and precipitated carbonates. About 70% of the original magnesium content was leached and mobilized to the main veins, while the remaining 30% was incorporated into the host rock as carbonate disseminations and veinlets. The calculated volume of magnesite, resulting from magnesium mobilization of a unit volume of serpentinite, is consistent with the observed volumetric proportion between main carbonate veins and altered serpentinites in the field.

In summary, we identified the following processes: 1) dissolution at low temperature of the fractured serpentinites by slightly acidic CO_2-rich and silica-rich hydrothermal fluids; 2) in situ silica precipitation penecontemporaneous with serpentine dissolution; 3) hydraulic fracturing and subsequent CO_2 loss (boiling) resulting in a brecciated texture, and local magnesite precipitation; 4) migration of fluids into a network of fractures and consequent focusing along main structural pathways; 5) boiling of the escaped fluids and beginning of the massive precipitation of magnesite and late dolomite (Boschi et al., 2008, 2009, 2010). The two-step-reaction proposed here – congruent dissolution of serpentinite and precipitation of carbonates away from the host-rocks – led to an increase of the initial porosity, allowing for a more efficient fluid infiltration into the rock.

6.3 The Montecastelli carbonated area

A body of serpentinite several kilometers across at the Montecastelli site, embedded in shales, has been deeply eroded by the Pavone River and provides good geological exposures. The central portion of the serpentinite body (near the river) hosts a small copper ore deposit that was intermittently exploited during the 19th century, and was definitively closed in 1869. Bornite, chalcopyrite, chalcocite and pyrite veinlets and nodules, in a chlorite-serpentine-brucite-amphibole soapy gangue, characterize narrow deformation zones crosscutting the serpentinites. The ore bodies contain very low grades and most of the material extracted during the exploration period was not high enough grade for industrial processing and it was dumped directly in front of the entrances of the mine, forming a

DOI: 10.3301/GFT.2015.02

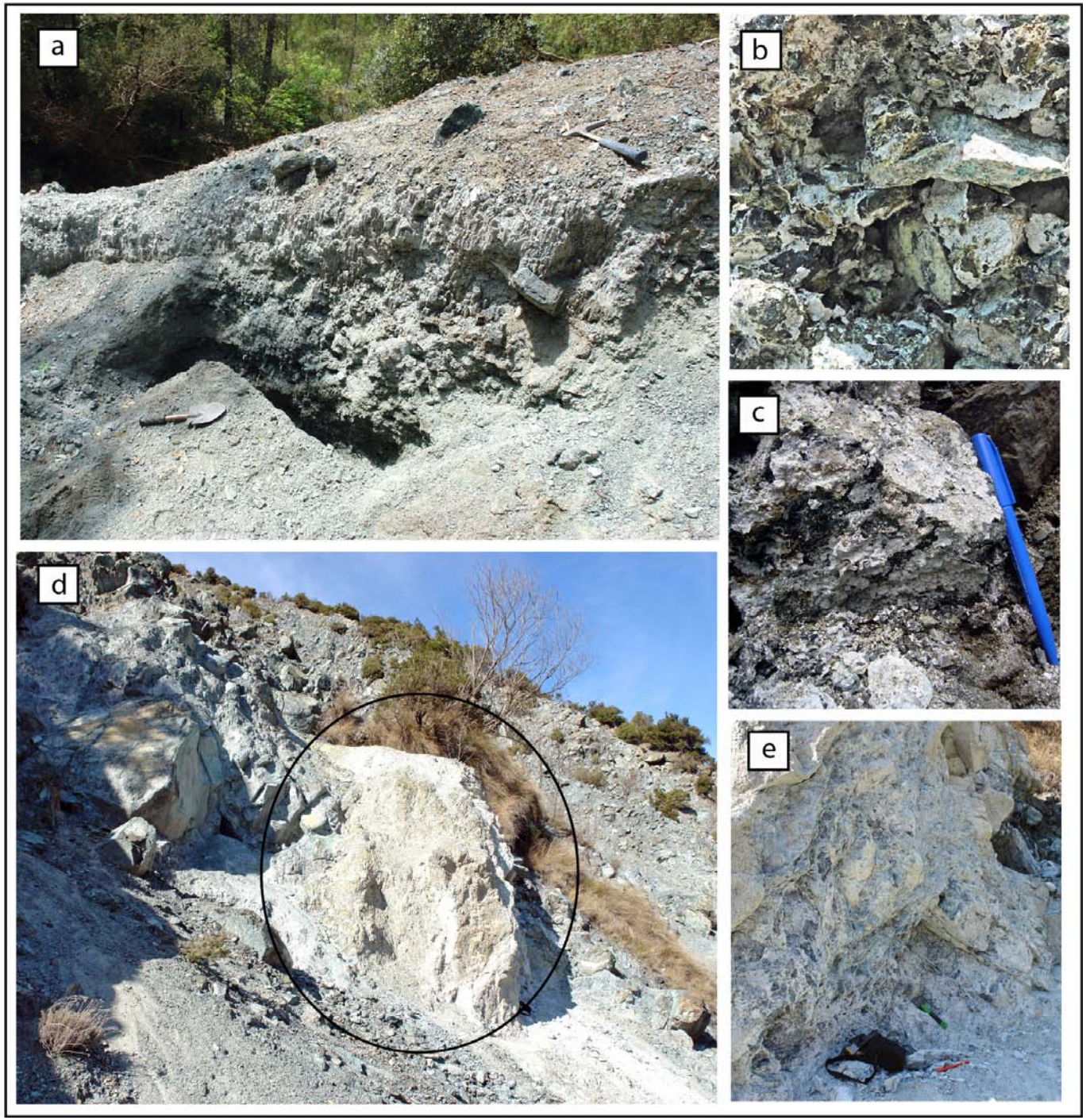

small mining dump. Further exploration activities inside the mine are younger than 60 years. Intense carbonation produced a crust of hydrated Mg-carbonates coating the serpentinite clasts of the mining dump and the serpentinite walls of the mine adits (Boschi et al., 2013). On the western side of the Pavone River, a large escarpment of incoherent serpentinites shows scattered, narrow spots, some meters wide, of whitish carbonated serpentinites that were shielded from alkaline spring waters (Fig. 32). These altered areas are characterized by an intense precipitation of hydrated Mg-carbonates and aragonite along the fractures and at the rock surface.

Fig. 32 - Pictures of: **(a)** the distal part of the mine tailing and; **(d)** the serpentinite escarpment; **(b)** and **(c)** are close up views of (a), showing clasts of serpentinite encrusted by whitish carbonates; **(e)** represents a particular of the carbonated wall of the serpentinite escarpment (d). Modified from Boschi et al., 2013.

DOI: 10.3301/GFT.2015.02

In the serpentinites escarpment (Figs. 32d, e), a network of fractures crosscut the rocks, showing large cavities partially filled by hydrated Mg-carbonates. Fractures are randomly oriented, clearly post-dating the early oceanic serpentine veining. Tailings at the Montecastelli mine (Figs. 32a, c) are composed of a bottom incoherent layer, up to 4m thick, of serpentinite clasts (up to 60 cm in diameter) that are randomly distributed with frequent voids between clasts. An intermediate layer, ranging from 10 cm to 1 m in thickness, consists of very fine-grained whitish carbonate-rich materials embedding altered clasts of serpentinites and copper sulfide-rich ore. At the top, a 15-40 cm of type c soil is alternating with minor quantities of serpentinite clasts and tree roots. On the distal part of the tailings, the bottom layer disappears, and very-fine grained and incoherent carbonate-rich layers alternating with a greenish serpentinite- and clay-rich part prevail.

In the mine, an inclined rising adit, approaching the Cu-rich orebody, intercepted a gently dipping fracture in massive serpentinite. Continuous water flow from the fractures produces a film of water along the roof and the walls of the adit as well as water dripping from the fractured hanging wall. Aragonite and hydrated Mg-carbonates continuously form on the wet surfaces of the adit.

6.3.1 The serpentinite and the hydrated Mg-carbonates

The Montecastelli serpentinites mostly preserve their original texture. OM and SEM-EDS observations indicate that the mesh texture of the serpentine after olivine, surrounded by magnetite-enriched mesh rims and relicts of primary spinel (Mg-chromite), typical of oceanic serpentinites, are easily recognized. Very fine-grained Fe-poor and Fe-rich brucites are frequently observed at SEM-EDS observations either associated with serpentine in the mesh texture, or as veins cutting the earlier minerals. A later network of light green chrysotile veins, with variable thickness up to several centimeters, pervasively crosscut the outcrops. These veins represent preferential zones of weakness where later meteoric fluids could be concentrated.

Actually, the hydrated Mg-carbonate precipitate is often observed along these fractures, growing on the external vein surfaces. Carbonate veining is accompanied by carbonate precipitation as a laminar/rounded whitish crust on the external surface of the rocks and/or as spherules up to 1 cm in diameter with radiating needles above the laminar crust or directly on the top of the rock (Fig. 33). In addition to these types, a fibrous whitish material has been observed to be intermixed with them.

DOI: 10.3301/GFT.2015.02

XRD analyses of selected samples revealed that the hydrated Mg-carbonate minerals are mostly hydromagnesite, with minor and variable amount of nesquehonite, $MgCO_3 \cdot 3(H_2O)$, manasseite, $Mg_6Al_2(CO_3)(OH)_{16} \cdot 4(H_2O)$, pyroaurite, $Mg_6Fe_3+2(CO_3)(OH)_{16} \cdot 4(H_2O)$, brugnatellite, $Mg_6Fe_3+(CO_3)(OH)_{13} \cdot 4(H_2O)$ and minor amounts of aragonite (Boschi et al., 2013; Bedini et al., 2013). No silica has been detected or observed in the field.

Spring water fluids (sampled close to the serpentine escarpment) show high pH (~8.2) and Mg and Ca concentrations (57 and 6.1 mEq/l, respectively), compared to the local rainwater (pH = 5.7; Mg= 0.04 and Ca= 0.02 mEq/l). These data suggest that infiltrated rainwater interacted with the host serpentinite rock, increasing pH and Mg content, without buffering its isotope composition.

The three areas show evidence of a rapid precipitation of hydrated Mg-carbonates as result of interaction between rainwater and serpentinites with ongoing atmospheric CO_2 uptake.

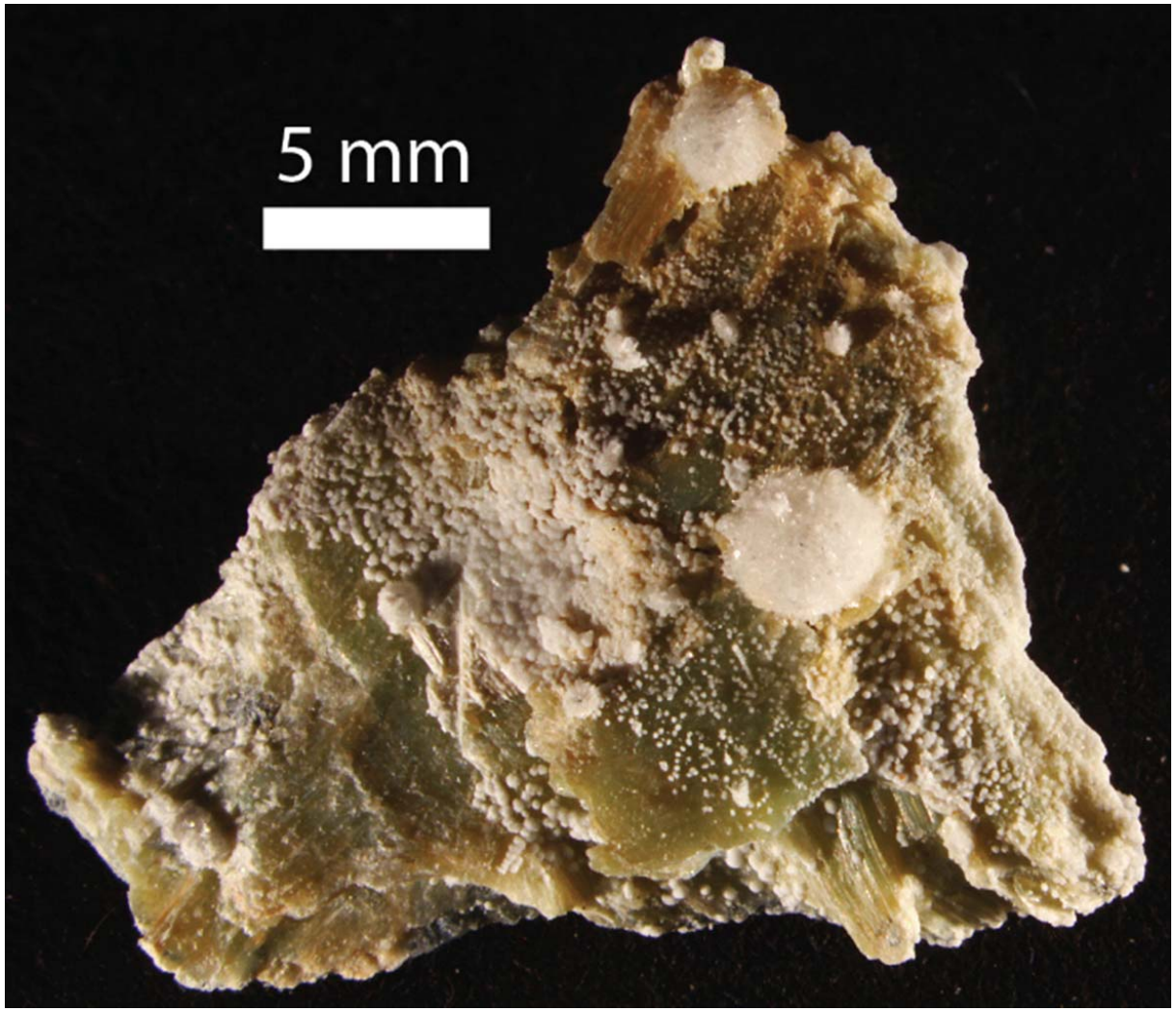

Fig. 33 - Examples of hydrated Mg-carbonates on serpentinites of the Mantecastelli area. The sample shows the two main type of precipitation: laminar whitish crust and spherules on the external surfaces of the rock.

DOI: 10.3301/GFT.2015.02

1st Day

From ores (Temperino mine, Campiglia M.ma) to
metals (Baratti-Populonia archaeometallurgical site)

STOP 1.1 – The Temperino adit, from Etruscan to modern exploitation
STOP 1.2 – Earle shaft and Gran Cava stope, the Cu-Pb-Zn-Ag skarn deposit
STOP 1.3 – Rocca San Silvestro, a time travel in a medieval mining village
STOP 1.4 – Short visit to the Acropolis of Populonia
STOP 1.5 – The beach slag deposit at Baratti (Populonia)
STOP 1.6 – The Etruscan "Chariots Tomb" (S. Cerbone necropolis, Populonia)

Stops 1.1-1.3: The Temperino Cu-Pb-Zn-Ag skarn deposit, Campiglia Marittima

Mining activity started at the Temperino mine during the 9th-6th century BC. Narrow shafts and inclined tunnels were excavated directly on the Cu-rich orebodies at the surface, and driven to significant depth (around 100 m) below the surface. Archaeologists discovered several fragments of Etruscan ceramics (oil lamps, vases) in the underground works. The intensive exploitation led to the formation of quite large rooms at depth that were invaded by water when the mine was abandoned in the 1st century BC.
After almost one millennium, between the 900 and 1300, mining activities flourished again. Chalcopyrite- and galena-rich ores at Temperino are particularly rich in silver (up to 2 kg per ton) and medieval activity was triggered by the increasing silver demand for coinage at the Pisa mint. The powerful family Della Gherardesca established a settlement in the mine area (Rocca San Silvestro) to control the whole process: from ore exploitation to metal production (mainly Ag). Medieval miners excavated underground works similar in shape and size to the Etruscan ones. The discovery of richer Pb-Ag deposits in other areas and the political decline of Pisa contributed to the rapid abandonment of the area at the beginning of the 14th century.
During the 16th century, the Grandukes of Tuscany undertook new exploration and small-scale production for silver but we must wait the 19th century for a systematic exploitation of the Cu-Pb-Ag ores. From 1841 several mining companies began to explore the deeper part of ore deposits by excavation of crosscut adits and shafts.

DOI: 10.3301/GFT.2015.02

Modern underground works intercepted many old stopes, draining off water and exposing beautiful rooms with walls covered by blue-green crusts of chrysocolla, malachite and azurite and lined by large crystals of gypsum and dendrites of native copper (Fig. 34). Exploration and small-scale exploitation intermittently continued until the Second World War, but all the companies had severe problems with water availability and the mineral separation processes. Between 1950 and 1976 a small mining company ran the mine and introduced flotation, and discovered a significant water resource in karstic marbles at the bottom of the main Earle shaft. Total production during the last management consisted of 40000 t of galena/sphalerite and 30000 t of chalcopyrite concentrates with about 24 tons of silver. In 1983, mining permits expired and since 1996 the whole area of the Temperino mine has been part of the San Silvestro Archaeomining Park.

Fig. 34 – Gypsum crystals on chrysocolla crusts from Etruscan exploitation openings (15 cm).

STOP 1.1: The Temperino adit, from Etruscan to modern exploitation

After arrival at the Archaeological Mines Park of San Silvestro (Website), you could start the (guided) visit of the Temperino mine from the so-called "Temperino" adit (Fig. 35); the entrance is located in an old mining building. The Temperino adit was dug around the mid-1800s to explore the southern end of the skarn deposit and the deepest part of the ore bodies reached by Etruscans and medieval miners. The first part of the

DOI: 10.3301/GFT.2015.02

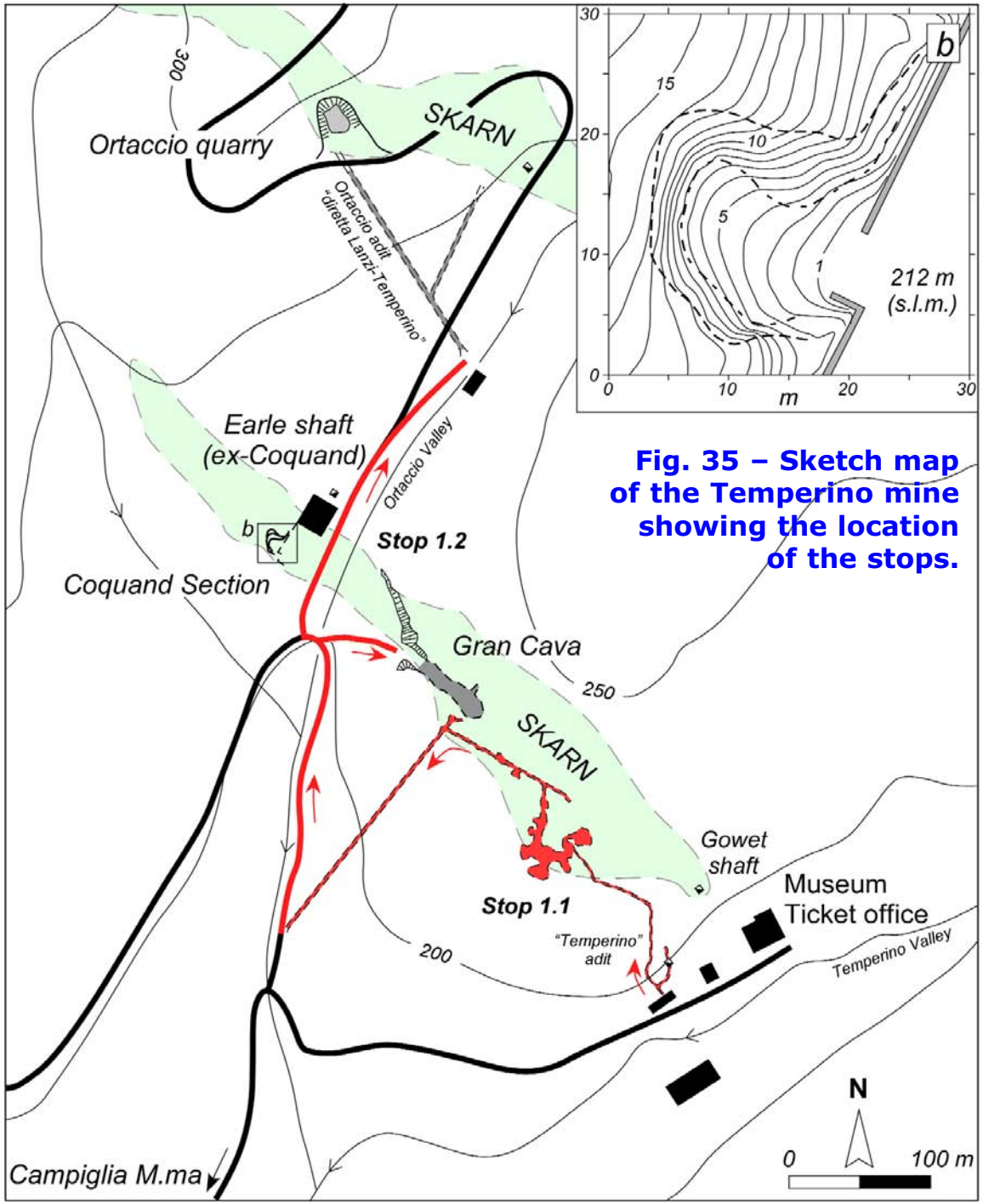

Fig. 35 – Sketch map of the Temperino mine showing the location of the stops.

underground path is a typical meandering 19th century drift crosscutting marble host rocks. After about 70 m we enter the skarn orebody that exhibits rhythmic layers of dark-green hedenbergite and black ilvaite with disseminations, veinlets and masses of chalcopyrite, pyrite, pyrrhotite, galena and sphalerite.

At this point the morphology of underground works suddenly change from a narrow adit to an irregular "rooms and pillars" excavation opening that resulted from the overlap of old (Etruscan, medieval?) and modern (19th and 20th century) exploitation activities. Most of the narrow Etruscan excavation openings are partially or totally occupied by mining infill (poorly sorted clasts of both barren and ore-rich skarn) cemented by chrysocolla, malachite, azurite, gypsum and native copper. A similar mineral assemblage encrusts the exposed walls in the upper part of the old excavation openings (not visible along the tourist path; Fig. 36). The large "rooms and pillars" excavation opening was mainly dug during the 20th century because it was one of the main access paths for miners to the lower levels of the mine (see the inclined shaft on the right descending to the level 2 and 3).

DOI: 10.3301/GFT.2015.02

Fig. 36 – Upper part of an old excavation opening showing encrustation of chrysocolla and gypsum.

The walls and roof of the main opening provide a very good 3D picture of textures/mineralogy of skarn orebody and mafic porphyry masses. Masses and dykes of mafic porphyry, entirely hosted by skarn, display the typical greenish-grey colour and a prominent porphyritic texture with phenocrysts of plagioclase, pyroxene, olivine and biotite associated with resorbed xenocrysts of sanidine (centimetric megacrysts) and quartz. Several residual voids (geodes) are found in the skarn. Most of the geodes show pipe-like or irregular spheroidal geometries but, sometimes, they mimic the cuspate geometry of rhythmically layered hedenbergite-ilvate skarn. Their dimensions range from few cm^3 up to several m^3. The surfaces of geodes are lined by prismatic crystals of quartz (up to 40 cm in length) and more rarely by fine crystals of ilvaite (1-8 cm), pyrite and, more rarely, garnet. Marble, skarn, and mafic porphyry are crosscut by a NW-SE trending subvertical dyke of acidic

DOI: 10.3301/GFT.2015.02

porphyry. The acidic porphyry (originally syenogranitic in composition) is made by small phenocrysts of quartz, K-feldspar, plagioclase and biotite set in a very fine-grained groundmass. When hosted by marble, the acidic porphyry maintains its original magmatic texture (in spite of the pervasive potassic alteration; sericite and adularia), while portions hosted by skarn are totally replaced by a propylitic assemblage (epidote ± calcite ± quartz) resulting in a beautiful olive-green, fine-grained epidosite.

At the northern end of the main "rooms and pillars" excavation we enter a long, straight drift, wider than the previous one: it was dug in the 1960s as a minor haulage drift of the mine. Walking along this drift you encounter other old excavation openings, beautiful outcrops of skarn and ore minerals, and spectacular drapes of blue chrysocolla covering the lateral surface of the tunnel. It is an ongoing process triggered by meteoric water that, after having leached copper and silica from the Cu-rich skarn above, followed a downward path along tiny fractures until it dripped off at the top of the tunnel. Dripping of Cu-saturated water is frequently observed (depending on the season) and the blue crusts and drapes are still soft.

After a few metres you leave the skarn body and you walk through the marble host until the exit of the tunnel. Now we walk uphill through the Ortaccio Valley, quickly reaching the next stop.

STOP 1.2: Earle shaft and Gran Cava stope, the Cu-Pb-Zn-Ag skarn deposit

Walking uphill along the Ortaccio Valley you can observe the south-western slope of the hill mantled by large mining dumps (Fig. 35). They represent the residue of old and modern excavations. In fact, several narrow inclined shafts pierce the hill connecting the surface to the excavation opening seen previously in the Temperino adit. In a few minutes you reach the Earle shaft (212 m elevation): the main shaft for ventilation, drainage and for hoisting of personnel and materials (Fig. 37). The original headframe, hoist house, cage and steel wire

Fig. 37 – The Earle shaft, Temperino mine.

DOI: 10.3301/GFT.2015.02

ropes are still in good condition and the last descent was performed in 1998. It was originally (second half of 19th century) called the "Coquand shaft" from the name of the French mining engineer that reopened the mine after many centuries of neglect. The main skarn orebody passes to the west of the shaft. Here, there is a small quarry exposing a complete section of skarn and porphyries that was known as the "Coquand Section". This geological section represents the first locality in the world where skarn textures and mineralogy were described in detail (vom Rath, 1868; Burt, 1982). Recently, the "Coquand Section" was cleared of vegetation and mapped in great detail (Fig. 38). Different skarn types (hedenbergite, massive ilvaite, and rhythmically layered hedenbergite-ilvaite), mafic porphyry and epidotized acidic porphyry are well exposed but the observation is made difficult by widespread oxidation coatings.

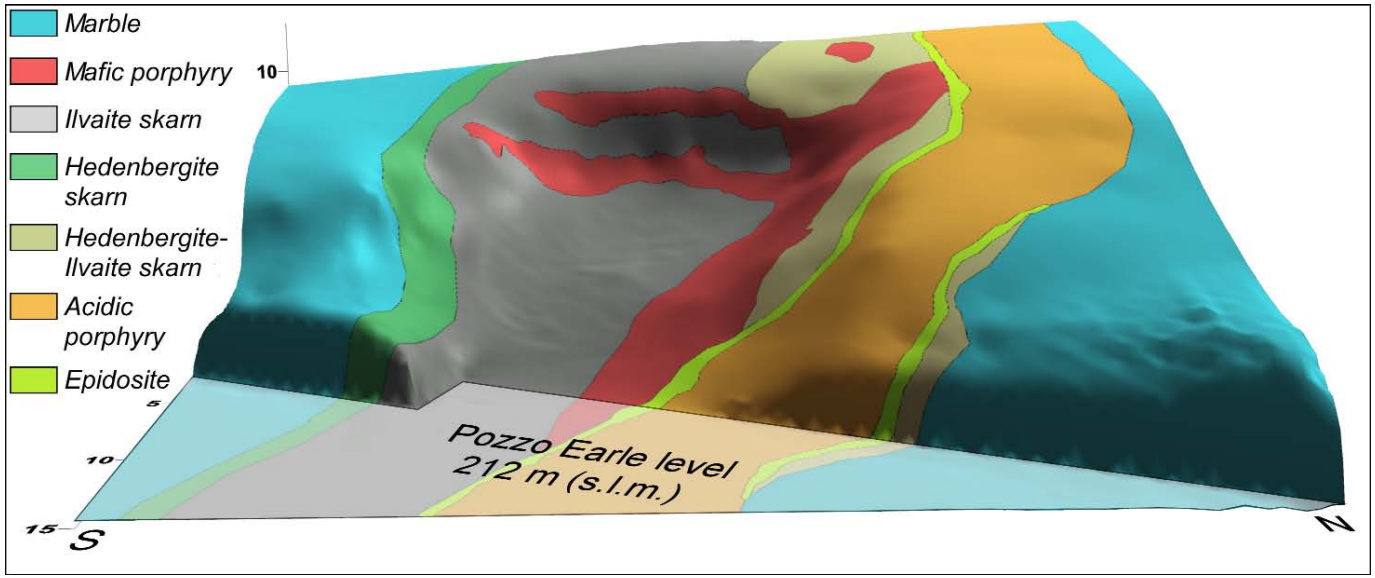

Fig. 38 – 3D view of the Coquand Section (modified after Da Mommio et al., 2010).

From the Earle shaft, moving north-east along the Ortaccio Valley, you arrive at the station of the mine train for tourists. The tourist railway follows the path of the Ortaccio adit (the so-called "diretta Lanzi-Temperino"), a 20th century tunnel connecting the Ortaccio Valley to the Lanzi Valley (to the north-west) where the ore minerals were treated in the flotation plants. The Ortaccio adit was dug in marbles but, after a few hundred metres, it crosscuts a second main skarn orebody, parallel to the one we visited in the Temperino adit. A thick dyke of acidic porphyry passes through the valley near the entrance of the Ortaccio adit (north side). The magmatic rock shows a prominent porphyritic texture with centimeter-scale sanidine phenocrysts and smaller quartz, plagioclase, and biotite phenocrysts set in a yellowish fine-grained groundmass (the so-called "yellow porphyry"). This dyke is quite different from the acidic porphyry that we saw earlier: it represents the last magmatic event crosscutting skarn, mafic porphyry, and also the epidotized acidic porphyry.

DOI: 10.3301/GFT.2015.02

The last outcrop to be visited is the "Gran Cava" stope (Great Quarry): a large, horizontal excavation opening (20x15x60 m), (possibly) excavated by the Etruscans and then enlarged during subsequent exploitation workings in medieval, renaissance and modern times. The entrance of the "Gran Cava" is on the opposite side of the Ortaccio Valley from the Earle shaft. Beautiful outcrops of hedenbergite-ilvaite skarn, mafic porphyry, and epidotized acidic porphyry occur at the "Gran Cava".

STOP 1.3: Rocca San Silvestro, a time travel in a medieval mining village

Rocca San Silvestro, a medieval village of miners and smiths (Fig. 39), was founded as a seigniorial enterprise between the 10th and 11th centuries AD in order to exploit the local deposits of copper and silver-rich lead ore (Fig. 6). These metals were used for coin production principally in the Tuscan mints ("zecche toscane") of Pisa and Lucca; the village lords enjoyed close commercial relations with these cities during the period. In medieval times this village was known by the name of "Rocca a Palmento" (a millstone, or "palmentum", has been discovered in the oil press below the church) and owes its present name to the saint to whom the church was dedicated.

The first archaeological excavations at the medieval village of Rocca San Silvestro were started in 1984 by the Department of Teaching of Archaeology and History of Arts of the University of Siena, in collaboration with numerous European university departments. The excavation, involving two thirds of the site, has revealed the complex layout of the village and allowed the functional organization of the living quarters to be defined. It is precisely the internal spatial organization of the settlement, with areas set up for metallurgical production, the living quarters, the church, and the castle, which reveal Rocca San Silvestro as a center whose birth, development and decline depended on its industry and on the managerial skills of its lords.

Fig. 39 – The medieval village of Rocca San Silvestro

The visitor follows an itinerary designed to show the social and economic organization, the eating habits, the building, and metallurgical techniques of a medieval community. The access to the Rocca is via a path starting from Villa Lanzi, walking uphill, for about 20 minutes, through old mining areas (from Etruscan to modern time).

DOI: 10.3301/GFT.2015.02

Stops 1.4-1.6: The archaeological Park of Populonia-Baratti

We move back towards Piombino, and take the road to Populonia. Thus we enter the "Populonia-Baratti Archaeological Park" (Website), a real open-air museum which includes a significant part of the ancient "Pupluna", a unique Etruscan settlement built directly on the sea. After parking the car at the S. Cerbone parking area, we can get on the shuttle bus to reach the ancient Acropolis of Populonia (Fig. 40).

Fig. 40 – Sketch map of the "Populonia - Baratti Archaeological Park" with location of stops. The dotted circle encloses the "Industrial area" (modified after Benvenuti et al., 2000).

DOI: 10.3301/GFT.2015.02

STOP 1.4: Short visit to the Acropolis of Populonia

The acropolis extended over two hills at the top of the promontory: Poggio del Castello and Poggio del Molino (o del Telegrafo) (Fig. 41). From the very hilltop of the Acropolis you can enjoy the spectacular view of the promontory of Piombino and the Gulf of Baratti, with the island of Elba at some distance and the Etruscan necropolises, the calcarenite quarries, and the industrial ironworking quarters below along the Baratti plain.

You join the Villanovian "Villaggio delle capanne" ("village of huts"), where in the 8th-9th century BC important houses were built on the Acropolis, to accommodate the most ancient aristocracies of Populonia. There remain faint and picturesque traces of these houses on the summit of the acropolis, not far from the monumental structures of another Populonia, the Roman one, which around the 2nd cent. BC built important temples, thermal spas, and sanctuaries right in the heart of the city.

Fig. 41 – The Acropolis of Populonia: view of the paved street connecting the Temples with "Le Logge" edifice (courtesy of the Società Parchi Val di Cornia SpA).

DOI: 10.3301/GFT.2015.02

STOP 1.5: The beach slag deposit at Baratti (Populonia)

After returning to the S. Cerbone necropolis, we leave the shuttle bus and arrive at the beach to see the remains of the slag deposit, a poorly cemented heap of Etruscan and Roman slag discharged over an erosional terrace (Fig. 42). The bottom portion of the deposit mostly consists of large plano-convex cakes and fragments of copper slags, clearly identifiable by the greenish spots (due to exogenous alteration of copper sulfides) on their surfaces. Copper slags from these layers have been radiocarbon dated to the IX-VIII century BC. (Cartocci et al., 2007). Slag cakes have diameters in the range of 26 to 40 cm (Fig. 43a); some of them are multilayered, each layer made of small needle-like crystals of olivine separated by tiny films of magnetite (Chiarantini et al., 2009b). Mineralogy of most of the copper slag is quite homogeneous: a groundmass of fayalitic olivine, hedenbergite, magnetite and scarce glass includes variable (but always minor) amounts of "matte"(Cu-Fe±Zn) sulphides and metallic phases (Fig. 43b). Two preliminary main types of copper slags based on relative proportions of matte sulphides and metallic phases were distinguished by Benvenuti et al.

Fig. 42 – The Baratti beach slag deposit (photo by M. Benvenuti, 2007).

DOI: 10.3301/GFT.2015.02

(2000): (1) slags enriched in metallic copper (called "type-A" slags), and (2) matte-rich slags ("type-B" slags), although in a small group of samples the two types of metal-bearing phases occur almost in equal amounts. The first group of copper slags ("Cu-rich slags") is characterized by the presence of a silicate groundmass with abundant magnetite and droplets (up to 400 μm in diameter) of metallic copper (Fig. 43c), sometimes associated with rare metallic bismuth, lead and copper sulphides like covellite, chalcocite, and digenite (Fig. 43c). However, magnetite is scarce in the "matte-rich slags", and copper does not occur in the form of metallic copper but as matte droplets (50-150 μm in diameter) showing fine exsolution textures (Figs. 43a-b). These features could indicate a multi-stage copper smelting process, with type-B slag belonging to an earlier (matte production) stage than type-A slags.

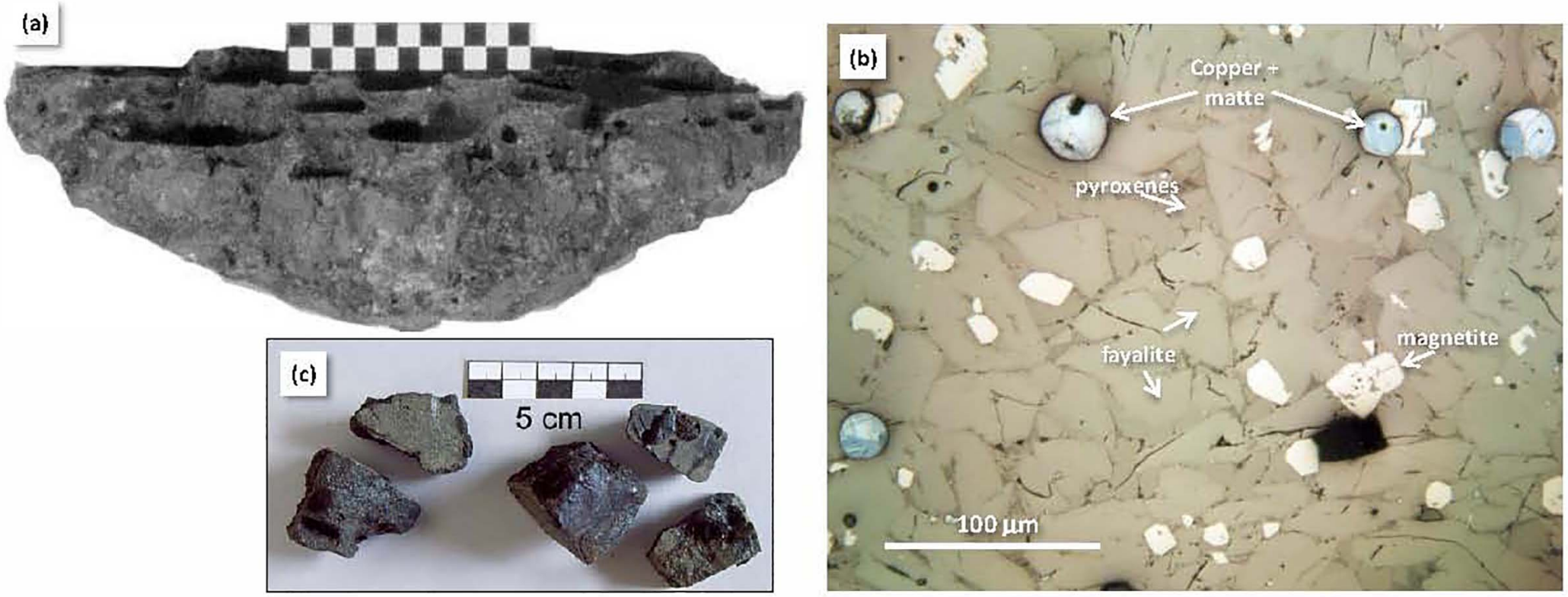

Fig. 43 – Macroscopic and microscopic features of copper slag from the Baratti beach slag deposit: **(a)** copper slag cake; **(b)** reflected light microscope image of a matte-rich copper slag showing several matte (±copper) droplets in a matrix of fayalite, pyroxenes and subhedral magnetite crystals; **(c)** fragments of copper slag.

DOI: 10.3301/GFT.2015.02

The largest portion of the archaeometallurgical deposit consists of iron slag produced by both primary (bloomery) smelting and by post-reduction ironworking (smithing, etc.). The iron bloomery slags (Fig. 44a) are mainly a silicate groundmass of fayalitic olivine (with up to 1.45% CaO) in an iron-rich interstitial glassy matrix (up to about 25 wt.% FeO), which in itself is normally a eutectic of anorthite and fayalite. Wüstite, magnetite, hercynite, and partially smelted, relic phases like quartz, hematite and scheelite, occur in variable amounts, and are especially abundant in furnace slags. Fayalite crystals in tapped slags occur as small laths associated with micrometric dendrites of wüstite (Fig. 44b), while in furnace slags both minerals show a significant increase in size. Unlike tapped and furnace slags, furnace conglomerates show abundant relics of hematite and quartz and a more silica-rich (and FeO-poor) glassy groundmass. Iron slags almost invariably contain droplets of metallic iron (Fig. 44b). Some iron slags are enriched in tin and tungsten and may contain micrometric globules of iron-tin alloys, approximating FeSn and $FeSn_2$ in composition, as well as calcium tungstates (Figs. 44c-d). These mineralogical and geochemical features are in agreement with a provenance of smelted iron ore from the hematite-rich deposits of nearby Elba Island, which show characteristic W–Sn-rich geochemical signatures (Benvenuti et al., 2013).
Fragments of smelting furnaces are also commonly present in the Baratti beach deposit. They are made up of local Macigno sandstone and baked clay (Benvenuti et al., 2003b).

Archaeological excavations carried out in the last decades in the upper portion of the beach slag deposit unearthed a number of simple hearths made with local sandstone blocks and bricks lined with clay (Fig. 45). These structures, interpreted as smithing/reheating hearths for iron working (Chiarantini et al., 2009a), have been dated to the V-II century BC (Cartocci et al., 2007). These hearths closely resemble the III-II century BC furnaces described by Voss (1988) in the upper portion of the slag beach deposit, although the latter author described it as a smelting furnace rather than a forge. Abundant plano-convex slag occurs in the upper part of the deposit (Fig. 44e). Most of them are made up of fayalite and iron oxides (wüstite, magnetite) and could be related genetically to slagging and metal oxidation which are the dominant processes occurring during the heating of metal for hot forging. The relatively high amounts of iron particles and iron oxides/hydroxides, observed in some samples (Fig. 44f), indicate that a significant loss of iron took place during iron working, while the abundance of quartz relics could imply the use of siliceous fluxes added to the surface of the metal during welding operations and/or to minimise iron oxidation during the fashioning of objects (Chiarantini et al., 2009a).

DOI: 10.3301/GFT.2015.02

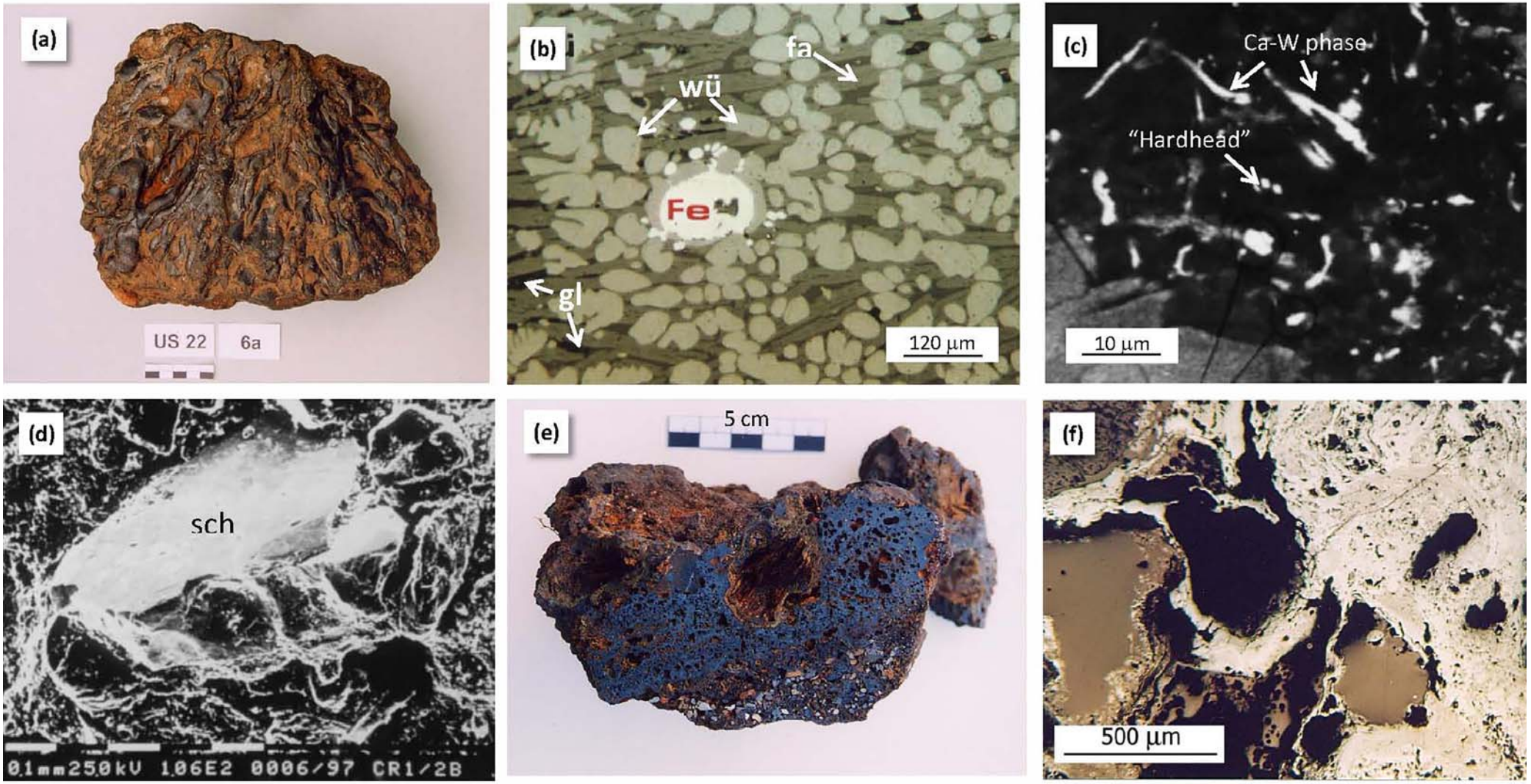

Fig. 44 – Macroscopic and microscopic features of iron slag from the Baratti beach slag deposit. **(a)** Tapped slag; **(b)** reflected light image of a tapped iron smelting slag showing a droplet of metallic iron (Fe) associated with wustite (wü), fayalitic olivine (ol) and glass (gl); **(c)** Reflected light image of an iron slag showing lamellar Ca-W phases (probably scheelite) and droplets of FeSn and $FeSn_2$ ("hardhead"); **(d)** backscattered image of a furnace slag, showing a grain of relic scheelite (sch). Scale = 10µm; **(e)** Cross-section of a plano- convex slag showing inclusion of charcoal and, on the lower surface, hammerscale and particles from ground level; **(f)** Reflected light image of globular hammerscale from sample shown in (e).

DOI: 10.3301/GFT.2015.02

Fig. 45 – "Furnace III" (V-III cent. BC). This furnace, interpreted as a smithing hearth, was partly excavated in a slag-rich layer. It has an internal diameter of about 25 cm; furnace walls are made of sandstone blocks and clay bricks or tiles, arranged in a horseshoe, quadrangular shape.

STOP 1.6: The Etruscan "Chariots Tomb" (S. Cerbone necropolis, Populonia)

It's surely worth visiting at least one of the most famous Etruscan tombs located in the nearby S. Cerbone necropolis: the "Chariots Tomb", a fine example of the so called "tombe a tumulo", made up of rectangular burial chambers covered with an earthen tumulus (Fig. 46). This monumental type of burial (with a diameter of 28 metres) appeared at Populonia in the VII cent. BC. The Chariots Tomb is the largest burial edifice found at Populonia. It owes its name to the presence of a chariot with four-spoked wheels within the burial chamber. The tomb was discovered in 1914 by A. Minto.

Fig. 46 – The Charriots Tumb at Baratti: aerial view (courtesy of the Società Parchi Val di Cornia SpA).

DOI: 10.3301/GFT.2015.02

2nd Day

The geothermal field of Larderello and the Malentrata mine

STOP 2.1 – The Geothermal museum of Larderello
STOP 2.2 – The geothermal demonstrative well
STOP 2.3 – The geothermal equipment at the "Nuova San Martino" geothermal power plant
STOP 2.4 – Natural gas vents at Monterotondo Marittimo
STOP 2.5 – Malentrata mine: The Mio-Pliocene sedimentary cover
STOP 2.6 – Malentrata mine: The sedimentary envelope of the ophiolites
STOP 2.7 – Malentrata mine: The serpentinite protolith
STOP 2.8 – Malentrata mine: The serpentinite-argillite contact
STOP 2.9 – Malentrata mine: Carbonated serpentinites and carbonate-silica veins

Stops 2.1-2.4: The geothermal field of Larderello

STOP 2.1: The Geothermal museum of Larderello

Leaving Massa Marittima, follow the signs to Larderello. The first stop is dedicated to the Geothermal museum (Fig. 47). The museum is located in one of the first buildings, recently restored, that the de Larderel family built during the initial period of

Fig. 47 – Location of Larderello geothermal museum and of demonstrative geothermal well (Stop 2.1 and Stop 2.2).

DOI: 10.3301/GFT.2015.02

industrial exploitation (18th century). The museum, founded by the Larderello Joint Stock Company in the late 1950s, outlines the local history of geothermal energy (Website). It hosts finds and tools from Etruscan and Roman periods when the geothermal resources were mainly used for thermal baths, continuing through the period of borax production in the 17th and 18th centuries, to the present time with exploitation and exploration for electricity production, and showing drilling methods (well-illustrated with models and original equipment) and different ways of using geothermal fluids to produce thermal and mechanical energy, as well as certain aspects of the social development of the area. Samples with minerals from the Larderello area are also exhibited.

STOP 2.2: The geothermal demonstrative well

The geothermal well N120 is located about 700 m ESE from the Geothermal Museum (Fig. 47). This well is used for demonstration purposes. It was drilled in 1956 into the first geothermal reservoir and it is equipped with an electrically controlled opening valve. Both the depth and capacity of this well are considered moderate. This well, when it is opened, gives rise to an impressive column of steam at about 220°C (Fig. 48). The main well features are:

- Total depth: 740 m
- Casing: up to 600 m depth
- Steam capacity: 20 t/h
- Steam temperature: 220°C
- Output pressure: 5 bar
- Outflow speed: 400 m/s
- Stratigraphic sequence: formations belonging to the Ligurid unit and the tectonic wedge complex.

Fig. 48 – The Geothermal demonstrative well at Larderello.

DOI: 10.3301/GFT.2015.02

STOP 2.3: The geothermal equipment at the "Nuova San Martino" geothermal power plant

From Larderello follow the road signs to Monterotondo Marittimo, pass the village along the SS398 route, and at about 1.5 km from Monterotondo Marittimo turn on the left following the sign for the Nuova Centrale San Martino of ENEL (Fig. 49). This Stop will visit examples of different geothermal equipment involved in the geothermal production process. The equipment (comprising drilling technology of geothermal wells, a sectioned turbine with an alternator, the AMIS system, and examples of the use of steam for multiple purposes) are exhibited for educational purposes along the perimeter of the Nuova San Martino geothermal power plant (Fig. 50).

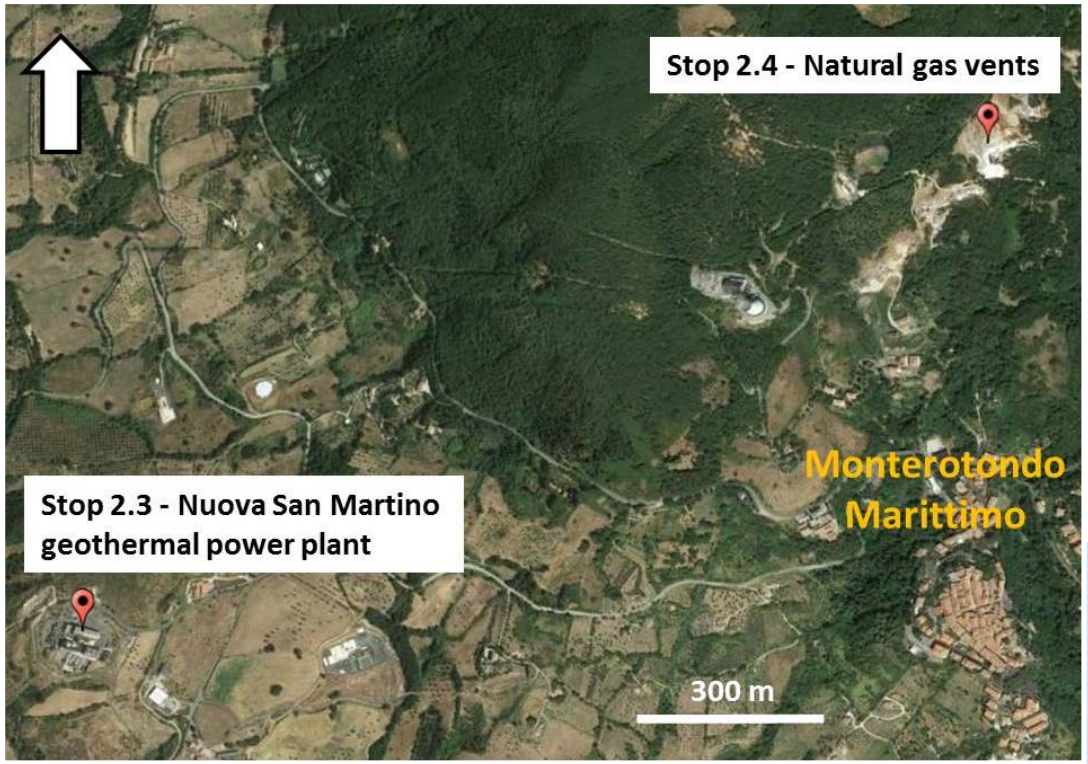

Fig. 49 – Location of Stop 2.3 (Nuova San Martino geothermal power plant) and Stop 2.4 (Natural gas vents at Monterotondo Marittimo).

Fig. 50 - Nuova San Martino geothermal power plant (built 2005).

DOI: 10.3301/GFT.2015.02

AMIS is the acronym for "Abatement of Mercury and Hydrogen Sulfide" in the Italian language. The italian geothermal power plants are characterized by a high Non Condensable Gas (NCG) content, averaging 4.4% by weight in the steam fed to the turbines. NCG is composed mainly of CO_2 (over 95% by weight of the NCG). Hydrogen sulfide is partitioned between the gas discharged to the atmosphere and the cooling water and it is stripped from the latter stream in the cooling towers. Since it has a characteristic bad smell, it constituted a problem from an environmental point of view. Owing to the particular features of the italian power plants (small sizes and unattended) and of the geothermal fluids (high content of NCG), the abatement technologies available on the market were not suitable and entailed excessive costs. As a consequence, it became necessary to develop an innovative abatement process. This objective was achieved through the invention of the AMIS® technology (Baldacci & Sabatelli, 1997), entirely designed and developed by ENEL (Baldacci, 2001). The AMIS® abatement system is placed before the gas enters the cooling towers and treats the NCGs with efficiencies near 100% removal for H_2S and 95% for Hg. The first commercial unit (Figs. 51 and 52) was installed in 2002 on a 20 MW power plant in the Mt. Amiata area, where the steam characteristically had high mercury concentrations. The AMIS® system has been installed on new and existing geothermal power plants in a continuing program that is still in progress. A recent study (Pertot et al., 2013) evaluated the air quality controlled by the AMIS® system and indicated a significant reduction of the geothermal power plant's contribution to the annual average atmospheric concentration of H_2S and Hg.

The drilling equipment on display are part of the drilling technology utilized by ENEL for a geothermal drilling project. ENEL develops both well design and drilling of geothermal wells over 4000 m deep. The geothermal well design is a "bottom-up" process: the location of the production zone determines the well's depth, and the expected flow rate determines the diameter at bottom hole. ENEL standards usually consist of 9" 5/8 production casings and an 8" ½ open hole. The well's profile continues by successively larger casing strings at shallower levels as required by drilling or geological considerations in order to isolate the well from the surrounding grounds (Fig. 53). At the surface, a wellhead controlled by valves connects the well to the steam gathering system.

At present, ENEL has eight drilling rigs including MASS6000 and the HH300 automatic rig, specially designed according to ENEL specifications. During the drilling process the drill string movement can be provided by the rotary table or by top-drive, electric or hydraulic motors suspended from the hook and connected to a short section of pipe. In this case the rotary mechanism is free to travel up and down the derrick. The lower portion of

DOI: 10.3301/GFT.2015.02

the drill-string consists mainly of bit, mud motor (in directional drillings), stabilizers, drill collar, heavy-weight drill-pipe and jarring devices. The bottom hole assembly must provide force for the bit to break the rock, survive a hostile mechanical and chemical environment, and provide the directional control of the well in case of a target

Fig. 51 - AMIS® abatement system (patentee: ENEL SpA). **1)** inlet water; **2)** inlet gas; **3)** mercury removal; **4)** HR2RS reactor; **5)** SOR2R scrubber; **6)** treated gas; **7)** gas cooler; **8)** cooled gas output; **9)** gas inlet to the blower; **10)** gas outlet from the blower. Photo from ENEL (2009).

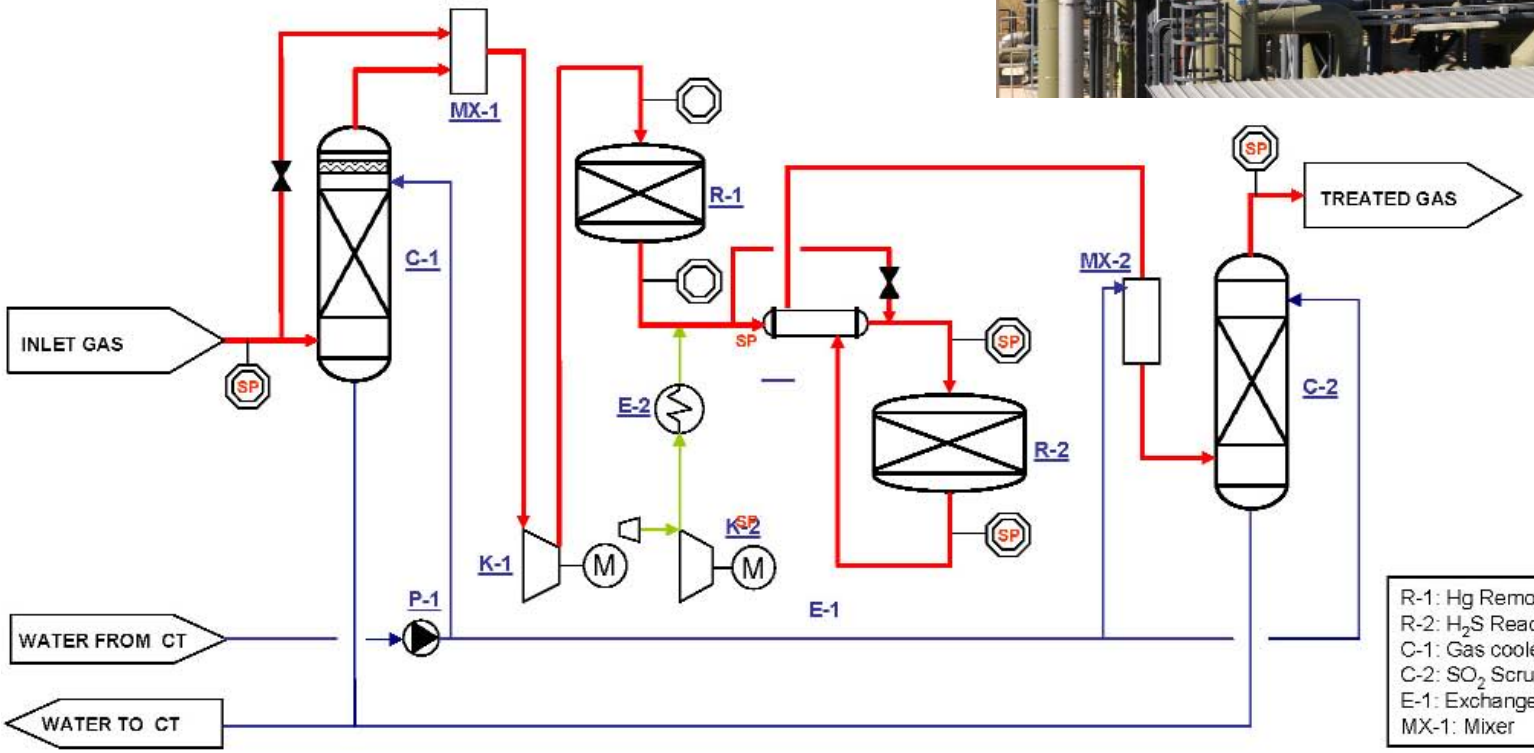

Fig. 52 - Simplified process flow diagram of an AMIS® plant (Sabatelli et al., 2009).

DOI: 10.3301/GFT.2015.02

displaced from the well vertical axis (Fig. 53). The most common rock bit is composed of three cones with hard metal inserts free to rotate at the bottom of the hole. Mud (water plus bentonite clay) is usually used for drilling through cover formations. Otherwise, the reservoir formations, usually characterized by high temperature and total loss of circulation, are drilled with water as the circulating fluid. The main features of the Nuova San Martino power plant are:

Type	Direct contact condenser
Cooling tower	6 units (mechanical drafts)
AMIS® plant	Yes
Installed Capacity	40 MW
N ° groups	1

STOP 2.4: Natural gas vents at Monterotondo Marittimo

The natural environment of the boraciferous region has been modified by human activity. Steam is completely utilized for energy production, and the hydrothermal manifestations are now present in limited areas only. At present, of the many and impressive natural manifestations of the Larderello-Travale geothermal field found in the past, a few can be seen in the area between Sasso Pisano and Monterotondo Marittimo along a normal fault system that displaces the Tuscan nappe sequence.

Returning to the Monterotondo Marittimo village the road crosses the neoautochtonous deposits, covered by recent

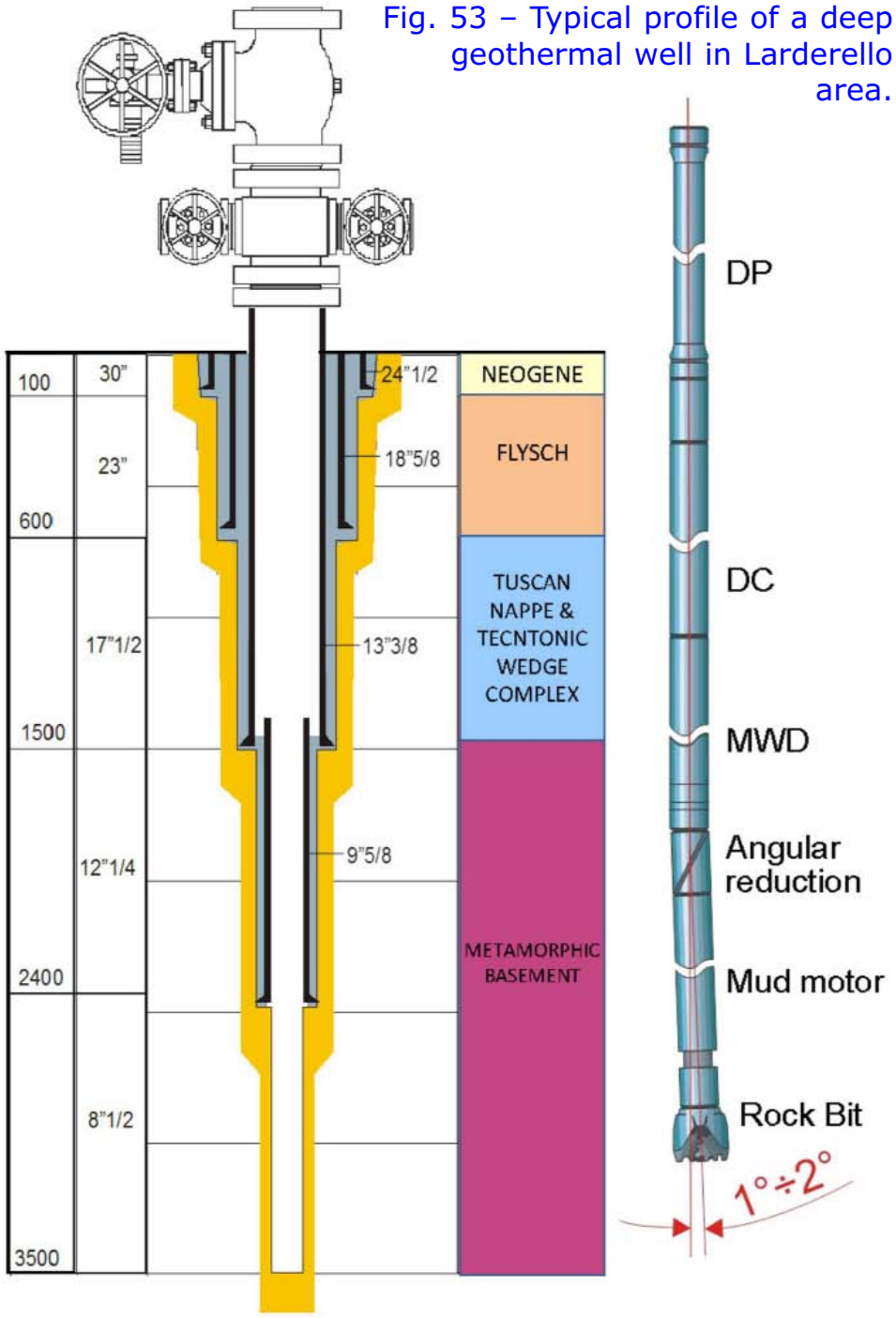

Fig. 53 – Typical profile of a deep geothermal well in Larderello area.

DOI: 10.3301/GFT.2015.02

detritus in places, and also crosses modest outcrops of the flysch units. As it approaches the village, the road plunges into the largest outcrop of the non-metamorphic Tuscan unit that is characteristic of the zone (Fig. 54). Follow the road signs for the "biancane" and go up to the hill to the extensive thermal manifestations of

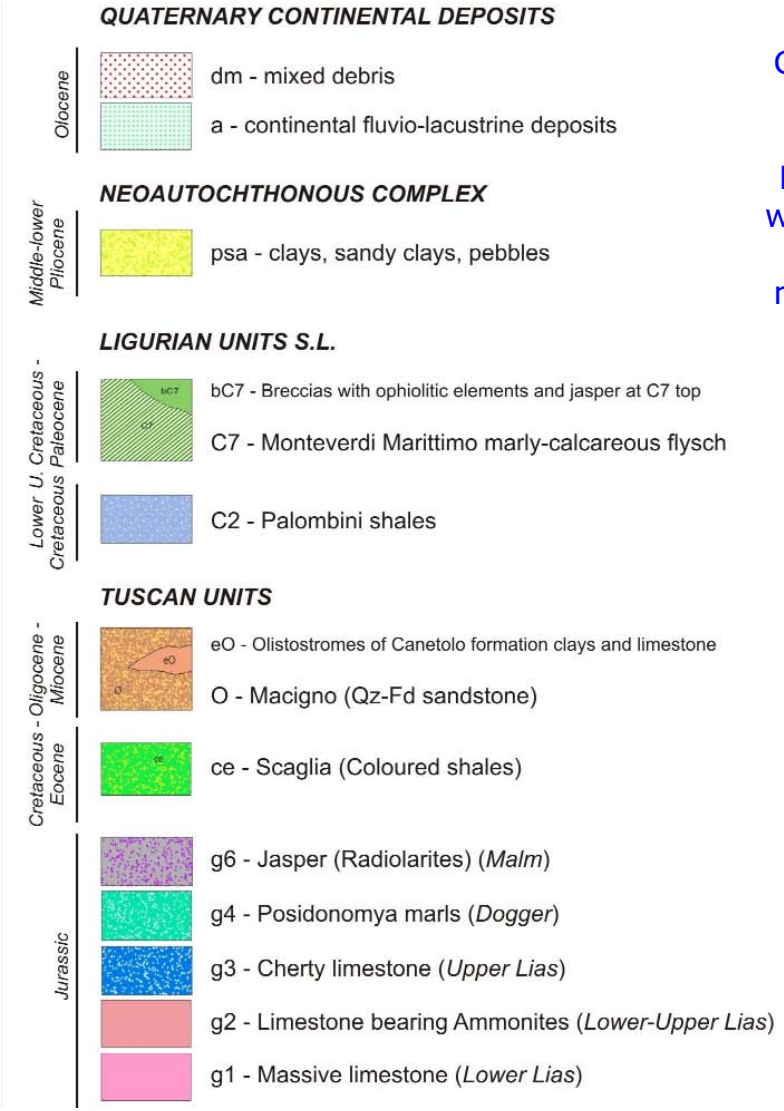

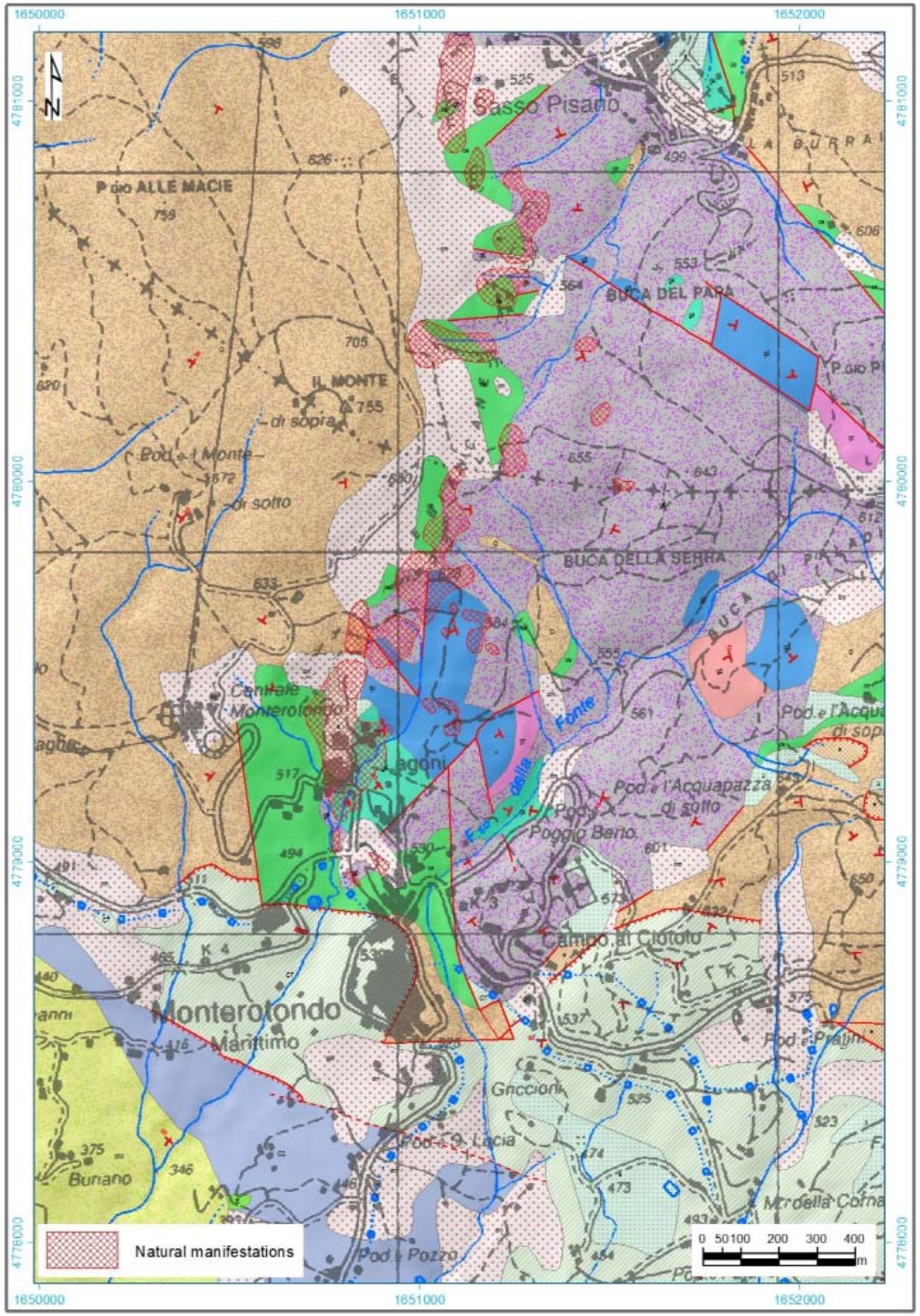

Fig. 54 - Geological map of the Monterotondo Marittimo area with locations of the natural manifestations. Modified from Lazzarotto (1967).

DOI: 10.3301/GFT.2015.02

Monterotondo (Fig. 49), which are characterized by steam and gas emanations and intense alteration of the outcrops. The rocks that usually constitute the top of the shallow geothermal reservoir are exposed in this zone: the Tuscan unit, from "massive limestone" (Lias) to "Macigno sandstone" (Upper Oligocene - Lower Miocene), is exposed in the southern and eastern part of "Il Monte" hill (755 m elevation) thanks to a tectonic window of an anticline structure. The fumaroles are located in the Middle Jurassic radiolarites (jasper) formation that, despite its thinness, shows a particularly broad outcrop. These are deeply altered by circulation of hydrothermal fluids channelled to the surface through a fracture network, mostly with a nearly vertical attitude. Hydrothermal circulation produced a complete "bleaching" (= whitening and hence the local name "biancane") of the siliceous layers, usually variegated, and weight loss. Widespread beautiful sulphur crystal blooms are present at the hydrothermal vents (Fig. 55).

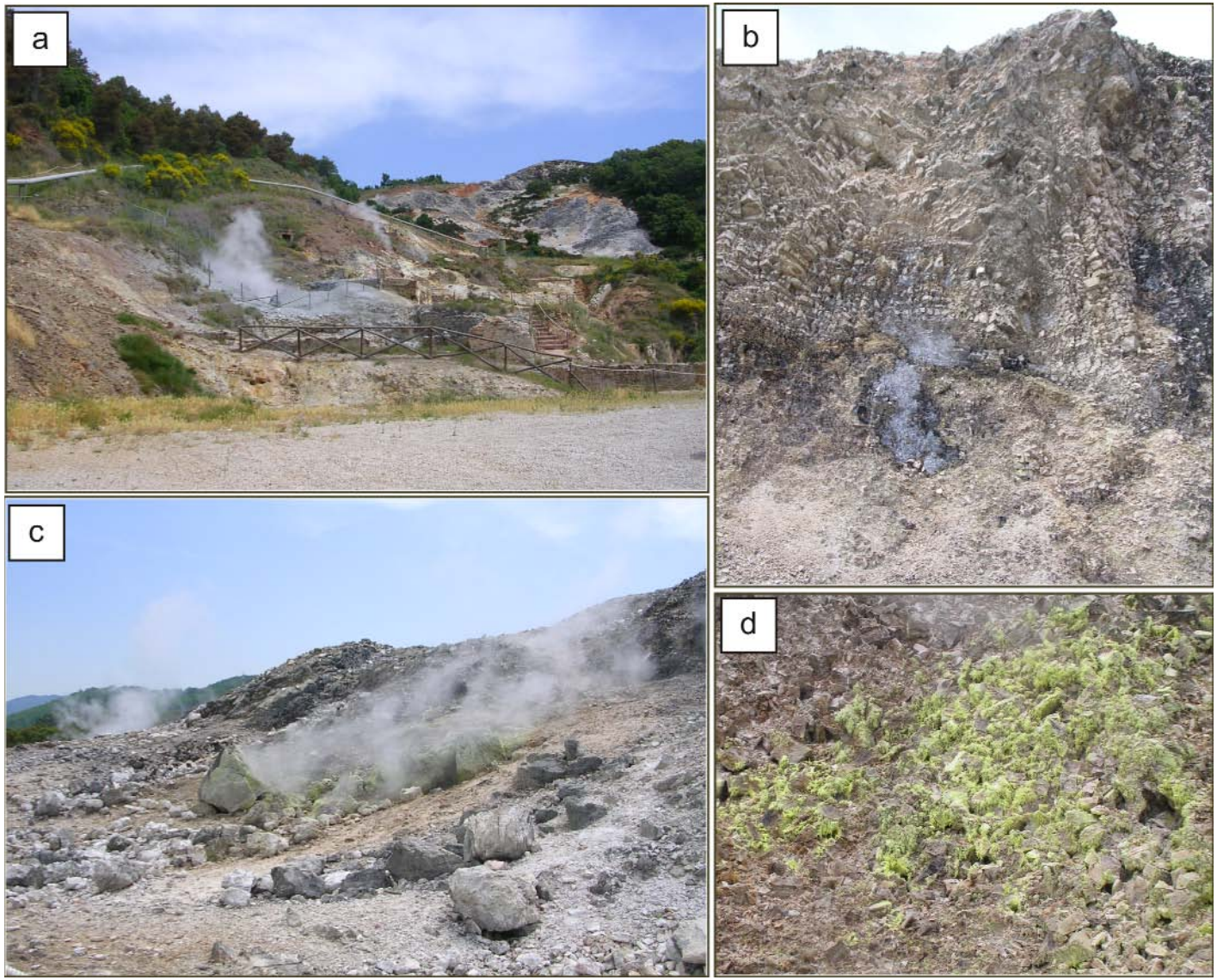

Fig. 55 – Monterotondo natural manifestations: **(a)** general view; **(b)** altered and fragmented radiolarites; **(c)** detail on natural manifestations; **(d)** growth of tiny sulphur crystals needles at the hydrothermal vents.

DOI: 10.3301/GFT.2015.02

This Stop also offers a panoramic view of the whole southwest sector of the Larderello area: looking south, on your right the Nuova Monterotondo is a direct steam power plant (10 MW installed capacity) built in 2002 in place of the old Monterotondo power plant (in operation since 1958).

Stops 2.5-2.9: The Malentrata mine. Natural analogues of CO_2 mineral sequestration (I)

Tuscany hosts several small hydrothermal deposits of magnesite, embedded in the serpentinites of the Ligurian ophiolitic units. Most of the magnesite ores are located in central-southern Tuscany: Monti Livornesi (Castiglioncello and Campolecciano mines), Colline Pisane (Malentrata, Monterufoli and San Dalmazio mines), and Val d'Elsa (Querceto mine). Minor outcrops occur on Elba Island.
Magnesite was discovered for the first time on Elba Island and has been locally exploited for the production of ceramics since the Renaissance. During the nineteenth century several mineralogists debated the composition of the white earthy mineral dug in Elba Island, alternately attributing it to magnesite (named "giobertite"), sepiolite, or kaolin. The real industrial phase starts at the beginning of the 1900s with the opening of large open pits in Elba Island. Later, massive veins of magnesite were discovered and exploited in the Monti Livornesi and Colline Pisane (1915), and in Val d'Elsa (1917). Exploitation continued intermittently until the beginning of World War II and covered the national needs at the time (refractory bricks for the metallurgical industry). Total production of magnesite was about 0.3 Mt while reserve estimation amounts to ca. 3 Mt, corresponding to 1.5 Mt of naturally sequestered CO_2. Production of magnesite in Tuscany displays three peaks that correspond to the "Great War" (1915-18), the 1920s (expansion of the Italian steel industry) and the autarkic period of fascism (1936-43). Magnesite production was conducted at a very local scale using simple exploitation techniques and manual sorting. The significant amount of silica (quartz, chalcedony, opal) was a detractive character of the Tuscan magnesite ore that, when coupled with the relatively high transport costs, caused the closure of the mines.

The Malentrata magnesite deposit is exposed along a lateral creek of the La Sterza River, near the Canneto village and at the periphery of the Larderello geothermal area. It consists of several carbonate–silica veins hosted by silicified, carbonated and argillized serpentinites of the Ligurian units. Some veins were dominated by silica phases (chalcedony, opal) and they were relatively famous and used in Tuscany (during the main activity of the Opificio delle Pietre Dure; Firenze) since the 16th century AD for the production and workmanship of semiprecious stone furnishings (Targioni Tozzetti, 1768-79).

DOI: 10.3301/GFT.2015.02

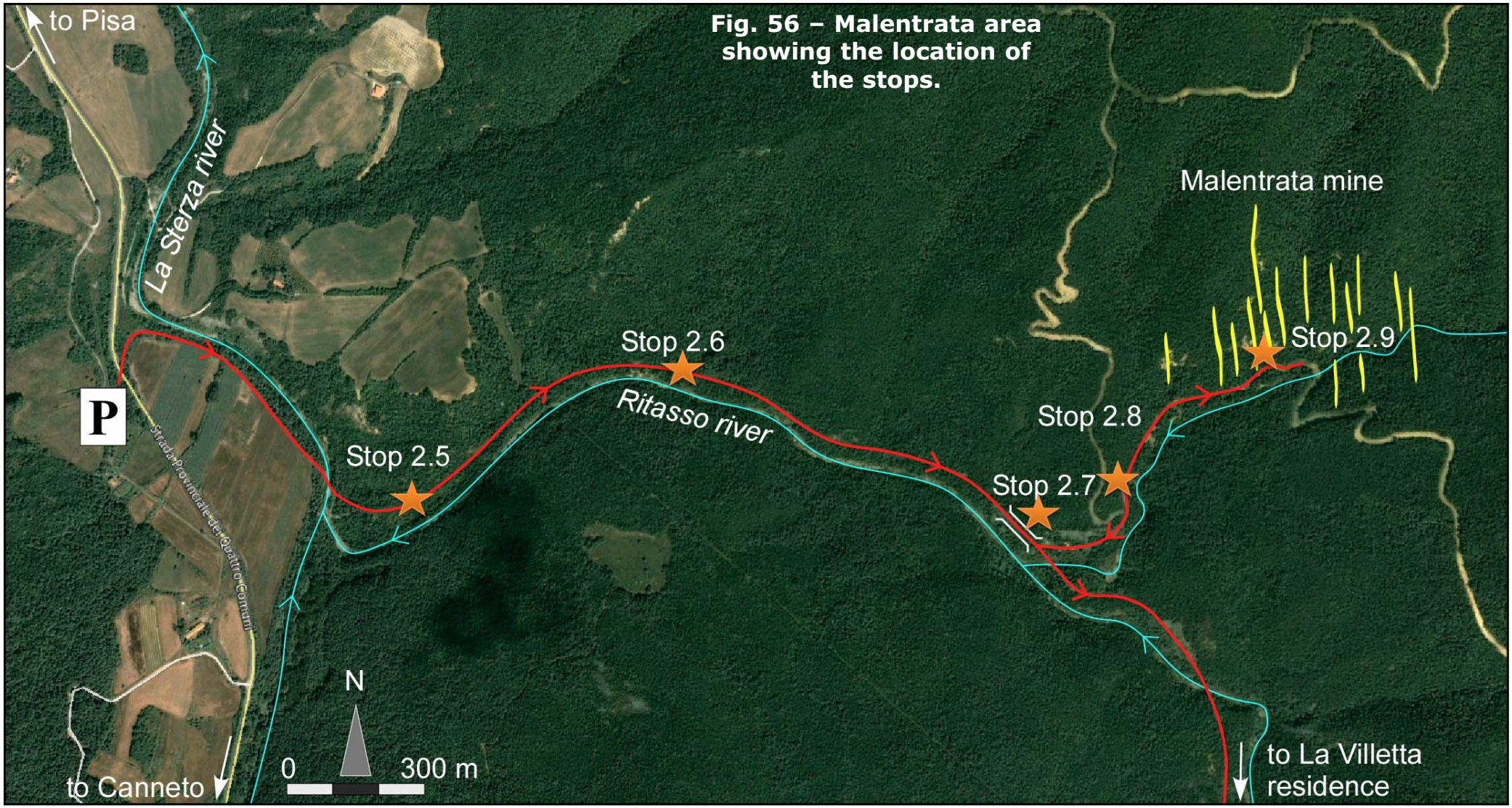

Fig. 56 – Malentrata area showing the location of the stops.

From a parking area near the La Sterza River you walk uphill (30-40') following the path of the old mining railroad that connected the abandoned La Villetta mine of lignite to the railway station of Casino di Terra (ca. 10 km to the north; Fig. 56). This path displays a nice geological section from the sedimentary envelope to the ophiolite body that hosts the magnesite deposit.

DOI: 10.3301/GFT.2015.02

STOP 2.5: Malentrata mine, the Mio-Pliocene sedimentary cover

Ophiolite outcrops in southern Tuscany are scattered because Neogene extensional tectonics dismembered the orogenic stack. Several sedimentary basins developed since Late Miocene and mantled the ophiolitic units with alluvial and shallow-marine deposits. Along the first part of the trail, after fording the La Sterza River, on the flank of the hill one can observe sub-horizontal layers of sands and conglomerates (Pliocene) (Fig. 57). This formation represents the upper part of the sequence, while the Miocene sediments are buried in the deeper part of the basin. Near the bottom of the sequence, some clay layers (Late Miocene) contain abundant lenses of lignite that were exploited by the La Villetta mine between 1850 and 1925. Some shafts and inclined drifts were dug down to 180 m below the surface, where a pluri-kilometric net of tunnels provided a total production of ca. 1.5 Mt of lignite. The remains of this activity are represented by the headframe of the main shaft and the rail loading station, now restored and transformed into a touristic residence.

Fig. 57 – Pliocenic sands and conglomerates at the top of Neogene sedimentary cover of the ophiolitic suite.

STOP 2.6: Malentrata mine, the sedimentary envelope of the ophiolites

Continuing along the path of the old lignite mining train, you leave the Neogene sediments and enter the sedimentary envelope of the ophiolite bodies (Fig. 58). Several stratigraphic and tectonic sub-units have been defined inside the Ligurian units on the basis of the relative age, paleogeographic position and internal stacking. However, the overall compositions of the sedimentary units are similar, ranging from argillites to marls, with

DOI: 10.3301/GFT.2015.02

Fig. 58 – Large boulder of serpentinite completely encased by argillites and marls of the sedimentary cover.

limestone, calcilutite and sandstone layers. The net result is the almost complete wrapping of ophiolite lenses (from decametric to pluri-kilometric in size) by quite impermeable argillitic envelopes (Fig. 58). The significant deformation of these sedimentary cover is responsible for the sudden changes in bedding attitude as well as the local folding. The sedimentary cover of Ligurian units stay on top of a large, sub-horizontal serpentinite body but the contact is not visible here due to the detrital cover.

Fig. 59 – The steep trench excavated through the serpentinites.

STOP 2.7: Malentrata mine, the serpentinite protolith

After a few hundred metres the path enter a steep trench that was excavated through the serpentinites and allowed the passage of the mining train (Fig. 59). Beautiful outcrops of serpentinites are here exposed and show the

DOI: 10.3301/GFT.2015.02

typical structure with lenses of massive porphyroclastic serpentinite wrapped by an anastomosing network of fibrous veins of serpentine. This outcrop represents the westernmost edge of the serpentinite body where the carbonation effects were very limited. Within a few hundred metres from here, the carbonation effects progressively increase and reach their maximum at the Malentrata mine.

STOP 2.8: Malentrata mine, the serpentinite-argillite contact

Immediately after the trench, you leave the path of the mining train and take (on the left) the uphill path, a small gravel road that intersects the old mining dumps. Abundant magnesite-dolomite-silica blocks and fragments may be easily observed in the mining dumps and among road's gravel. If you take a secondary road to the left and walk for about 100 metres uphill you could observe a nice outcrop along the road cut exposing the contact between serpentinites and argillites/marls (Fig. 60). Here, serpentinites show strong deformation, boudinage and carbonation.

The contact between argillites/marls and serpentinites may also be observed along the main gravel road, moving towards the mining site (Fig. 61).

Fig. 60 – Contact between boudined serpentinites (below) and argillites (above).

DOI: 10.3301/GFT.2015.02

Fig. 61 – Contact between serpentinites and argillites/marls along the main gravel road.

STOP 2.9: Malentrata mine: Carbonated serpentinites and carbonate-silica veins

We walk along the gravel road for some 300-400 meters and we finally reach the lower part of the excavations with small open pits and adits. Beautiful outcrops and large blocks of carbonate-silica veins are exposed everywhere in the area above the road (Fig. 62).

Fig. 62 – **(A)** On the left an example of brecciated and carbonated serpentinite, infilled by dolomite veins; **(B)** On the right, brecciated magnesite vein, partially cemented by dolomite and silica.

DOI: 10.3301/GFT.2015.02

Textures and mineralogy of both veins and carbonated serpentinites can be examined either by comfortable observation on block surfaces in the dumps or by climbing the steep walls of the open pits and adventuring into the old adits. Main carbonate–silica veins are characterized by an early massive infill of cryptocrystalline creamy-white magnesite containing angular fragments (millimetric to decimetric in size) of the carbonated-silicified serpentinite. Locally, massive magnesite veins acquire a nodular structure with magnesite nodules and cauliflower aggregates cemented by dolomite. Most of the massive veins are brecciated and show a "cement supported" structure (cement up to 50% vol.) with fragments of the early magnesite infill and host rocks cemented by banded Fe-rich magnesite, dolomite, chalcedony, quartz and opal. Beautiful samples of magnesite clasts encrusted by banded, green and creamy-white dolomite can be easily collected. Sliced and polished, they provide amazing natural artistic compositions showing large variations in geometry and colours. Quartz, chalcedony and opal represent the last phases to crystallize into the residual voids (geodes).
After a reasonable break for field observation and sampling you could turn back to the mining train path and continue to walk uphill (along gentle slopes), crossing the river twice over old bridges, and finally reaching the old rail loading station where you could spend the night (Website). Alternatively, you could follow the entire pathway in the opposite way to reach your car.

DOI: 10.3301/GFT.2015.02

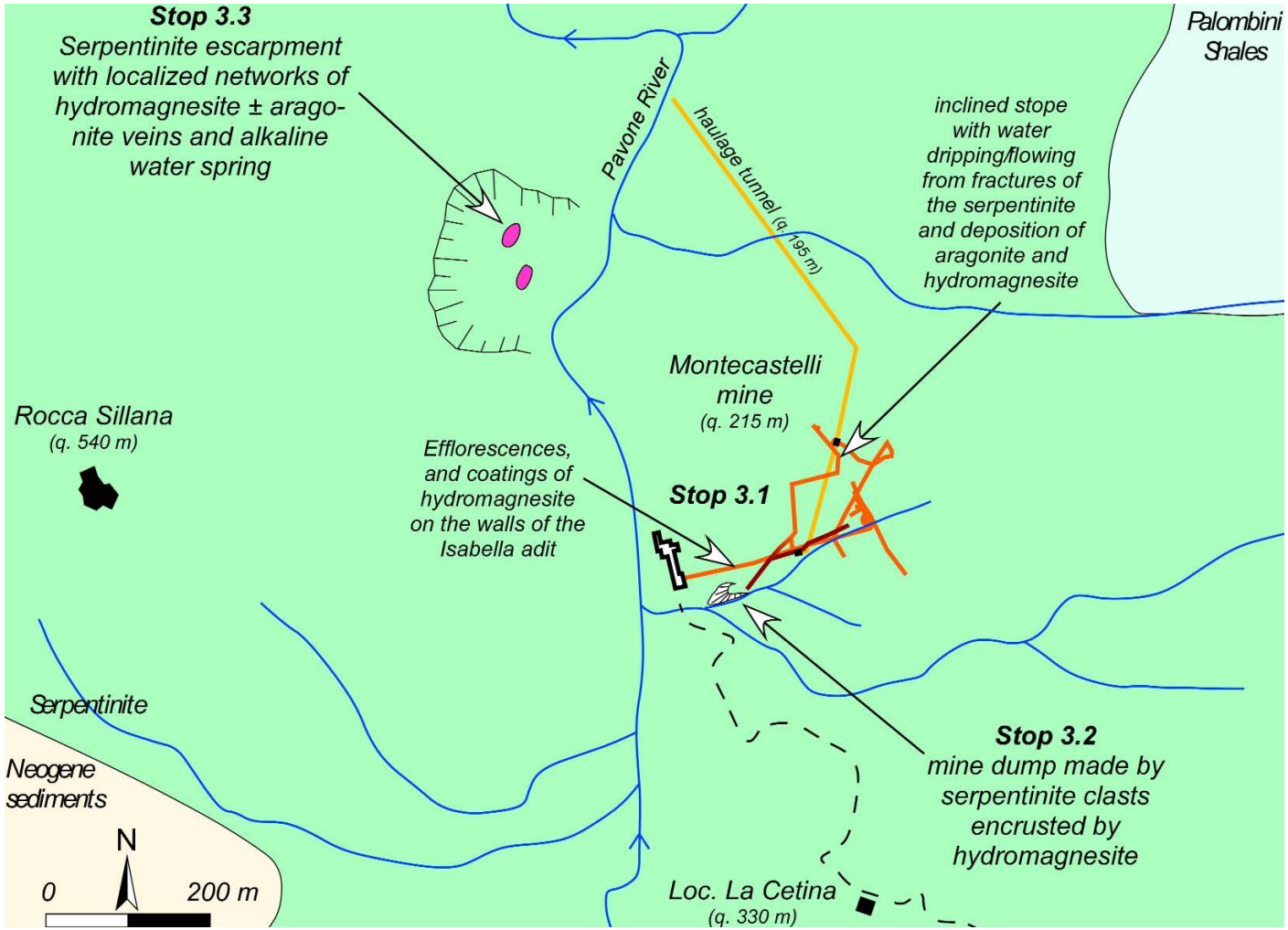

3rd Day

The Montecastelli copper mine. Natural analogues of CO_2 mineral sequestration (II)

Stop 3.1 – The Montecastelli copper mine: ongoing carbonation in the underground works.
Stop 3.2 – The Montecastelli copper mine: ongoing carbonation in mining dumps.
Stop 3.3 – The Pavone river: hydromagnesite-aragonite vein network and water spring.

Fig. 63 – Montecastelli area showing the location of the stops.

The ophiolitic sequence of the Ligurian units host several small copper deposits that were formed by oceanic hydrothermal circulation during Jurassic time. The original ore deposits were dismembered and locally mobilized by the complex tectonic and hydrothermal processes that affected the Tuscan portion of the Apennine chain. During the first half of the 19th century, one of these copper deposits (Montecatini Val di Cecina) became famous due to the discovery of a large bonanza where more than 50000 tons of copper were extracted. For a few years the Montecatini mine was the most productive copper mine in Europe, and the huge profits stimulated exaggerated expectations among prospectors exploring the rest of the ophiolite outcrops in

DOI: 10.3301/GFT.2015.02

Tuscany. Private investors lost large sums of money building oversize industrial plants and digging exploratory adits/shafts in Tuscan ophiolites. The Montecastelli mine is a representative example of this story: many kilometers of adits and shafts penetrate the hills, and ruins of large industrial buildings are strewn in the woods. The net result of such a big effort (1841-1869) was the production of a few tons of bornite and chalcopyrite. Minor exploration activities were carried out at the beginning of the 20th century but after 1941 the area was completely abandoned. Since 1970 this area was frequented by mineral collectors looking for nice specimens of aragonite (prismatic crystals) and hydromagnesite (fibrous-radiating spherules) in the fractures of serpentinites (Brizzi & Meli, 1989). This information sparked new scientific interest in the area of Montecastelli, because the presence of hydrated Mg-carbonates (mainly hydromagnesite) and aragonite highlights a different CO_2 sequestration process with respect to Malentrata (magnesite, dolomite and opal).
From the old medieval village of Montecastelli you walk downhill for about 30' along a small gravel road, and reach the Pavone River and the mining site (Fig. 63). Remember to contact the owner of the copper mine before planning your trip (Website).

STOP 3.1: The Montecastelli copper mine, ongoing carbonation in the underground works

The road cuts show good exposures of serpentinites crosscut by fibrous veins of serpentine along the path from Montecastelli to the abandoned copper mine. Arriving at the mine site near the Pavone River, you can observe the ruins of mining plants scattered through the woods. The entrance of the main adit (*Isabella adit*) is located inside one of these buildings. The owner of the property recently restored part of the underground works and included a new lighting system. The adits are safe and scenically lightened. An iron gate at the entrance allows the survival of a small bat colony that will accompany us along the visit.
The adit is completely dug in serpentinites that are crosscut by serpentine veins and late tectonic structures lined by breccias and soapy serpentine. This adit is connected by inclined stopes to the upper levels and, during the summer, the colder underground air column flows out from the Isabella adit. After a few tens of metres inside the adit we can make a first observation: the colours of the walls and the roof of the adit change when observed from two different directions (Fig. 64). Looking inward, the rock surfaces are covered by white coatings and spots, while looking outward the typical dark colour of serpentinite is dominant. This phenomenon is caused by the preferential growth of hydromagnesite coatings, efflorescences and cauliflower aggregates over the surfaces exposed towards the entrance of the adit. The study of these efflorescences is in progress but the

DOI: 10.3301/GFT.2015.02

Fig. 64 – The main adit of the Pavone mine. The colours of the adit's walls and roof change when observed in two different opposite directions (A and B).

asymmetric distribution of hydromagnesite may be related to seasonal variations of airflow and pCO_2 (Fig. 64). The Isabella adit reaches the main internal shaft that connects all of the underground works. The concrete walls of the shaft show several examples of writing left by the miners during the activity in the 19th century. Following a narrow deviation on the left, we explore a more adventurous part of the mine (optional part). This adit connected the Isabella adit to the exploitation zone but it is now interrupted. However, walking for a few tens of metres we observe an interesting zone with significant water dripping at the top of an inclined stope. Water dripping and flow along the lateral walls are responsible for the continuous growth of an aragonite flowstone associated with spotted aggregates of hydromagnesite (Fig. 65).

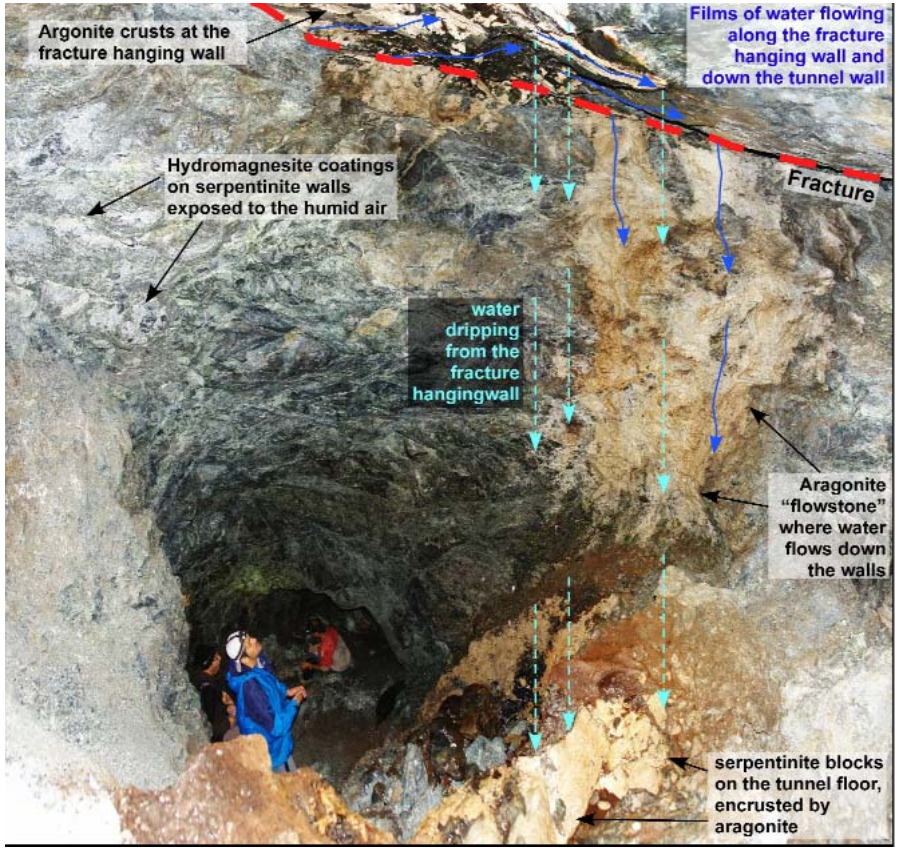

Fig. 65 – Dripping and flow of water along the lateral walls responsible for the continuous growth of an aragonite flowstone associated with spotted aggregates of hydromagnesite.

DOI: 10.3301/GFT.2015.02

STOP 3.2: The Montecastelli copper mine, ongoing carbonation in mining dumps

You walk uphill from the entrance of the Isabella adit and follow a narrow creek connecting the mining plants to the upper levels of the mine. The erosion along the creek exposes an interesting section of an old mining dump (Fig. 66). The dump is mainly made up of serpentinite clasts, with minor amounts of Cu-ore fragments. A prominent character of this site is the widespread precipitation of hydrated Mg-carbonates in voids between the clasts. White coatings, crusts, spherules, and cauliflower aggregates act as weak cement for the dump material.

Fig. 66 – Carbonated serpentinite clasts of the mine dump.

DOI: 10.3301/GFT.2015.02

STOP 3.3: The Pavone river, hydromagnesite-aragonite vein network and water spring

From the mine you reach the Pavone River. After the simple ford of the river, you walk downhill for a few hundred metres and reach the base of a large and steep wall of serpentinites. Serpentinites at this site are strongly fractured and rock falls sometimes happen. In the middle of the large serpentinite wall, a whitish spot represented by a few m^3 of serpentinite crosscut by a widespread network of hydromagnesite and aragonite veins is quite evident (Fig. 67). Many blocks of this outcrop fell to the base of the wall and can be easily observed and sampled. Persons interested in having a closer view of the outcrop can carefully climb the wall. Hydromagnesite spherules and crusts fill a network of fractures, and recently exposed surfaces of the rock are also rapidly covered by hydromagnesite coatings. Aragonite occurs either as fibrous radiating aggregates with hydromagnesite or as an exclusive infill made by large prismatic crystals (up to 10 cm). A small water spring is visible to the right of this outcrop. The spring water has an alkaline character (pH =8.5) and high Mg and Ca concentrations, as compared to the local rainwater (pH = 5.7; Mg= 0.04 and Ca= 0.02mEq/l).

Fig. 67 – Carbonated serpentinites of the serpentinite escarpment.

DOI: 10.3301/GFT.2015.02

DOI: 10.3301/GFT.2015.02

References

Acocella V., Rossetti F., Faccenna C., Funiciello R. & Lazzarotto A. (2000) - Strike-slip faulting and pluton emplacement in southern Tuscany; the Campiglia Marittima case. Boll. Soc. Geol. Ital., 119, 517-528.

Arias A., Dini I., Casini M., Fiordelisi A., Perticone I. & Dell'Aiuto P. (2010) - Geoscientific feature update of the Larderello–Travale geothermal system (Italy), for a regional numerical modelling. In: Proceedings World Geothermal Congress 2010, Bali, Indonesia, p. 11.

Baldacci A. (2001) - Italian Patent #01305033 dated 10 April 2001 (applied for 16 October 1998).

Baldacci A. & Sabatelli F. (1997) - Perspectives of Geothermal Development in Italy and the Challenge of Environment Conservation. Proceedings of NEDO International Geothermal Symposium, 31-41.

Baldi P., Bellani S., Ceccarelli A., Fiordalisi A., Squarci P. & Taffi L. (1995) - Geothermal anomalies and structural features of southern Tuscany. In: Proceedings of Geothermal Congress 1995, 18–31 May, Florence, Italy (E. Barbier et al. eds.), 693–696.

Barbier E., Musmeci F. & Saracco L. (1998) - Banca nazionale dati geotermici. Istituto Internazionale per le Ricerche Geotermiche CNR, Pisa.

Barelli A., Bertini G., Buonasorte G., Cappetti G. & Fiordelisi A. (2000) - Recent deep exploration results at the margins of the Larderello–Travale geothermal system. In: Proceedings World Geothermal Congress 2000, Kyushu-Tohoku, Japan, 965–970.

Barelli A., Cappetti G. & Stefani G. (1995) - Results of deep drilling in the Larderello–Travale/Radicondoli geothermal area. In: Proceedings World Geothermal Congress 1995, Florence, Italy, 1275–1278.

Batini F., Bertini G., Gianelli G., Pandeli E. & Puxeddu M. (1983) – Deep structure of the Larderello field: contribution from recent geophysical and geological data. Mem. Soc. Geol. Ital., 25, 219–235.

Batini F., Brogi A., Lazzarotto A., Lotta D. & Pandeli E. (2003) – Geological features of the Larderello-Travale and Mt. Amiata geothermal areas (southern Tuscany, Italy). Episodes, 26, 239–244.

Bedini F., Boschi C., Meìnez B., Perchiazzi N., Natali C. & Zanchetta G. (2013) - Interaction between Geosphere and Biosphere in CO_2-mineral sequestration environment. Abstract FIST2013.

Benvenuti M., Boni M. & Meinert L. (2004) – Skarn deposits in Southern Tuscany and Elba Island (Central Italy). IGC 2004 Field trip guide book - B18. Mem. Descr. Carta Geol. d'It., LXIII (Vol. 2), 24 pp.

Benvenuti M., Chiarantini L., Norfini L., Casini A., Guideri S. & Tanelli G. (2003a) - The "Etruscan tin": a preliminary contribution from researches at Monte Valerio and Baratti-Populonia (southern Tuscany, Italy). In G. Mair & F. Lo Schiavo (eds) "Le problème de l'étain à l'origine de la métallurgie" XIV UISSP Congress, Liège, 2-8 septembre 2001, Colloquium 11.2. Archeopress, BAR, 1199, 55- 65.

Benvenuti M., Costagliola P., Corretti A. & Dini A. (2012) - I minerali di ferro elbani: un viaggio tra mito, storia, industria, cultura e scienza. In: G. Pratesi (ed.), Il Museo di Storia Naturale dell'Università di Firenze. Volume IV. Le collezioni mineralogiche. Firenze University Press, ISBN: 978-88-6655-318-2, pp. 229-243.

Benvenuti M., Dini A., D'orazio M., Chiarantini L., Corretti A. & Costagliola P. (2013) - The tungsten and tin signature of iron ores from Elba island (Italy): a tool for provenance studies of iron production in the Mediterranean region. Archaeometry, 55(3), 479-506.

DOI: 10.3301/GFT.2015.02

Benvenuti M., Mascaro I., Costagliola P., Tanelli G. & Romualdi A. (2000) – Iron, copper and tin at Baratti (Populonia): smelting processes and metal provenances. Hist. Metal., London, 34 (2), 67-76.

Benvenuti M., Pecchioni E., Chiarantini L., Chiaverini J., Mariani A. & Mascaro I. (2003b) - An investigation on iron smelting furnaces from the Etruscan site of Baratti-Populonia (Tuscany). Proceedings Volume of the 6th Int. Congress on Ancient Ceramics (EMAC '01), Fribourg (Svizzera), 3-6 Ottobre 2001, 1-18.

Bertani R. & Cappetti G. (1995) - Numerical simulation of the Monteverdi zone (western border of the Larderello geothermal field). In: Proceedings World Geothermal Congress 1995, Florence, Italy, 1735–1740.

Bertini G., Cameli G.M., Costantini A., Decandia F.A., Dini I., Elter F.M., Lazzarotto A., Liotta D., Pandeli E. & Sandrelli F. (1994) – Structural features of southern Tuscany along the Monti di Campiglia-Rapolano Terme cross-section. Mem. Soc. Geol. Ital., 48, 51–59.

Bertini G., Casini M., Gianelli G. & Pandeli E. (2006) - Geological structure of a long-living geothermal system, Larderello, Italy. Terra Nova, 18, 163–169.

Bertini G., Cornamusini G., Lazzarotto A. & Maccantelli M. (2000) - Stratigraphic and tectonic framework of the Ligurian Units in the Castellina M.ma Hills (southern Tuscany, Italy). Boll. Soc. Geol. It., 119, 687–701.

Bertini G., Gianelli G. & Battaglia A. (1996) - Risultati ed interpretazione delle datazioni radiometriche (metodo 230Th/234U) dei campioni di minerali idrotermali presenti nelle rocce attraversate dai sondaggi geotermici (Larderello e Monteverdi) e negli affioramenti di rocce mineralizzate (Sassa e Canneto-Malentrata). ENEL-CNR-CISE, Atti Joint Report, Pisa, 12 pp.

Bertolani M. (1958) - Osservazioni sulle mineralizzazioni metallifere del Campigliese (Livorno). Periodico di Mineralogia, 27, 311-344.

Boccaletti M., Elter P. & Guazzone G. (1971) - Plate tectonics models for the development of Western Alps and Northern Apennines. Nature, 234, 108–111.

Boiron M.C., Cathelineau M., Ruggieri G., Jeanningros A., Gianelli G. & Banks D.A. (2007) - Active contact metamorphism and COR2R–CHR4R fluid production in the Larderello geothermal field (Italy) at depths between 2.3 and 4 km. Chem. Geol., 237, 303–328.

Bonini M. & Sani F. (2002) - Extension and compression in the northern Apennines (Italy) hinterland: evidence from the late Miocene-Pliocene Siena-Radicofani Basin and relations with basement structures. Tectonics, 22, 1-35.

Bonini M., Boccaletti M., Moratti M. & Sani F. (2001) - Neogene crustal shortening and basin evolution in Tuscany (northern Apennines). Ofioliti, 26, 275-286.

Bonini M., Moratti G. & Sani F. (1999) - Evolution and depocentre migration in thrust-top basins: Inferences from the Messinian Velona Basin (northern Apennines, Italy). Tectonoph., 304, 95-108.

Boschi C., Dallai L., Dini A., Gianelli G., Ruggieri G. & Trumpy E. (2010) - Fluid chemistry evolution during the natural carbonation of the Tuscan serpentinites: insights for CO_2 mineralogical sequestration. Proceeding of the 3th International Conference on accelerated carbonation for environmental and materials engineering, 29 Novembre-1 Dicembre 2010, Turku (Finlandia). pp. 139-146. ISBN 978-952-12-2505-5 (ISBN 978-952-12-2506-2 .pdf version)

Boschi C., Dini A., Baneschi I., Bedini F. Dallai L. & Perchiazzi N. (2013) - Direct carbon dioxide uptake from the atmosphere: examples from Montecastelli serpentinites (Tuscany, Italy). Proceeding of the 4th International Conference on accelerated carbonation for environmental and materials engineering, (Belgio). pp. 431-441. ISBN 978-94-6018-655-4.

Boschi C., Dini A., Dallai L., Gianelli G. & Ruggieri G. (2008) - Mineralogical sequestration of carbon dioxide: new insights from the Malentrata magnesite deposit (Tuscany, Italy). Proceeding of the 2th International Conference on accelerated carbonation

DOI: 10.3301/GFT.2015.02

for environmental and materials engineering, 1-3 Ottobre 2008, Rome (Italy), pp. 55-63.
Boschi C., Dini A., Dallai L., Gianelli G. & Ruggieri G. (2009) - Enhanced CO_2-mineral sequestration by cyclic hydraulic fracturing and Si-rich fluids infiltration into serpentinites at Malentrata (Tuscany, Italy). Chem. Geol., 265, 209–226.
Bossio A., Costantini A., Lazzarotto A., Liotta D., Mazzanti R., Mazzei R., Salvatorini G. & Sandrelli F. (1993) - Rassegna delle conoscenze sulla stratigrafia del neoautoctono toscano. Soc. Geol. Ital. Mem., 49, 17–98.
Brizzi G. & Meli R. (1989) - Le pietre silicee della Fattoria di Monterufoli (PI). Riv. Min. It., 3, 101-110.
Brogi A., Lazzarotto A., Liotta D. & Ranalli G. (2003) - Extensional shear zones as imaged by reflection seismic lines: the Larderello geothermal field (central Italy). Tectonoph., 363, 127-139.
Brogi A., Lazzarotto A., Liotta D. & Ranalli G. (2005) - Crustal structures in the geothermal areas of Southern Tuscany (Italy): insights from the CROP 18 deep seismic reflection lines. J. Volcan. Geotherm. Res., 148, 60-80.
Brogi A. & Liotta D. (2008) - Highly extended terrains, lateral segmentation of the substratum, and basin development: the middle-Late Miocene Radicondoli Basin (inner Northern Apennines, Italy). Tectonics, 27, TC5002.
Brozzetti F., Boncio P. & Pialli G. (2002) - Early-middle Miocene evolution of the Tuscan Nappe-western Umbria foredeep system: insights from stratigraphy and structural analysis. Boll. Soc. Geol. It., 121, 319-331.
Brunet C., Monié P., Jolivet L. & Cadet J.P. (2000) - Migration of compression and extension in the Tyrrhenian Sea, insights from $^{40}Ar/^{39}Ar$ ages on micas along a transect from Corsica to Tuscany. Tectonoph., 321,127-155.
Burgassi P.D., Cataldi R. & Donati C. (1995) - Scientific investigations and technological development in the Larderello region from XVI through XIX centuries, Proceedings World Geothermal Congress, Florence, Italy, 18-31 May 1995, 1, 433-440.
Burt (1982) - Skarn deposits – historical bibliography through 1970. Econ. Geol., 77, 755-763.
Cappetti G., Fiordelisi A., Casini M., Ciuffi S. & Mazzotti A. (2005) - A new deep exploration program and preliminary results of a 3D seismic survey in the Larderello–Travale geothermal field (Italy). In: Proceedings World Geothermal Congress 2005, Antalya, Turkey, p. 8.
Cappetti G., Passaleva G. & Sabatelli F. (2000) - Italy Country Update Report 1995-1999. Proceedings World Geothermal Congress, Kyushu-Tohoku, Japan, May 28-June 10, 2000, 109-116.
Carmignani L., Decandia F.A., Fantozzi P.L., Lazzarotto A., Liotta D. & Meccheri M. (1994) - Tertiary extensional tectonics in Tuscany (Northern Apennines, Italy). Tectonoph., 238, 295-315.
Cartocci A., Fedi M.E., Taccetti F., Benvenuti M., Chiarantini L. & Guideri S. (2007) - Study of a metallurgical site in Tuscany (Italy) by radiocarbon dating. Nucl. Inst. Meth. Ph. Res. B, 259, 384-387.
Cataldi R., Lazzarotto A., Muffler P., Squarci P. & Stefani G. (1978) - Assessment of geothermal potential of central and southern Tuscany. Geothermics, 7, 91–131.
Cathelineau M., Marignac C., Boiron M.C., Gianelli G. & Puxeddu M. (1994) - Evidence for Li-rich brines and early magmatic fluid rock interaction in the Larderello geothermal system. Geochim. Cosmochim. Acta, 58, 1083–1099.
Cavarretta G., Gianelli G. & Puxeddu M. (1982) - Formation of authigenic minerals and their use as indicators of physico-chemical parameters of the fluid in the Larderello-Travale geothermal field. Econ. Geol., 77, 1071–1084.
Celati R., Squarci P., Taffi L. & Stefani G.C. (1975) - Analysis of water levels and reservoir pressure measurement in geothermal wells. In: Proceedings 2nd U.N. Symposium on the Development and Use of Geothermal Resources, San Francisco, CA, USA, 1583–1590.

DOI: 10.3301/GFT.2015.02

Chiarantini L., Benvenuti M., Cartocci A., Costagliola P., Fedi M.E. & Guideri S. (2009a) – Iron production in the Etruscan site of Populonia: new data. In W. Nicodemi (Ed.), Archaeometallurgy in Europe 2007. Selected papers, AIM, Milano, 221-231.

Chiarantini L., Benvenuti M., Costagliola P., Fedi M. E., Guideri S. & Romualdi A. (2009b) - Copper production at Baratti (Populonia, southern Tuscany) in the early-Etruscan period (IX-VIII cent. BC). J. Archaeolog. Sci., 36, 1626–1636.

Cipriani C. & Tanelli G. (1983) - Risorse minerarie ed industria estrattiva in Italia. Atti e memorie dell'Accademia Toscana di Scienze e Lettere "La Colombaria", XLVIII, 241-283.

Corretti A. & Benvenuti M. (2001) - The beginning of iron metallurgy in Tuscany; with special reference to Etruria Mineraria. Proceedings of the First International Colloquium on The Archaeology of Africa and the Mediterranean Basin, The Museum of Natural History in Geneva, 4-7 June, 1999, Mediterranean Archaeology, 14, 127-145.

Corsini F., Cortecci G., Leone G. & Tanelli G. (1980) - Sulfur isotope study of the skarn-(Cu-Pb- Zn) sulfide deposit of Valle del Temperino, Campiglia Marittima, Tuscany, Italy. Econ. Geol., 75, 83-96.

Craig H. (1963) - The isotope geochemistry of water and carbon in geothermal areas. In: Nuclear Geology on Geothermal Areas, E. Tongiorgi (Ed.), Pisa, Lab. di Geol. Nucl., CNR, Pisa.

D'Amore F. & Bolognesi L. (1994) - Isotopic evidence for a magmatic contribution to fluids of the geothermal systems of Larderello, Italy, and The Geysers, California. Geothermics, 23, 21–32.

Da Mommio A., Iaccarino S., Vezzoni S., Dini A., Rocchi S., Brocchini D., Guideri S. & Sbrilli L. (2010) - Valorizzazione del geosito «Sezione Coquand», miniera del Temperino (Parco Archeominerario di San Silvestro, Campiglia Marittima). Atti Soc. Tosc. Sci. Nat., Mem., Serie a, 115, 55-72.

Dini A., Gianelli G., Puxeddu M. & Ruggieri G. (2005) - Origin and evolution of Pliocene-Pleistocene granites from the Larderello geothermal field (Tuscan Magmatic Province, Italy). Lithos, 81, 1-31.

Direzione generale delle miniere (1975) - Relazione generale mineraria: (art. 6, legge 7 marzo 1973, n. 69). Roma, Ministero dell'Industria, Commercio e Artigianato, 230 pp.

Elter F.M. & Pandeli E. (1990) – Alpine and Hercynian Orogenic phases in the Basement rocks of the Northern Apennines (Larderello Geothermal field, Southern Tuscany, Italy). Eclogae Geol. Helv., 83/2, 241–264.

Elter P. (1975) - Introduction à la géologie de l'Apennin septentrional. Bull. Soc. Geol. Fr. 7, 956–962.

ENEL (2009) - Visita la nostra Centrale. Percorso di visita turistico-didattico della centrale "San Martino". Pannelli illustrativi.

Ferrara G.C., Gonfiantini R. & Panichi C. (1965) - La composizione isotopica del vapore di alcuni soffioni di Larderello e dell'acqua di alcune sorgenti e mofete della Toscana, Atti Soc. Tosc. Sc. Nat., 72, 3–21.

Finetti I.R. (2006) - Basic regional crustal setting and superimposed local pluton-intrusion related tectonics in the Larderello-Monte Amiata geothermal province, from integrated CROP seismic data. Boll. Soc. Geol. Ital., 125, 117-146.

Finetti I.R., Boccaletti M., Bonini M., Del Ben A., Geletti R., Pipan M. & Sani F. (2001) - Crustal section based on CROP seismic data across the North Tyrrhenian-northern Apennines-Adriatic Sea. Tectonoph., 343, 135-163.

Gianelli G. & Ruggieri G. (2002) - Evidence of a contact metamorphic aureole with high-temperature metasomatism in the deepest part of the active geothermal field of Larderello, Italy. Geothermics, 31, 443– 474.

Gianelli G., Manzella A. & Puxeddu M. (1997) - Crustal models of the geothermal areas of southern Tuscany (Italy). Tectonoph., 281, 221–239.

DOI: 10.3301/GFT.2015.02

Goff F. & Lackner K.S. (1998) - Carbon dioxide sequestering using ultramafic rocks. Environ. Geosci., 5, 89–101.
Grassellini-Troysi M. & Orlandi P. (1972) - Sulla melanoflogite del Fortullino (Livorno). Soc. Tosc. Sc. Nat., Serie A, 79, 245–250.
Jolivet L., Dubois R., Fournier R., Goffé B., Michard A. & Jourdan C. (1990) - Ductile extension in alpine Corsica. Geology, 18, 1007-1010.
Lackner K.S. (2003) - A guide to CO_2 sequestration. Science, 300, 1677–1678.
Lattanzi P. (1999) - Epithermal precious metal deposits of Italy—an overview. Miner. Deposita, 34, 630–638.
Lattanzi P., Benvenuti M., Costagliola P. & Tanelli G. (1994) - An overview on recent research on the metallogeny of Tuscany, with special reference to the Apuane Alps. Mem. Soc. Geol. Ital. 48, 613–625.
Lazzarotto A. (1967) - Geologia della zona compresa fra l'alta valle del fiume Cornia ed il torrente Pavone (prov. di Pisa e Grosseto). Mem. Soc. Geol. Ital., 6, 151-197.
Liotta D. (2002) - D2 asymmetric folds and their vergence meaning in the Montagnola Senese metamorphic rocks (inner Northern Apennines, central Italy). J. Struc. Geol., 24 (9), 1479-1490.
Liotta D. & Ranalli G. (1999) – Correlation between seismic reflectivity and rheology in extend lithosphere: southern Tuscany, inner Northern Apennines, Italy. Tectonoph., 315, 109–122.
Locardi E. & Nicolich R. (1988) - Geodinamica del Tirreno e dell'Appennino centromeridionale: la nuova carta della Moho. Mem. Soc. Geol. Ital., 41, 121-140.
Magro G., Ruggieri G., Gianelli G., Bellani S. & Scandiffio G. (2003) - Helium isotopes in paleofluids and present day fluids in the Larderello geothermal field: constraints on the heat source. J. Geophys. Res., 108, 1–12.
Marinelli G. (1955) - Il giacimento di marcasite e magnesite nelle serpentine di Macchia Escafrullina (Rosignano Marittimo). Atti Soc. Tosc. Sc. Nat., Serie A, 62, 418–443.
Marini L. & Manzella A. (2005) - Possible seismic signature of the α–β quartz transition in the lithosphere of Southern Tuscany (Italy). J. Volcanol. Geotherm. Res., 148, 81–97.
Martini I.P. & Sagri M. (1993) - Tectonosedimentary characteristics of Late Miocene–Quaternary extensional basins of the Northern Apennines, Italy. Earth-Sci. Rev., 34, 197–233.
Mascaro I., Guideri S. & Benvenuti M. (1991) – Inventario del patrimonio minerario e mineralogico in Toscana. Aspetti naturalistici e storico-archeologici, Firenze, Regione Toscana (Ed.), 2 vv.
Molli G. (2008) - Northern Apennine-Corsica orogenic system: an updated review. Geol. Soc. London Spec. Publ., 298, 413-442.
Mongelli F., Palumbo F., Puxeddu M., Villa I. M. & Zito G. (1998) – Interpretation of the geothermal anomaly of Larderello, Italy, Mem. Soc. Geol. Ital., 52, 305–318.
Musumeci G., Bocini L. & Corsi R. (2002) - Alpine tectonothermal evolution of the Tuscan metamorphic Complex in the Larderello geothermal field (northern Apennines, Italy). J. Geol. Soc., 159, 443– 456.
Pandeli E., Gianelli G. & Morelli M. (2005) - The crystalline units of the middle-upper crust of the Larderello geothermal region (southern Tuscany, Italy): new data for their classification and tectono-metamorphic evolution. Boll. Soc. Geol. Ital. (Special Issue), 3, 139–155.
Pandeli E., Gianelli G., Puxeddu M. & Elter F.M. (1994) - The Paleozoic basement of the Northern Apennines: stratigraphy, tectono-metamorphic evolution and Alpine hydrothermal processes. Soc. Geol. Ital. Mem., 48, 627–654.

DOI: 10.3301/GFT.2015.02

Panichi C., Scandiffio G. & Baccarin F. (1995) - Variation of geochemical parameters induced by reinjection in the Larderello area. In: Proceedings of the Geothermal Congress 1995, 18–31 May, Florence, Italy (E. Barbier et al. eds.), 1845–1849.

Pertot C., Sabatelli F., Messia M. & D'Aleo M. (2013) - Assessment of Geothermal Power Plants Impact on Air Quality – Effect of H2S Abatement with AMIS® in the Larderello-Travale-Radicondoli Geothermal Area (Tuscany). Proceedings European Geothermal Congress 2013, Pisa, Italy, 3-7 June 2013, 10 pp.

Rath vom G. (1868) - Die Berge von Campiglia in der Toskanischen Maremme. Zeitschr. Deutsch. Gesell. Geow., 20, 307-364.

Romagnoli P., Arias A., Barelli A., Cei M. & Casini M. (2010) - An updated numerical model of the Larderello – Travale geothermal system, Italy. Geothermics, 39, 292–313.

Ruggieri G., Cathelineau M., Boiron M.C. & Marignac C. (1999) – Boiling and fluid mixing in the chlorite zone of the Larderello geothermal field. Chem. Geol., 154, 237–256.

Sabatelli F., Mannari M. & Parri R. (2009) - Hydrogen Sulfide and Mercury Abatement: Development and Successful Operation of AMIS Technology. GRC Transactions, 33, 343-347.

Sartori F. (1967) - La wolchonskoite di Castiglioncello (Livorno). Per. Mineral., 36, 103–124.

Scandiffio G., Panichi C. & M. Valenti (1995) - Geochemical evolution of fluids in the Larderello geothermal field. In: Proceedings of the Geothermal Congress 1995, 18–31 May, Florence, Italy (E. Barbier et al. eds.), 1839–1843.

Seifritz W. (1990) - CO_2 disposal by means of silicates. Nature, 345, 486.

Serri G., Innocenti F. & Manetti P. (1993) - Geochemical and petrological evidence of the subduction of delaminated Adriatic continental lithosphere in the genesis of the Neogene-Quaternary magmatism of central Italy. Tectonoph., 223, 117-147.

Sestini A. (1981) - Introduzione all'Etruria Mineraria. Il quadro naturale e ambientale. In: L'Etruria Mineraria. Atti del XII Convegno di Studi Etruschi e italici, Firenze - Populonia - Piombino 1979, Firenze, Leo S. Olschki (Ed.), 3-21.

Tanelli G. (1977) - I giacimenti a skarn della Toscana. Rend. Soc. It. Mineral. Petrol., 33(2), 875- 903.

Tanelli G. (1983) - Mineralizzazioni metallifere e minerogenesi della Toscana. Mem. Soc. Geol. Ital., 25, 91–109.

Targioni Tozzetti G. (1768-79) - Relazione di alcuni viaggi fatti in diverse parti della Toscana. Stamperia Granducale, Firenze, tomo III.

Trumpy E., Boschi C. & Dini A. (2010) - 3D geological reconstruction of serpentinite bodies in Tuscany: insights for in-situ CO_2 sequestration. Rend. Soc. Geol. Ital., 11(1), 85-86.

UGI (2007) - 5000 years of geothermal energy in Italy: historical outline. Chapter 4 in: Geothermal Energy, Yesterday, Today, Tomorrow. Special Issue of UGI's Newsletter, November 2007, 33-41.

Vai G.B. (2001) - Structure and stratigraphy: an overview. In: Anatomy of an Orogen, the Apennines and Adjacent Mediterranean Basin (G.B. Vai & I.P. Martini, eds), Kluwer Academic Publishers, Dordrecht/Boston/ London, 15–32.

Villa I.M., Ruggieri G., Puxeddu M. & Bertini G. (2006) – Geochronology and isotope transport systematics in a subsurface granite from the Larderello–Travale geothermal system (Italy). J. Volcan. Geotherm. Res., 152, 20–50.

Voss O. (1988) - The Iron Production in Populonia, in: PACT, The First Iron in the Mediterranean (Strasbourg), 91-100.

Editorial responsability and handling by R. Cioni

DOI: 10.3301/GFT.2015.02